

MOLECULAR MECHANISMS OF DEREGULATED TRANSLATION IN
PARKINSON'S DISEASE-LINKED G2019S LEUCINE-RICH REPEAT KINASE 2
(LRRK2) NEURONS

by
Jungwoo Wren Kim

A dissertation submitted to Johns Hopkins University in conformity with the requirements
for the degree of Doctor of Philosophy

Baltimore, Maryland

March, 2017

©2017 Jungwoo Wren Kim
All Rights Reserved

Abstract

Parkinson's disease (PD) is a neurodegenerative disorder affecting approximately 1.5% of the population over 65 years of age (Lees, Hardy, & Revesz, 2009). Pathologically, PD is characterized by a selective loss of dopamine neurons in the substantia nigra pars compacta and subsequently reduced dopamine signaling in the central nervous system. Over the last two decades, genetic studies have revealed a number of genes that can cause familial forms of PD when mutated. Among the PD-linked genes, G2019S missense mutation in leucine-rich repeat kinase 2 (LRRK2) gene is the most common disease-causing mutation in familial PD. The G2019S mutation is known to increase its kinase activity (Greggio et al., 2006; Smith et al., 2006). Recent studies have suggested that the increased kinase activity can cause translational abnormality, however, the mechanistic relationship between LRRK2 kinase activity and translation has not yet been established (Imai et al., 2008; Martin, Kim, Lee, et al., 2014).

Our laboratory has previously identified the ribosomal small subunit protein S15 as a pathogenic substrate of G2019S LRRK2. In this study, we revealed that global translation is increased in G2019S LRRK2 expressing *Drosophila* brain, and that the increased translation is important for its neurotoxicity. To gain a deeper understanding of the increased translation, we performed ribosome profiling experiments with LRRK2 mammalian models. We found that mRNAs harboring complex 5' untranslated region (UTR) secondary structure are preferentially translated in the presence of G2019S LRRK2, and it is dependent on phosphorylation of S15. Structured 5'UTR-mediated alteration in translation was observed in G2019S LRRK2 transgenic mice, LRRK2 knockout mice, and in human dopamine neurons

differentiated from G2019S LRRK2 PD patient-derived induced pluripotent stem cells. Notably, translation of $\text{Ca}_v1.2$ L-type voltage-gated Ca^{2+} channel, which is continuously active in substantia nigra pars compacta dopamine neurons, is enhanced through its 5'UTR in G2019S LRRK2 neurons. This increased expression leads to the elevation of neuronal Ca^{2+} influx and intracellular Ca^{2+} concentration in dopamine neurons. This study provides a novel finding between deregulated translation and increased Ca^{2+} influx, which may be crucial to understand progressive and selective dopamine neuronal death.

(Readers: Valina L. Dawson, Ph.D. and Nicholas T. Ingolia, Ph.D.)

Acknowledgements

First of all, I want to thank the Cellular and Molecular Physiology graduate program for giving me the opportunity to study at the Johns Hopkins University School of Medicine and providing me with an outstanding research environment.

I would like to express my sincerest gratitude to my doctoral advisors, Drs. Valina and Ted Dawson, for their exceptional support, mentorship, and being my ‘academic parents’.

Working in this laboratory to perform cutting-edge research and being trained by the leading scientists in the field has been a tremendous training experience to me. I am certain that the lessons and training I have obtained from Drs. Dawson will last for the rest of my scientific career.

I am very fortunate to have truly great dissertation committee members. This study could not have been possible without their support. Dr. Rachel Green, Dr. Mollie Meffert, and Dr. Nicholas Ingolia have not only provided professional and technical advices but have also shown a track of great scientist that I wish to follow. I am deeply obliged for their guidance and encouragements.

I have met many wonderful colleagues since I joined the laboratory and I deeply appreciate their professionalism and collaborative spirit. I particularly thank Dr. Ian Martin and Dr. Stephen Eacker for their close ‘benchtop’ mentorship, scientific excellence, and friendship that have nurtured me to an independent scientist.

Support from my family and friends has undoubtedly been vital for me to complete the extensive doctoral training. Although my parents are living in my hometown, Seoul, their love always finds me regardless of the distance, and my courage stands on the love I received from my family. I would like to acknowledge Adeline Yong, who has been showing great love to me and with whom I have shared laughter and tears.

Our path to reveal the molecular details of the deregulated protein synthesis regulation in Parkinson's disease-associated G2019S LRRK2 mutation has led us to an unexpected finding of defective calcium homeostasis in human dopamine neurons. It is my hope that our finding can contribute to deepen our understanding on the etiology of Parkinson's disease, and will ultimately help the patients who are suffering from this incurable disease.

Lastly, I would like to acknowledge the laboratory animals that have been sacrificed for this research.

Table of Contents

Abstract.....	ii
Acknowledgements.....	iv
Table of Contents.....	vi
List of Figures.....	vii
Chapter 1. Introduction.....	1
Chapter 2. Characterization of Global Protein Synthesis in G2019S LRRK2 Transgenic Drosophila Models.....	16
Chapter 3. 5' Untranslated Region (UTR)-mediated Translatome Alteration Leads To Calcium Homeostasis Dysregulation in G2019S LRRK2 Expressing Neurons.....	27
Chapter 4. Discussion and Conclusions.....	80
References.....	86
Appendices.....	99
Curriculum Vitae	119

List of Figures

Figure 1-1. A schematic of eukaryotic translational initiation.	12
Figure 1-2. Parkinson’s disease-linked LRRK2 mutations and their molecular mechanisms.	13
Figure 2-1. Elevated protein synthesis in G2019S LRRK2 transgenic flies is blocked by T136A S15.	23
Figure 2-2. Ribosomal run-off following harringtonine treatment is unaffected by G2019S LRRK2.	25
Figure 3-1. Broad alteration in mRNA translation through structured 5’UTR in GS LRRK2 mouse brain.	52
Figure 3-2. LRRK2 protein expression levels in LRRK2 mouse models.	55
Figure 3-3. Translation regulatory mechanisms unchanged in LRRK2 mouse models.	57
Figure 3-4. Phosphorylation of S15 mediates structured 5’UTR bias in GS LRRK2 neurons.	59
Figure 3-5. Reporter transcript levels measurement for stem-loop and IRES reporter assays.	62
Figure 3-6. DA differentiation and ribosome profiling of LRRK2 hiPSC lines.	64
Figure 3-7. GS LRRK2 human DA neurons have increased cytosolic Ca ²⁺ concentration. ..	66
Figure 3-8. Pathway analyses of human DA neuron ribosome profiling.	69
Figure 3-9. Cav1.2 expression is increased in GS LRRK2 human DA neurons.	71
Figure 3-10. Increased L-VGCC current in GS LRRK2 human DA neurons.	74
Figure 3-11. Cav1.2 expression is increased in GS LRRK2 human DA neurons.	76
Figure 3-12. Translation-mediated stress model in GS LRRK2 DA neurons.	78

Chapter 1. Introduction

I. Messenger RNA translation and its regulation in neurons

Messenger RNA (mRNA) translation is a fundamental cellular process, and its regulation serves as a major post-transcriptional regulatory mode of gene expression. Translation is a crucial part of protein homeostasis, and is tightly linked to vital cell physiology, such as the cell cycle, metabolism, stress and even cell death.

The core molecular machinery for mRNA translation is the ribosome. The ribosome is a large and complex molecular machinery specialized in protein synthesis, consisting of two subunits, the large subunit and the small subunit. Translation consists of three functionally distinct but mechanistically continuous steps: initiation, elongation and termination. Each step of translation is subject to tight regulation to meet the physiological needs of the cell. Although translational regulation is relatively less known compared to transcriptional regulation, there is growing evidence suggesting that it comprises diverse and complex regulatory mechanisms. Initiation is a crucial step to decide the mRNA to decode and to select the start codon to initiate translation, thereby choosing the open reading frame (ORF). Therefore, it is not surprising that the majority of currently known regulatory mechanisms focus on the proper control of the initiation process. During translational initiation in eukaryotes, eukaryotic initiation factors (eIFs) are recruited to the mRNAs to facilitate ribosomal loading and scanning. The initiation step is over when the ribosome and the

initiation factors locate the start codon, and then elongation proceeds (Jackson, Hellen, & Pestova, 2010; Sonenberg & Hinnebusch, 2009). During elongation, the actual coding information is 'translated' by the ribosome through codon-anticodon interaction between mRNA and aminoacyl-transfer RNA (tRNA) and subsequent peptide bond formation. Therefore, elongation is directly related to the fidelity of protein synthesis. For instance, speed of elongation influences pairing of a codon with its cognate tRNA, which is required for proper amino acid incorporation and appropriate folding of the growing polypeptide chain, underlining the importance of elongation regulation (Crombie, Swaffield, & Brown, 1992). Finally, ribosomal recognition of a stop codon triggers its release from the mRNA, thereby terminating the process. Translational termination is tightly connected to ribosome recycling and re-initiation of translation, and thus regulates the balance between free and active ribosomes (Dever & Green, 2012).

Translation in eukaryotic cells

In eukaryotes, mature mRNAs are exported from the nucleus to the cytosol after splicing. The cap-binding eukaryotic initiation factor 4F (eIF4F), a complex that consists of eIF4E, eIF4G, eIF4A, binds to the mRNAs and activates them (see Fig. 1. for the outline of the entire process). With the help of initiation factors such as eIF1, eIF1A and eIF3, the small ribosomal subunit (40S in eukaryotes) and ternary complex, comprised of initiator methionyl-tRNA (Met-tRNA_i^{Met}), eIF2 and GTP, form the 43S pre-initiation complex (PIC). The eIF4F cap complex recruits the PIC to the mRNA and forms the 48S initiation complex. Once the 48S complex is formed, it scans the mRNA until it finds a start codon. Upon the recognition of the start codon, the GTP in the ternary complex is hydrolyzed with the aid of

eIF5, an eIF2-specific GTPase-activating protein (GAP). eIF5 and eIF5B facilitate the dissociation of the initiation factors and the joining of the large ribosomal subunit (60S in eukaryotes). The large subunit joins to make the 80S ribosome, which has peptidyltransferase activity and thereby synthesizes a polypeptide by forming peptide bonds between amino acids. With the help of eukaryotic elongation factor 2 (eEF2), an aminoacyl-tRNA is recruited to the acceptor site (A site) of the ribosome. A new peptide bond is formed between the amino acids in the peptidyl (P)- and A-sites. eEF2 also promotes ribosomal translocation, and the whole cycle repeats until the ribosome encounters a stop codon. At the stop codon, instead of a charged tRNA, release factors enter the P-site and mediate termination of protein synthesis (Dever & Green, 2012).

eIF2 is thought to be one of the major regulatory targets in translational initiation. eIF2 is a component of the ternary complex and it binds to GTP and Met-tRNA_i^{Met}. More specifically, it delivers the Met-tRNA_i^{Met} to the 40S small ribosomal subunit. With the help of other initiation factors, the ternary complex forms the 48S initiation complex and enables the 40S subunit to scan, find the start codon, and initiate protein synthesis. Once the 48S complex finds the start codon, GTP is hydrolyzed to GDP, which is an essential step for initiation factor dissociation and 60S large subunit joining. eIF2 is a heterotrimeric protein consisting of subunits alpha, beta and gamma. Serine 51 on eIF2 α can be phosphorylated by various kinases in response to stress signals, and phosphorylated eIF2 α is resistant to the guanine nucleotide exchange factor (GEF) activity of eIF2B, therefore it remains in an inactive eIF2-GDP-tRNA_i state (Jackson et al., 2010; Sonenberg & Hinnebusch, 2009). Hence, it decreases active ternary complex availability and thereby reduces global protein synthesis, e.g. under

conditions of stress (Harding et al., 2000). It is also known that the phosphorylation of eIF2 α increases the expression of a group of genes with stress-responsive functions, such as activating transcription factor 4 (ATF4), through upstream open reading frame (uORF)-mediated translational regulation (Harding et al., 2000; Vattem & Wek, 2004). uORF-mediated regulation is involved in start codon selection; based upon arrangement of the different start codons, different ORFs can be chosen, resulting in the production of different proteins. Briefly, when ternary complex availability is low, start codon recognition by the 48S complex is hampered and the balance of start codon selection is skewed towards the downstream start codons. Several stress-responsive genes have multiple uORFs encoding non-functional gene products. Under normal conditions, the uORFs prevent the major ORF from being translated. However, when the ternary complex is depleted, the downstream start codons are preferred, leading to the synthesis of the desired functional protein (Harding et al., 2000; Jackson et al., 2010; Sonenberg & Hinnebusch, 2009). It is noteworthy that eIF2 α -mediated translational regulation has been shown to play important roles in processes relevant to neurons, like synaptic plasticity or neurodegeneration (H.-J. Kim et al., 2013; Moreno et al., 2012; Scheper, van der Knaap, & Proud, 2007).

Translation and neurological disorders

Aberrant translational regulation can lead to various neurological disorders, including neurodegenerative diseases. In fact, mouse models with straight overexpression/knockout of translation initiation factors or translation regulation factors show cognitive defects (Bhattacharya et al., 2012; Gkogkas et al., 2013; Santini et al., 2013). For example, eIF4E overexpression or eukaryotic initiation factor 4E-binding protein (4E-BP) knockout animals

have phenotypes reminiscent of autism-spectrum disorders (Gkogkas et al., 2013; Santini et al., 2013). 4E-BP acts as a negative regulator of eIF4E by directly binding to eIF4E and thereby sequesters eIF4E from the eIF4F complex formation. This suggests that neurons may be highly susceptible to translational abnormalities. Furthermore, protein aggregation-related neurodegenerative diseases – such as prion-mediated neurodegeneration or Alzheimer’s disease (AD) – might be linked to eIF2 α -mediated protein synthesis defects (Ma et al., 2013; Moreno et al., 2012). It has been suggested that the unfolded protein response (UPR) triggered by protein aggregates increases the levels of phosphorylated eIF2 α , thereby reducing global mRNA translation. As a result, many genes that are important for neuronal activity and synaptic function are downregulated and this eventually leads to cognitive defects and neuronal cell death. Notably, it has been reported that chemical modulators of eIF2 α including salubrinal and ISRIB may be neuroprotective in AD and prion-mediated neurodegenerative model, respectively (Halliday et al., 2015; Huang et al., 2012). However, their molecular mechanisms are unclear. Fragile X syndrome (FXS) and fragile X-related tremor and ataxia syndrome (FXTAS) is caused by loss of function of a single gene, fragile X mental retardation 1 (FMR1) (Sharma et al., 2010). FMR1 is an RNA-binding protein and it has been reported to function as translational repressor. Translational profiling identified that FMR1 target genes are important for neuronal function (Darnell & Klann, 2013). Recently, repeat-associated non-ATG (RAN) translation has been suggested as a key mechanism to understand triplet expansion-related homopolymeric protein disorders, such as spinocerebellar ataxia (SCA), myotonic dystrophy (DM) and amyotrophic lateral sclerosis / frontotemporal dementia (ALS/FTD) (Cleary & Ranum, 2013).

II. PD-linked LRRK2 mutations and their impact on mRNA translation

Recent studies on the familial forms of Parkinson's disease (PD) have revealed that there is a clear link between PD and protein synthesis. Leucine-rich repeat kinase 2 (LRRK2) G2019S mutation has been linked to increased protein synthesis and microRNA (miRNA) deregulation (S. Gehrke, Imai, Sokol, & Lu, 2010; Imai et al., 2008). Furthermore, PD-associated eukaryotic initiation factor 4 gamma-1 (eIF4G1) mutations were identified in genome-wide association studies (GWAS), and PTEN-induced putative kinase 1 (PINK1) was suggested to have a role in protein synthesis of mitochondrial proteins (Chartier-Harlin et al., 2011; Stephan Gehrke et al., 2015). Although there is increasing evidence suggesting the role of disrupted protein synthesis in PD, the detailed molecular mechanisms are still under investigation.

Parkinson's disease

PD is a neurodegenerative disorder affecting approximately 1.5% of the population over 65 years of age, and there are currently over 6 million people suffering from Parkinson's disease worldwide (Lees et al., 2009). As PD is an age-related disease and the portion of aged individuals continues to increase globally, this number will surely continue to rise, causing an increased burden not only on patients and their families, but also on our society as a whole. Pathologically, PD is characterized by a selective loss of dopamine (DA) neurons in the substantia nigra pars compacta and subsequently reduced dopamine signaling in the central nervous system (Moore, West, Dawson, & Dawson, 2005). The cause of this degeneration remains unknown. For many years, PD was considered to have little or no

genetic component. However, over the last two decades, genetic studies have revealed a number of genes that can cause familial forms of PD when mutated. Interestingly, it has been known that many PD-linked genes are linked to protein synthesis; either their gene products have a direct involvement in protein synthesis or certain phenotypes associated with these genes are susceptible to changes in translational regulation.

Table 1: Summary of PD genes linked to translation, modified from Taymans J-M. *et al.* (2015) (Taymans, Nkiliza, & Chartier-Harlin, 2015)

Gene	Protein	Mendelian inheritance ¹	Link to mRNA translation
SNCA	α -synuclein	AD	Alternate transcript usage through 3'UTR, genetic interaction with EIF4G1 (Dhungel et al., 2015; Rhinn et al., 2012)
PARK2	Parkin	Early-onset AR	E3 ligase substrate in translational machinery, genetic interaction with 4E-BP (Lee et al., 2013; Ottone et al., 2011)
DJ-1	DJ-1	Early-onset AR	Interacts with ribosomes in <i>Escherichia coli</i> (Kthiri et al., 2010)
PINK1	Pten-induced kinase 1	Early-onset AR	Genetic interaction with 4E-BP, regulation of translation of respiratory chain complex mRNAs on mitochondrial outer membrane (Stephan Gehrke et al., 2015; W. Lin et al., 2014)
LRRK2	Leucine-rich repeat kinase 2	Late-onset AD	Interaction with translational regulatory proteins, kinase substrates in translation machinery, increases bulk translation, involved in miRNA pathway (S. Gehrke et al., 2010; Gillardon, 2009; Imai et al.,

¹ AD: autosomal dominant, AR: autosomal recessive

			2008; Martin, Kim, Lee, et al., 2014)
VPS35	Vacuolar protein sorting-associated protein 35	Late-onset AD	Genetic interaction with LRRK2 and EIF4G1 (Dhungel et al., 2015; D. A. Macleod et al., 2013)
EIF4G1	Eukaryotic translation initiation factor 4 gamma-1	Late-onset AD	Translation initiation factor, suggested to affect cap complex formation (Chartier-Harlin et al., 2011)

LRRK2 mutations and PD

The PARK8 locus was identified in 2002 in a large Japanese family with autosomal dominant parkinsonism, and subsequent screening studies with familial PD groups identified mutations of LRRK2 in the PARK8 locus (Funayama et al., 2002). Up to now, LRRK2 mutations are the most common genetic cause of familial PD identified, accounting for up to 20% of specific PD cases in some populations like Ashkenazi Jews. Postmortem analysis of brains of affected individuals demonstrated that LRRK2 mutations show variable pathology regarding the presence of Lewy bodies and tau-reactive lesions (Moore et al., 2005). LRRK2 is a large multi-domain protein with known GTPase and kinase enzymatic activities, and multiple protein-protein interaction domains flank the enzymatic domains. There are many LRRK2 mutations reported from PD patients; 6 of those mutations clearly segregate with the disease, all of which reside within the enzymatic Ras of complex (ROC) – C-terminus of ROC and kinase domains (Fig. 1-2A) (Martin, Kim, Dawson, & Dawson, 2014). This suggests that the enzymatic activities of LRRK2 are important to disease development. Despite the importance of enzymatic activities in PD, the normal biological role of LRRK2 is

still under investigation. A series of experimental evidences suggest a role for LRRK2 in vesicular trafficking, autophagy, cytoskeletal network formation, synaptogenesis and protein synthesis (Fig. 1-2B) (Mark R Cookson, 2012; M. R. Cookson, 2015; Dodson, Zhang, Jiang, Chen, & Guo, 2012; Imai et al., 2008; Kett et al., 2012; D. A. Macleod et al., 2013; Manzoni et al., 2013; Martin, Abalde-Atristain, Kim, Dawson, & Dawson, 2014; Martin, Kim, Dawson, et al., 2014; Ramonet et al., 2011). However, the major pathological mechanism contributing to disease progression is still unclear.

G2019S LRRK2 mutation and kinase activity of LRRK2

Among the LRRK2 mutations, G2019S in the kinase domain is the most prevalent. Globally, it constitutes 4% of familial and 1% of sporadic known cases. Studies have shown that the G2019S LRRK2 augments its kinase activity, and that the increased kinase activity is toxic to neurons (Mark R Cookson, 2012; Martin, Kim, Dawson, et al., 2014; Smith et al., 2006; West et al., 2005; West et al., 2007). Therefore, it has been thought that identifying LRRK2 kinase substrates is pivotal to gain insight into LRRK2-associated pathology. Notably, recent efforts to achieve an integrative understanding of the LRRK2-mediated neurotoxicity through augmented kinase activity suggest that the roles of LRRK2 kinase activity converge on the regulation of protein homeostasis, including protein synthesis (Fig. 1-2B) (S. Gehrke et al., 2010; Imai et al., 2008; Martin, Kim, Lee, et al., 2014). This allows us to hypothesize that the core disease mechanism of G2019S LRRK2 mutation is deregulation of protein homeostasis, and it also highlights the importance of understanding the roles of LRRK2 kinase activity in protein synthesis.

LRRK2 in mRNA translation

A series of studies showed that LRRK2 physically and functionally interacts with the mRNA translation machinery. These studies also showed that the defects in protein synthesis caused by PD-linked LRRK2 mutations incur toxicity in neurons. In 2008, Imai et al. reported that LRRK2 genetically interacts with the target of rapamycin (TOR) pathway components in *Drosophila*, suggesting a role of LRRK2 in translational regulation. In the study, genetic deletion of dLRRK either aggravated the TOR suppression-mediated impaired cell growth, or suppressed TOR hyperactivation-mediated enhanced cell growth. Therefore, LRRK2 was proposed to affect global protein synthesis through the TOR pathway (Fig. 1-2C) (Imai et al., 2008). In addition, a subsequent study from the same group reported that G2019S/I2020T PD-linked LRRK2 variants – both have increased kinase activity – impact translation through repressing miRNA activity. Transgenic flies expressing mutant human or fly LRRK2 showed suppression of let-7 and miR-184, thereby increasing expression of E2F1 and DP, respectively (Fig. 1-2C) (S. Gehrke et al., 2010). However, the molecular mechanism explaining how mutant LRRK2 disrupts the miRNA pathway remains unclear. In addition to the *Drosophila* models, Nikonova et al. reported that expression of the core components of the protein synthesis machinery is altered in LRRK2 mouse models. The authors performed microarray and subsequent gene set enrichment analysis to compare the expression profiles of LRRK2 knockout and G2019S transgenic mice. As a result, the authors reported that there was a significant increase in ribosomal gene expression in G2019S LRRK2 transgenic mice compared to LRRK2 knockout mice (Nikonova et al., 2012). This also suggests that there is an increased need of protein synthesis in G2019S LRRK2 mice. In addition to that, LRRK2 has been reported to interact with the translation elongation factor eEF1A in mammalian

cells. As eEF1A brings aminoacyl-tRNAs to the ribosomal A-site during elongation, it suggests the possibility that LRRK2 affects this step of translation as well (Fig. 1-2C) (Gillardon, 2009).

This chapter is modified from:

- 1) Kim JW, Abalde-Atristain L, Jia H, Dawson VL, Dawson TM. Protein translation in Parkinson's disease. In: Verstreken P, Ed., *Parkinson's Disease: Molecular Mechanisms Underlying Pathology*. San Diego: Academic Press, 2017:281-309.
- 2) Martin I, Kim JW, Dawson VL, Dawson TM. LRRK2 Pathobiology in Parkinson's Disease. LRRK2 pathobiology in Parkinson's disease. *J. Neurochem.* 2014 Dec;131(5):554–65. Review.

I-H. Wu created Fig. 1-1.

Figure 1-1. A schematic of eukaryotic translational initiation.

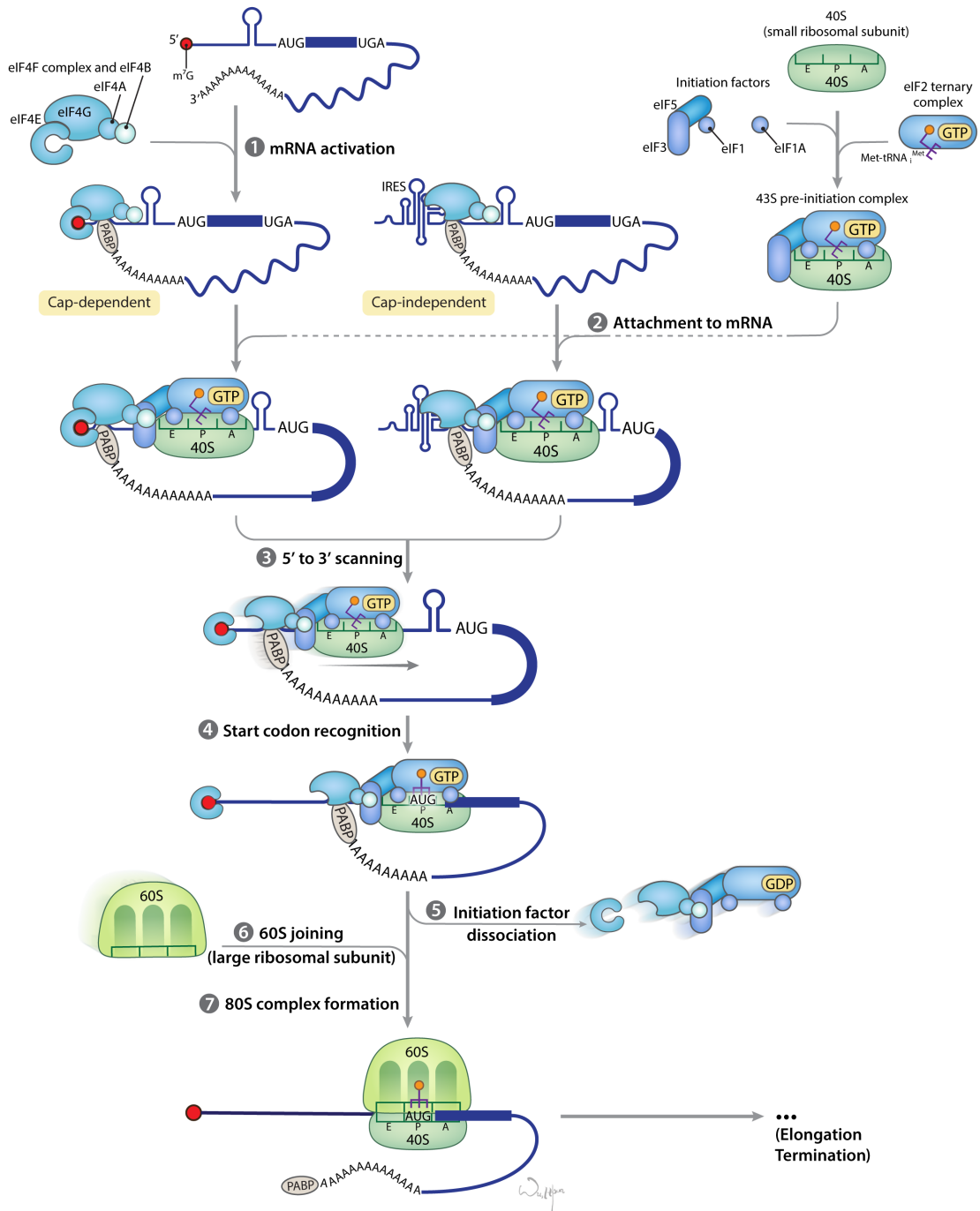


Figure 1-2. Parkinson's disease-linked LRRK2 mutations and their molecular mechanisms.

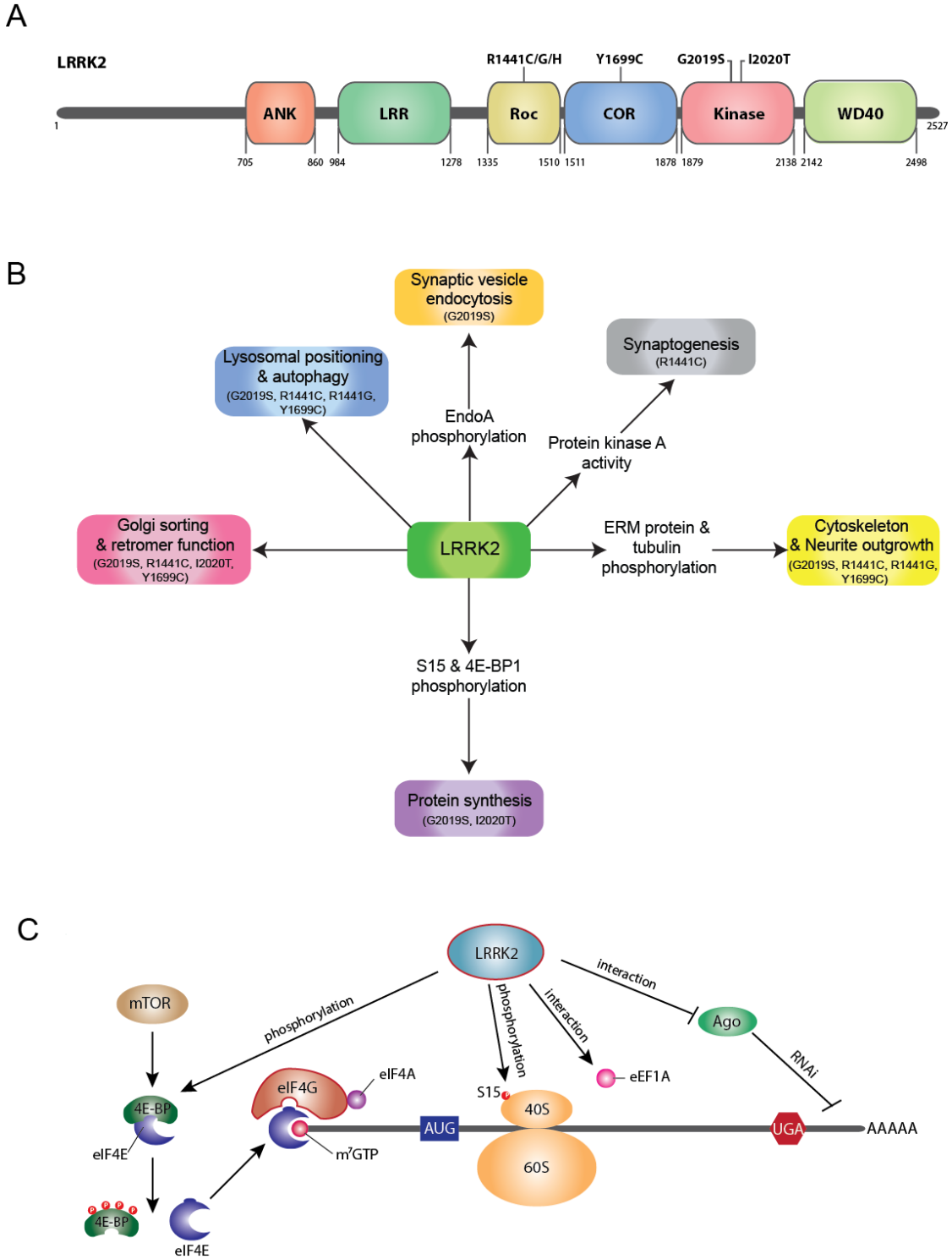


Figure 1-2. Parkinson's disease-linked LRRK2 mutations and their molecular mechanisms.

(A) The catalytic core of LRRK2 comprises Ras of complex proteins (Roc), C-terminal of ROC (COR) and kinase domains where all disease-segregating mutations identified are located. R1441 and Y1699 mutations decrease GTPase activity of LRRK2 whereas G2019S and I2020T mutations increase kinase activity. Flanking the catalytic domains are ankyrin-like repeats (ANK), leucine-rich repeats (LRR), and the WD40 domain that are thought to mediate protein-protein interactions, although binding partners for these domains are unknown. Numbers indicate amino acid boundaries for the domains and protein length.

Mutations that segregate with Parkinson's disease are annotated at their domain location. (B)

Putative functions of LRRK2 that are impacted by one or more pathogenic mutations.

LRRK2 has been reported to regulate lysosomal positioning and autophagy (Alegre-Abarategui et al., 2009; Dodson et al., 2012; Plowey, Cherra, Liu, & Chu, 2008; Su & Qi, 2013; Wang et al., 2012; Wu et al., 2012), synaptic vesicle endocytosis (Matta et al., 2012), synaptogenesis (Parisiadou et al., 2014), cytoskeleton and neurite outgrowth (Jaleel et al., 2007; D. MacLeod et al., 2006; Parisiadou et al., 2009; Smith et al., 2006; West et al., 2007), protein synthesis (Martin, Kim, Lee, et al., 2014), golgi sorting and retromer function (C. H. Lin, Tsai, Wu, & Chien, 2010; D. MacLeod et al., 2006; D. A. Macleod et al., 2013; Stafa et al., 2014). Mutations reported to affect each function are indicated in parentheses. (C)

A schematic illustration of LRRK2 effects on mRNA translation via several proposed mechanisms. LRRK2 may influence translation in an analogous manner to mTOR via phosphorylation of 4E-BP (eIF4E binding protein) that promotes dissociation of 4E-BP from eIF4E thus increasing levels of free eIF4E available for cap-dependent translation initiation.

LRRK2 interacts with Eukaryotic translation elongation factor 1A (eEF1A) with unknown consequences and LRRK2 may regulate miRNA function in a miRNA-specific manner involving unclarified mechanisms that may involve binding of LRRK2 and phospho-4EBP to Argonaute (Ago) proteins. This study contributes to the findings that LRRK2 phosphorylates ribosomal protein S15 to stimulate cap-dependent and cap-independent translation. The effects of LRRK2 on translation are kinase-dependent and pathogenic mutations that increase kinase activity (e.g. G2019S) cause toxicity at least in part via increased mRNA translation.

Chapter 2. Characterization of Global Protein Synthesis in G2019S

LRRK2 Transgenic Drosophila Models

Introduction

LRRK2 is a large multi-domain protein with several protein-protein interaction domains and a catalytic core containing GTPase, COR (C-terminal of ROC) and kinase domains are where most PD-linked mutations are found. It is likely that its physiologic and pathophysiologic functions are mediated through protein-protein interactions and/or phosphorylation of LRRK2 substrates (Cookson, 2010). A number of candidate LRRK2 substrates have been identified, and defects in protein synthesis in PD-linked LRRK2 models have been suggested. However, how elevated LRRK2 kinase activity is coupled to aberrant mRNA translation and neurodegeneration in PD remains to be clarified.

In order to understand the connection between LRRK2 kinase activity and neurotoxicity, we performed LRRK2-interacting phosphoprotein screening through LRRK2 tandem affinity purification and in vitro kinase screening of LRRK2-interacting phosphoproteins. We found that ribosomal proteins are major LRRK2 interactors and LRRK2 kinase targets, and that LRRK2 is markedly enriched in the ribosomal subcellular fraction. Interestingly, blocking phosphorylation of the small ribosomal subunit protein S15 rescues LRRK2 neurotoxicity in human dopamine neurons and Drosophila PD models.

Translation reporter assays suggest that G2019S LRRK2 increases global translation through phosphorylation of S15. To investigate the effects of G2019S LRRK2 on translation in vivo, we measured bulk protein synthesis rate in LRRK2 transgenic Drosophila models. We found

that G2019S LRRK2 induces an increase in bulk protein synthesis in flies, which is blocked by phospho-deficient S15. Furthermore, ribosome run-off assays suggest that the increased bulk translation in G2019S LRRK2 neuron is caused by elevated translation initiation.

Results

G2019S LRRK2 increases bulk translation in *Drosophila*

³⁵S-Methionine/Cysteine pulse labeling of newly synthesized protein shows that bulk protein synthesis is significantly increased in G2019S LRRK2 transgenic *Drosophila* heads, suggesting an increase in protein synthesis rates by LRRK2 (Fig. 2-1A). In accordance with its ability to block LRRK2 toxicity, T136A S15 co-expression abolishes this increase (Fig. 2-1A). SDS-PAGE analysis of lysates indicates a bulk increase in many proteins across a large range of molecular weights by G2019S LRRK2 (Fig. 2-1B). Assessment of housekeeping gene mRNAs undergoing translation in monosome and polysome fractions from fly heads reveals that G2019S LRRK2 expression leads to an enrichment of mRNAs in heavy polysome fractions, an effect which is attenuated by T136A S15 (Fig. 2-1C). This increase in density of ribosomes associated with mRNA indicates that LRRK2 stimulates mRNA translation and that an increased rate of protein synthesis underlies the augmented protein levels observed via ³⁵S-methionine/cysteine labeling.

Polysome profiling suggests that G2019S LRRK2 increases translational initiation

Increased ribosomal density typically indicates an increase in translation initiation but could theoretically signal a slower rate of ribosomal elongation or release upon termination. To test

the possibility whether reduced elongation/termination rates are accountable for the bulk translation reduction, ribosomal run-off experiments were performed. Harringtonine, a drug that prevents translocation of ribosomes engaged in initiation but not elongation, was treated and protein synthesis rate was measured by using polysome profiling or ³⁵S-Methionine/Cysteine pulse labeling (Fig 2-2, A to E). G2019S LRRK2 did not affect rates of ribosomal runoff following treatment of cells with harringtonine.

Discussion

Combined with the results from other experiments, these data contributed to our recent report that pathogenic G2019S LRRK2 increases phosphorylation of its substrate ribosomal protein S15, thereby increasing global protein synthesis and causing neurotoxicity (Martin, Kim, Lee, et al., 2014). In the study, we identified ribosomal proteins as targets of G2019S LRRK2, via proteomic screening and subsequent kinase assays. Among those ribosomal proteins, we showed S15 to be a ‘pathogenic’ target, as blocking S15 phosphorylation on the identified site as being phosphorylated by LRRK2, threonine 136, substantially reduced G2019S LRRK2 neurotoxicity in both human neuron and *Drosophila* models. Furthermore, phospho-deficient allele of S15 on threonine 136 (T136A S15) could block G2019S LRRK2-mediated neuronal injury, namely neurite shortening and cell death in human neuron models, while a phospho-mimetic version of S15 (T136D S15) could partially replicate the toxicity elicited by G2019S LRRK2. Subsequently, we confirmed phosphorylated S15-mediated neurotoxicity in *Drosophila* in vivo models.

When we tried to dissect out the role of LRRK2 in translation more specifically, G2019S LRRK2 showed increase translation in both a cap-dependent and -independent manner by in vitro reporter assays. We also detected elevated de novo protein synthesis in ³⁵S-methionine/cysteine incorporation assays. This increase in bulk translation was neutralized by co-expression of a phosphorylation-deficient form of S15. Furthermore, the elongation inhibitor anisomycin or phospho-deficient S15 rescued neurotoxicity in G2019S LRRK2 *Drosophila* models (Martin, Abalde-Atristain, et al., 2014). Those findings are in line with previous reports that increased protein synthesis serves as a key mechanism in pathogenic LRRK2 mutations, suggesting that protein synthesis inhibitors might have therapeutic potential for LRRK2 PD patients.

Materials and Methods

³⁵S-methionine/cysteine labeling in *Drosophila*

³⁵S-methionine/cysteine (100 µCi/ml) was added to standard food medium during cooling. The following day, flies were transferred to labeled food for 24h, and then heads were collected on dry ice and homogenized by pestle and mortar in 1% NP-40 extraction buffer on ice. Protein was precipitated by the addition of methanol and heparin (lysate:heparin(100mg/ml):methanol volume ratio of 150:1.5:600), centrifuged at 14,000 x g for 2 minutes, and supernatant was removed and the pellet air dried. Protein pellet was resuspended in 8M urea / 150 mM Tris, pH 8.5 and incorporation relative to total protein amount was measured by scintillation counting following assay of protein concentration by BCA assay.

mRNA polysome profiling by RT-PCR

Fly heads were homogenized in polysome lysis buffer (10 mM Tris-HCl/150 mM NaCl/5 mM MgCl₂/0.5 mM DTT/100 μG cycloheximide/EDTA-free protease inhibitor cocktail/40U/ml Suprase-in) and following clearing of the homogenate by centrifugation at 2,000 x g for 10 minutes, 1% NP-40 was added to the supernatant and incubated on ice for 10 minutes. The lysate was cleared by centrifugation at 16,000 x g for 10 min at 4°C, lysate was then layered onto a 10-60% sucrose gradient, centrifuged in a SW-41Ti rotor at 40,000 rpm for 2 hours at 4°C, and sampled using a Biocomp gradient station connected to a Gilson fraction collector with constant monitoring of optical density at 254 nm. 1 ml fractions were collected and spiked with 20 ng of polyA synthetic luciferase RNA to control for variations in downstream processing as previously described (Thoreen et al., 2012). Total RNA was extracted from each fraction using Trizol LS (Life Technologies) and precipitated with isopropanol following the manufacturer's protocol. cDNA was derived using Superscript III first-strand kit for RT-PCR using random hexamer primers and following the manufacturer's protocol. Transcript levels were measured by quantitative PCR using SYBR green master mix (Applied Biosystems) and primers for actin 5C, tubulin or luciferase. Actin 5C and tubulin levels in each fraction were normalized to luciferase and the percentage of translated mRNA in each fraction was calculated relative to the total RNA in all monosome and polysome fractions combined.

Assessment of ribosomal runoff

SH-SY5Y cells were transfected with LRRK2 and the following day, passaged to a new culture vessel at ~40% confluency to allow exponential growth. 24h after passaging, cells were treated with harringtonine (2 µg/ml) to freeze initiating ribosomes and allow runoff of elongating ribosomes. Total ribosomal translocation was blocked by adding cycloheximide (100 µg/ml) at fixed time intervals following harringtonine, and polysome profiles were generated by sedimentation of cell lysates made using polysome lysis buffer on 10-60% sucrose gradients. In a parallel experiment, transfected cells were pulse labeled with ³⁵S-methionine/cysteine (50 µCi/well) then immediately treated with harringtonine and cycloheximide together or harringtonine followed by cycloheximide at fixed time intervals. Cells were lysed and increase in ³⁵S-methionine/cysteine incorporation was measured and compared between groups as an indicator of relative ribosomal elongation rates.

Acknowledgements

This work was supported by NIH/NINDS P50NS038377, the JPB Foundation, Maryland Stem Cell Research Foundation (2013-MSCRFII- 0105-00), and the Adrienne Helis Malvin Medical Research Foundation's Parkinson's Disease Programs. We thank Dr. Rachel Green for the help on the polysome profiling experiments.

This chapter is modified from:

1) Martin I, Kim JW, Lee BD, Kang HC, Xu J-C, Jia H, Stankowski J, Kim M-S, Zhong J, Kumar M, Andrabi SA, Xiong Y, Dickson DW, Wszolek ZK, Pandey A, Dawson TM, Dawson VL. Ribosomal protein s15 phosphorylation mediates LRRK2 neurodegeneration in

Parkinson's disease. *Cell*. 2014 Apr 10;157(2):472–85.

2) Kim JW, Abalde-Atristain L, Jia H, Dawson VL, Dawson TM. Protein translation in Parkinson's disease. In: Verstreken P, Ed., *Parkinson's Disease: Molecular Mechanisms Underlying Pathology*. San Diego: Academic Press, 2017:281-309.

Figure 2-1. Elevated protein synthesis in G2019S LRRK2 transgenic flies is blocked by T136A S15.

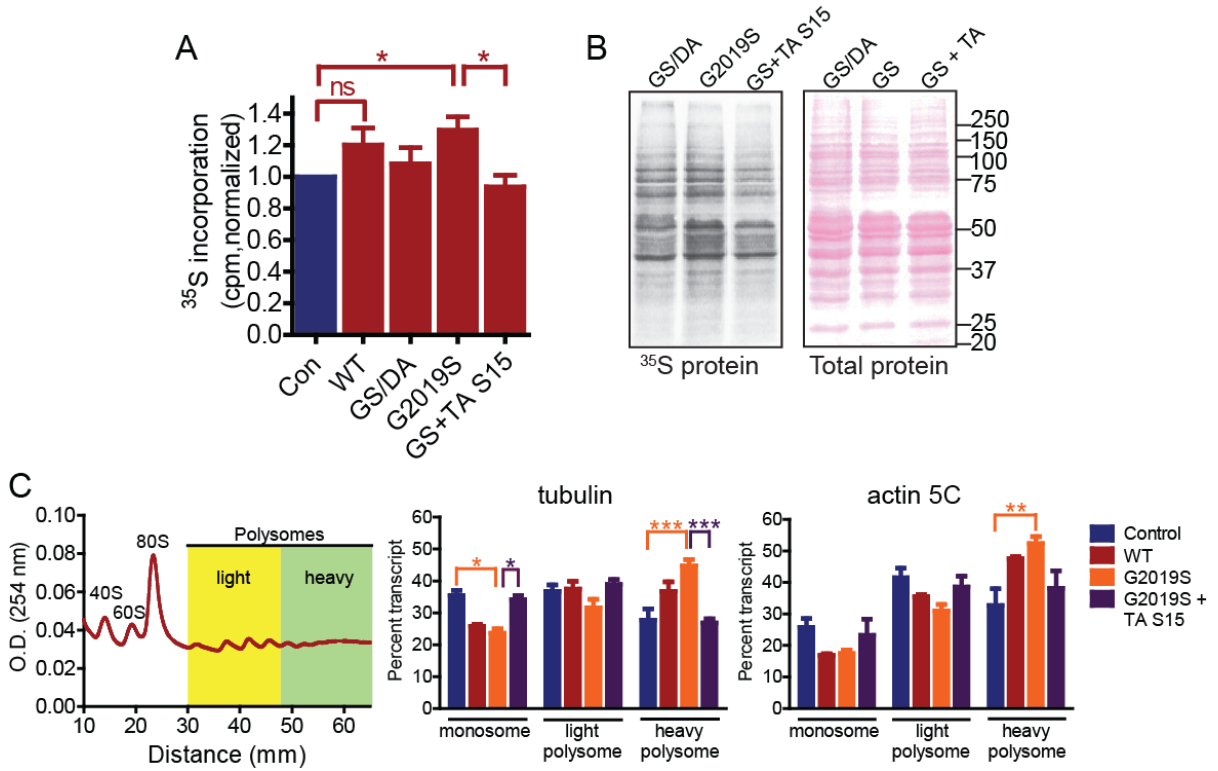


Figure 2-1. Elevated protein synthesis in G2019S LRRK2 transgenic flies is blocked by T136A S15.

(A) De novo protein synthesis, measured by ^{35}S -met/cys incorporation is significantly increased in protein precipitates from G2019S LRRK2 transgenic fly heads, which is blocked by T136A S15 co-expression (* $p < 0.05$, $n = 5$ groups of 50 heads/genotype). Genotypes are Da-Gal4 alone (Control), Da-Gal4; LRRK2 (WT), Da-Gal4/ GS/DA LRRK2 (GS/DA), Da-Gal4; G2019S LRRK2 (G2019S), Da-Gal4/T136A S15; G2019S LRRK2 (GS+TA S15). (B) Autoradiography from lysates reveals a widespread increase in ^{35}S -Met/Cys-labeled protein abundance. Ponceau staining for total protein. (C) Fractions collected from fly head polysome profiles and used for RT-PCR of translating mRNA indicates a G2019S LRRK2-mediated shift in tubulin and actin 5C to heavy polysome fractions, prevented by T136A s15 (two-way ANOVA, Bonferroni's post-test, * $p < 0.05$, ** $p < 0.01$, *** $p < 0.001$, $n = 3$ groups of 100 fly heads/genotype). Data are mean \pm SEM.

Figure 2-2. Ribosomal run-off following harringtonine treatment is unaffected by G2019S LRRK2.

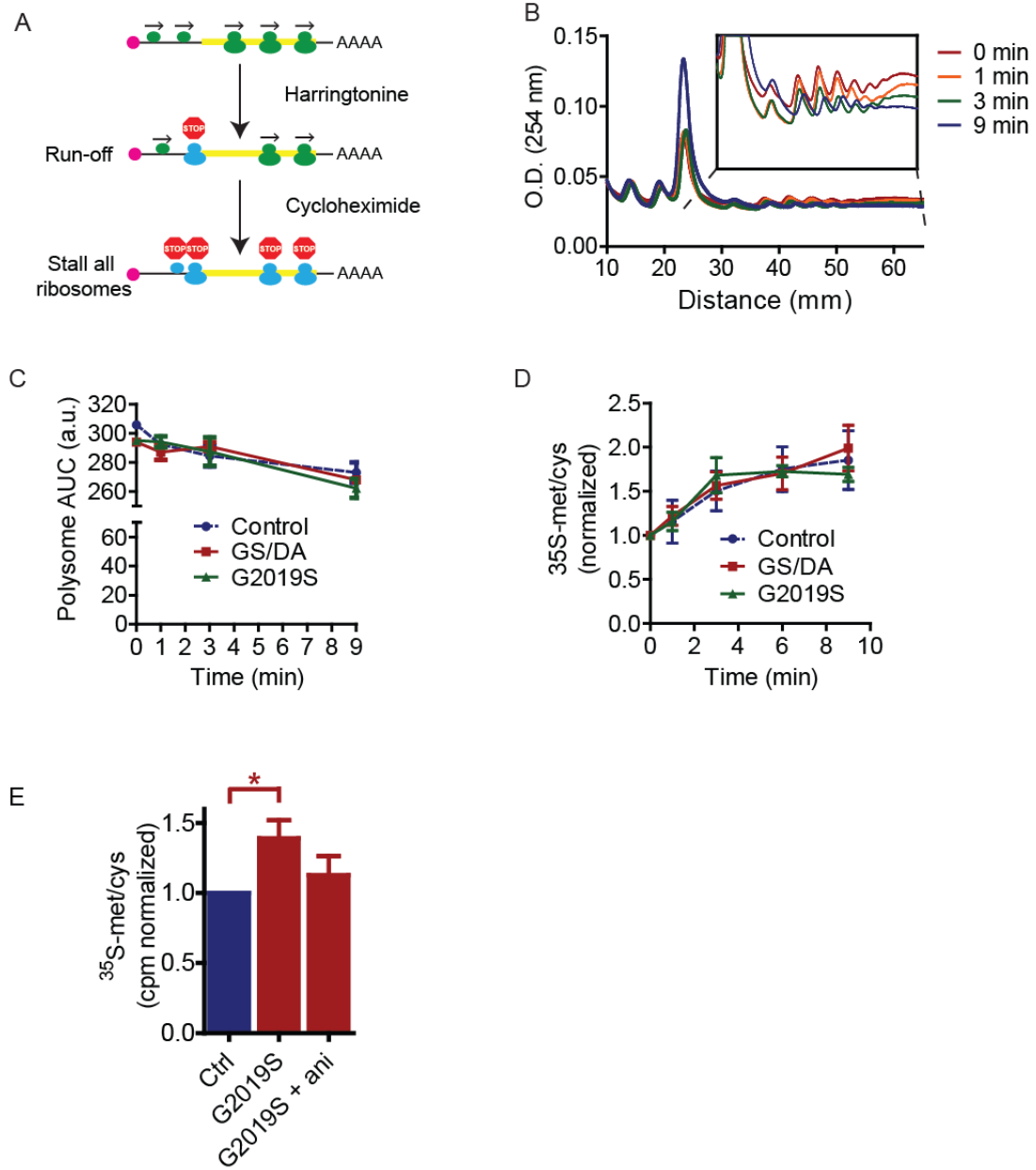


Figure 2-2. Ribosomal run-off following harringtonine treatment is unaffected by G2019S LRRK2.

(A) A schematic of harringtonine and cycloheximide treatment. (B) Polysome profiles generated at indicated time points following harringtonine treatment of SH-SY5Y cells demonstrate progressive ribosomal run-off. (C) No significant difference of ribosomal run-off, quantified as polysome area under curve (AUC) at each time point between cells transfected with vector, G2019S/D1994A LRRK2 or G2019S LRRK2 (two-way ANOVA, Bonferroni's post-test, n =3). (D) No significant difference in ribosomal run-off, measured by increase in ³⁵S-met/cys incorporation following harringtonine treatment (two-way ANOVA, Bonferroni's post-test, n =3). (E) Anisomycin treatment reduced the elevated protein synthesis in G2019S transgenic flies (ANOVA, Bonferroni's posttest, *p < 0.05, n = 3). Data are mean ± SEM.

Chapter 3. 5' Untranslated Region (UTR)-mediated Translatome Alteration Leads To Calcium Homeostasis Dysregulation in G2019S LRRK2 Expressing Neurons

Introduction

Mutations in the leucine-rich repeat kinase 2 (LRRK2) gene are the most common genetic cause of familial Parkinson's disease (PD) (Lees et al., 2009). G2019S missense mutation is the most frequent disease-causing mutation in LRRK2, and it enhances LRRK2 kinase activity that is known to be crucial for its neurotoxicity (Martin, Kim, Dawson, et al., 2014). While there are various cellular functions associated with LRRK2 kinase activity, emerging evidence suggests that translational abnormality caused by augmented kinase activity plays a role in PD pathogenesis (Taymans et al., 2015). However, the molecular mechanism linking defective mRNA translation to dopamine neurotoxicity remains unknown. We previously reported that G2019S LRRK2 increases global protein synthesis through phosphorylation of the ribosomal protein S15, and that reduction of global protein synthesis is protective against G2019S LRRK2 neurotoxicity in *Drosophila* models (See Chapter 2) (Martin, Kim, Lee, et al., 2014). The results led us to hypothesize that the increased translation in G2019S LRRK2 may lead to unfavorable induction of a subset of genes whose precise regulation is vital for the long-term survival of dopamine neurons. However, the translatome of G2019S LRRK2 mammalian brain has not been thoroughly assessed, impeding our insights on the mechanisms by which increased translation contributes to the neuronal stress in dopamine neurons. To further address the molecular mechanisms of G2019S LRRK2- and S15

phosphorylation-dependent translational abnormality, we performed ribosome profiling experiments with G2019S LRRK2 mammalian models.

Ribosome profiling and translation efficiency (TE)

In ribosome profiling, ribosome-protected mRNA fragments are captured and deep-sequenced, providing a quantitative measurement of translation and precise location of translating ribosomes in a genomic scale (Nicholas T Ingolia, Ghaemmaghami, Newman, & Weissman, 2009). RNase I treatment on mRNAs only leaves short RNAs, also called as ‘ribosome footprints’, which are protected by ribosomes, and subsequent deep sequencing of the footprints provides translational expression profile in genome-wide scale (Fig. 3-1A). The abundance of ribosome footprint is also coupled to the transcript abundance (N. T. Ingolia, 2016). To estimate the translational activity of a particular gene, translational efficiency (TE) is calculated by normalizing footprint frequency to the abundance of the corresponding transcript to decouple translational and transcriptional regulation.

5’ untranslated region (5’UTR) and translational regulation

Translation initiation is a tightly regulated process, with many eukaryotic initiation factors (eIFs) involved in the regulation and facilitation of the process. For example, the 5’UTR is known to possess a regulatory role in translational initiation. RNA secondary structure in the 5’UTR region is thought to repress scanning by the 43S ribosome, thereby serving as a negative modulator of translation initiation. DEAD-box RNA helicases including eIF4A, Ddx3, and Dhx29 are thought to resolve 5’UTR secondary structure of mRNAs with help of other initiation factors such as eIF4B (Parsyan et al., 2011; Sen, Zhou, Ingolia, &

Hinnebusch, 2015). Therefore, 5'UTR secondary structure and its resolution by RNA helicase have been suggested as a major regulatory step for translation initiation.

Internal ribosome entry site (IRES) reporters

The bicistronic internal ribosome entry site (IRES) reporter is a commonly used tool to distinguish cap-dependent and cap-independent translation. Different types of IRES sequences were identified with various translation initiation factors requirements (Jackson et al., 2010). In this study, bicistronic reporters with hepatitis C virus (HCV) or cricket paralysis virus (CrPV) IRES were used. HCV- and CrPV-IRES do not require RNA helicase activity to initiate translation. HCV-IRES is known to directly recruit 43S subunit to the start codon without eIF1, eIF4A, eIF4B and eIF4F. CrPV-IRES can mediate initiation without any known eIFs or tRNAⁱ (Jackson et al., 2010).

L-type voltage-gated calcium channels (L-VGCCs) in substantia nigra pars compacta dopamine neurons

Dopamine neurons are pacemaking neurons, and L-VGCCs are engaged during autonomous pacemaking in substantia nigra pars compacta dopamine neurons. This L-VGCC activity is known to elevate Ca²⁺ influx into the neurons (Chan et al., 2007). The elevated Ca²⁺ influx and subsequently increased mitochondrial oxidant stress have been implicated in the PD pathogenesis, supposedly through increased metabolic demands (Guzman et al., 2010; Pacelli et al., 2015). It is noteworthy that mitochondrial defects are regarded to be a common risk factor underlying PD etiology regardless of the cause, including genetic and pharmacological PD risk factors (Dawson & Dawson, 2017).

Results

Ribosome Profiling of LRRK2 mouse models

We implemented ribosome profiling to dissect the details of the translational abnormality in G2019S LRRK2 mammalian models. For this study, doxycycline-regulated LRRK2 transgenic mice were crossed with the CaMKII-tTA driver mice to obtain high expression of G2019S LRRK2 (GS LRRK2) or kinase dead G2019S/D1994A LRRK2 (GS/DA LRRK2) transgenes in excitatory neurons (Fig. 3-2, A to C) (Lee et al., 2013; Nikonova et al., 2012). Ribosome profiling was performed from the caudate putamen of GS LRRK2 or GS/DA LRRK2 transgenic and LRRK2 knockout mice. Translation efficiency (TE), which is a ratio between ribosome footprints abundance to mRNA abundance and used to infer translational activity of each transcript, was calculated (Brar & Weissman, 2015; N. T. Ingolia, 2016). The global distribution of TE values was compared between LRRK2 transgenic mice and non-transgenic control mice, or LRRK2 knockout mice and wild-type control mice. The results revealed that global TE distribution is altered in both GS LRRK2 transgenic and LRRK2 knockout mice (Fig. 3-1, B and C). GS/DA LRRK2 transgenic mice have a similar TE distribution as non-transgenic control mice (Fig. 3-1D), indicating TE changes in LRRK2 transgenic mice are kinase dependent (Greggio et al., 2006; Smith et al., 2006). The altered TE distribution indicates that there are genes more or less sensitive to GS LRRK2, and the enhanced mRNA translation in GS LRRK2 brain results in a wide distortion in its translato

5'UTR-mediated translational alteration in GS LRRK2 neurons

To gain a deeper understanding of the altered TE distribution, various modes of translational regulation were examined. The results do not show any significant TE differences on the targets of let-7 family miRNAs or the mRNAs with 5' terminal oligopyrimidine tract (5' TOP), which have been previously suggested by others as effectors of LRRK2-mediated translation control (Fig. 3-3, A to D) (S. Gehrke et al., 2010; Herzig et al., 2011). In contrast, there is a remarkable correlation when the 5'UTR secondary structure was compared between the most upregulated 'TE up' genes and the most downregulated 'TE down' genes from each dataset (Fig. 3-1, E to H). The TE up genes in GS LRRK2 brain tend to have more complex 5'UTR secondary structure, while the TE down genes tend to have simpler, less structured 5'UTR secondary structure. The opposite trend exists in LRRK2 knockout mice, further supporting the kinase-dependent roles of LRRK2 in 5'UTR-mediated translation (Fig. 3-1, G and H). No significant LRRK2-dependent bias was identified based on the structure of 3' UTRs (Fig. 3-3, E and F).

5'UTR reporter assays reveal S15 phosphorylation-dependent translational alteration

5'UTR luciferase reporters were designed to investigate if LRRK2 facilitates translation of a generic structured 5' UTR. 5'UTR sequences with no predicted secondary structure or strong hairpin structures were inserted into a firefly luciferase reporter vector, and the reporters were tested in mouse primary neurons (Fig. 3-4A). Consistent with the ribosome profiling results, the 5'UTR stem-loop luciferase reporters with complex 5'UTR secondary structure are translated more efficiently in GS LRRK2 expressing neurons (Fig. 3-4B). The effects of GS/DA LRRK2 are less and do not reach statistical significance. We previously reported that

the phosphorylation of ribosomal protein S15, a substrate of LRRK2, is crucial for the hyperactive translation in GS LRRK2 neurons (Martin, Kim, Lee, et al., 2014). Therefore, the role of S15 phosphorylation in 5'UTR-mediated translation was assessed. The increased reporter expression by GS LRRK2 was blocked by co-expression of T136A S15 (TA S15), a mutant that cannot be phosphorylated by LRRK2 (Fig. 3-4B) (Martin, Kim, Lee, et al., 2014). Furthermore, overexpression of phosphorylation-mimetic T136D S15 (TD S15) mimics the effects of GS LRRK2 in 5'UTR reporter assays (Fig. 3-4C). These results suggest that in GS LRRK2 expressing neurons, increased phosphorylation of S15 preferentially increases translation of the genes with complex 5'UTR secondary structure, thereby generating a structured 5'UTR bias in the translation profile. Transcriptional change is not attributable for the aforementioned expression changes (Fig. 3-5, A and B).

GS LRRK2 shows initiation factor-independent translation increase

To investigate potential crosstalk between GS LRRK2, phosphorylated S15 and eIFs, we employed bicistronic reporters with hepatitis C virus (HCV) or cricket paralysis virus (CrPV) internal ribosome entry site (IRES). In these assays, cap-dependent translation of firefly luciferase is dependent on helicase activity of eIFs, while IRES-driven cap-independent translation of *Renilla* luciferase is helicase independent. Surprisingly, both IRES reporters show the same cap-dependent and cap-independent translational induction by GS LRRK2 and TD S15 (Fig. 3-4, D to K). Since the CrPV IRES does not require any initiation factors to recruit ribosomes, the results indicate that the translational effects of GS LRRK2 are independent of translation initiation factors, and phosphorylation of S15 is sufficient to

enhance the translation of mRNAs with structured 5' UTRs. Transcriptional changes were not detected in the IRES reporter assays (Fig. 3-5, C to F).

Generation of GS LRRK2 dopamine neurons from patient-derived human induced pluripotent stem cells

Recent advances in the derivation of human induced pluripotent stem cells (hiPSCs) and differentiation into dopamine (DA) neurons allowed us to expand our findings to human DA neurons. Human iPSCs were derived from three GS LRRK2 PD patients and three healthy individuals. The six lines were differentiated into human DA neurons, and ribosome profiling was performed (Fig. 3-6, A to E). Similar to the findings from the LRRK2 mice, ribosome profiling in human DA neurons revealed an altered global TE distribution in GS LRRK2 neurons, and the TE up genes also tend to have more complex 5'UTR secondary structure (Fig. 3-7, A and B).

Ca²⁺ influx is increased in GS LRRK2 human dopamine neurons

To identify translationally dysregulated cellular pathways in GS LRRK2 human DA neurons, Ingenuity Pathway Analysis and Gene Ontology were performed with the TE values. Both analyses showed that the major cellular processes dysregulated in GS LRRK2 neurons are involved in neuronal physiology (Fig. 3-8A). Interestingly, the top pathways disturbed in human GS LRRK2 neurons converge on Ca²⁺ signaling (Fig. 3-7C and 3-8B). Furthermore, transcript levels of the activity-regulated genes are increased in the human GS LRRK2 neurons, suggesting that intracellular Ca²⁺ concentration is elevated (Fig. 3-7D) (Xiang et al., 2007). Fluorescent Ca²⁺ indicator Fluo-4 was used to compare intracellular Ca²⁺

concentrations in human DA neurons, and the results confirmed that GS LRRK2 neurons have significantly higher intracellular Ca^{2+} levels than wild-type neurons (Fig. 3-7E). In accordance with the effects of S15 phosphorylation in translation, overexpression of TA S15 rescues the elevated intracellular Ca^{2+} levels (Fig. 3-7E). Genes responsible for activity-dependent Ca^{2+} influx including L-type voltage-gated Ca^{2+} channel (L-VGCC) and *N*-methyl-D-aspartate (NMDA) receptors are among the major groups of induced genes, suggesting elevated neuronal Ca^{2+} influx in GS LRRK2 neurons. Whole cell Ca^{2+} current recordings were performed in human DA neurons, and the results demonstrate that GS LRRK2 neurons have increased Ca^{2+} current in both the peak and sustained current without affecting basal excitation characteristics (Fig. 3-7, F and G, and 3-8C). Overexpression of TA S15 reduces the increased Ca^{2+} current, indicating that the increased Ca^{2+} influx is S15 phosphorylation-dependent (Fig. 3-7, F and G, and 3-8C).

Increased L-type voltage-gated Ca^{2+} channel expression is accountable for the increased Ca^{2+} influx in GS LRRK2 human dopamine neurons

As L-VGCC activity serves as one of the major sources of Ca^{2+} influx in DA neurons, the L-VGCC antagonist isradipine was utilized to measure the contribution of L-VGCC to Ca^{2+} current in human DA neurons. Current-voltage relationships were examined by voltage ramp and peak Ca^{2+} current densities were calculated. The results show that GS LRRK2 neurons have significantly increased L-VGCC peak current density relative to wild-type neurons (Fig. 3-9, A and B). Furthermore, the ratiometric Ca^{2+} indicator Fura-2 was used to measure intracellular Ca^{2+} levels with isradipine treatment, and the results demonstrate that isradipine reduces the elevated intracellular Ca^{2+} level in GS LRRK2 human DA neurons (Fig. 3-9C

and 3-10A). There are two major isoforms of L-VGCC $\alpha 1$ pore-forming subunit expressed in the brain, $Ca_v1.2$ and $Ca_v1.3$ (Surmeier, Guzman, Sanchez, & Schumacker, 2012).

CACNA1C, a gene encoding the $Ca_v1.2$ subunit, has relatively long and complex 5'UTR sequences, while its paralog CACNA1D encoding the $Ca_v1.3$ subunit has a shorter and simpler 5'UTR sequence. To test the effects of the 5'UTR sequences on their expression, luciferase reporters with the 5'UTR sequences of both genes were generated and tested. The results confirmed that GS LRRK2 and TD S15 enhance the reporter expression of the 5'UTR sequences of CACNA1C, but not that of the 5'UTR sequences of CACNA1D (Fig. 3-9, D to F, and 3-10, B to F). Western blotting of L-VGCC confirmed the increased protein level of $Ca_v1.2$ in human DA neurons, which is reduced by TA S15 overexpression (Fig. 3-9, G and H, and 3-11A). Additionally, steady-state $Ca_v1.2$ protein levels in human GS LRRK2 postmortem PD brain samples are significantly increased over controls (Fig. 3-9, I and J).

Discussion

In this study, we show through ribosome profiling that mRNAs harboring complex 5' untranslated region (5'UTR) secondary structure are preferentially translated in the presence of G2019S LRRK2, thereby causing a broad alteration in the translome. Structured 5'UTR-mediated bias in translation were observed in G2019S LRRK2 transgenic mice, LRRK2 knockout mice, and in human dopamine neurons differentiated from G2019S LRRK2 PD patient-derived induced pluripotent stem cells. Structured 5' UTR bias is dependent on LRRK2 kinase activity and phosphorylation of S15. We found that LRRK2 enhances the translation of $Ca_v1.2$ L-type voltage-gated Ca^{2+} channel through its 5'UTR. The increased

expression of $Ca_v1.2$ channel elevates neuronal Ca^{2+} influx, thereby increasing intracellular Ca^{2+} concentration. Increased Ca^{2+} load in LRRK2 G2019S neurons is dependent on S15 phosphorylation, and is rescued by L-type Ca^{2+} channel antagonist isradipine treatment. This study provides cross-species, genome-scale translome profiles of G2019S LRRK2 neurons and reveals a previously undiscovered link between deregulated translation and increased Ca^{2+} influx, which may be crucial to understand progressive and selective dopamine neuronal death (Surmeier et al., 2012; Taymans et al., 2015).

5'UTR-mediated broad shift in translation profile in GS LRRK2 brain

A major finding of the study is that GS LRRK2 alters global translation by favoring mRNAs with complex 5'UTR secondary structure in a kinase-dependent and S15-dependent manner. The broad translome alteration correlating with 5'UTR secondary structure suggests the molecular mechanisms of translational regulation by LRRK2 and S15 phosphorylation. The 5'UTR is known to possess regulatory roles in translation, particularly complex secondary structure in the 5'UTR is thought to serve as a negative modulator of translation initiation by hindering ribosomal scanning (Hinnebusch, Ivanov, & Sonenberg, 2016). Thus, it is plausible to anticipate that the formation of hyperactive cap complex containing RNA helicases may preferentially regulate translation of the mRNAs with complex 5'UTR secondary structure. However, the IRES reporter assays indicate that phosphorylation of S15 enhances both cap-dependent and cap-independent translation, and initiation factors are dispensable for the effects. Our results suggest that the C-terminal phosphorylation of S15 may result in increased ribosomal processivity during initiation. Interestingly, there is no significant correlation between folding energy of the coding region sequences and the localized

translation efficiency when they were calculated on the exon structure in LRRK2 mouse models, suggesting that the exclusive roles of S15 phosphorylation during initiation (data not shown). Consistent with this idea, recent structural studies of mammalian 80S ribosome show the C-terminus of S15 projecting into the decoding sites of the ribosome (Anger et al., 2013). Future studies on the biophysical properties of phospho-S15 ribosome will be crucial to understand the precise molecular mechanisms of S15 phosphorylation in translation.

Increased Ca²⁺ influx and neuronal stress in dopamine neurons

Among various cellular pathways deregulated in GS LRRK2 neurons, increased translation was shown to play a role in GS LRRK2 neurotoxicity (Martin, Kim, Lee, et al., 2014). For example, by using transgenic *Drosophila* models, we previously reported that protein synthesis inhibitor anisomycin treatment is protective against GS LRRK2 DA neuron death (Martin, Kim, Lee, et al., 2014). However, the cellular mechanisms linking increased translation to DA neuronal stress were unknown. In this study, we demonstrate that structured 5'UTR bias in mRNA translation leads to an increase of Ca²⁺ influx, thereby increasing intracellular Ca²⁺ concentration in human GS LRRK2 DA neurons. Elevated intracellular Ca²⁺ concentration is known to increase mitochondrial respiration and oxidant stress in substantia nigra pars compacta DA neurons (Guzman et al., 2010). Consistent with this idea, transcript levels of ribosomal components and mitochondria respiratory chain complex genes are significantly increased in human GS LRRK2 neurons, reflecting elevated cellular metabolism (Fig. 3-11, B and C). Thus, elevated Ca²⁺ influx caused by GS LRRK2 may lead to higher mitochondrial oxidative stress, which is a common feature of PD (Scarffe, Stevens, Dawson, & Dawson, 2014).

Increased L-VGCC expression and its effects on substantia nigra dopamine neurons

It is noteworthy to mention that the differential L-VGCC activity profiles have been suggested to underlie the selectivity of neurodegeneration in PD. It has been shown that L-VGCC allows Ca^{2+} influx into the cytoplasm during autonomous pacemaking, generating oscillatory Ca^{2+} elevation in the dendrites of substantia nigra pars compacta DA neurons (Guzman et al., 2010; Philippart et al., 2016). This results in a sustained elevation in intracellular Ca^{2+} concentration, thereby causing higher basal levels of oxidative stress. In contrast, the Ca^{2+} oscillation is not present in the DA neurons in the ventral tegmental area, a region relatively spared in PD. This difference is attributable to lower basal expression of L-VGCCs and higher expression of the cytosolic Ca^{2+} binding protein calbindin (Khaliq & Bean, 2010; Surmeier et al., 2012). Thus, elevation of L-VGCC expression should be more detrimental to substantia nigra pars compacta DA neurons (Fig. 3-12A). Future experiments with segregation of distinct DA neuronal subtypes will enable us to test the selective vulnerability hypothesis.

Methods

Generation and maintenance of LRRK2 mouse models

Generation and characterization of the LRRK2 knockout mice were previously reported (Nikonova et al., 2012). For LRRK2 transgenic mice, we generated doxycycline-inducible (Tet-off), Tandem affinity purification (TAP)-tagged LRRK2 G2019S and G2019S/D1994A transgenic mice as previously described (Lee et al., 2013). The CaMKII-tTA driver line was

used to induce transgene expression (Mayford et al., 1996). Single transgenic mice were used for breeding, and the breeding cages were maintained with doxycycline chow (Diet-Sterile, 200 mg/kg doxycycline, Bio-Serv) and fed ad libitum. Doxycycline food was switched back to regular food after weaning for transgene induction. All animal protocols are in accordance with the regulations of the Johns Hopkins University Animal Care and Use Committee.

Ribosome profiling library generation

Ribosome footprinting and RNA-seq libraries were prepared by following a previously described protocol with several modifications made for mouse brain tissues (N. T. Ingolia, Brar, Rouskin, McGeachy, & Weissman, 2012). Mouse brain: brains of 3-4 months old mice were dissected in TBS buffer with 100 μ g/mL cycloheximide, and immediately frozen in dry ice. Caudate putamen tissues from three mice of mixed gender (1:2 or 2:1 male:female ratio) were pooled. The collected samples were homogenized in lysis buffer (10mM Tris pH 7.5, 150mM NaCl, 5mM MgCl₂, 0.5mM DTT, 100 μ g/mL cycloheximide, EDTA-free protease inhibitor (Roche), 40U/mL murine RNase Inhibitor (NEB)) with 12 strokes of high-speed motorized homogenizer at 40% power. The lysates were briefly centrifuged for 10 minutes at 2,000 \times g. The supernatant was transferred to a new tube, added NP-40 to 1% final concentration, incubated 5 minutes on ice. The samples were centrifuged again for 10 minutes at 20,000 \times g. Dopamine neurons: 100 μ g/mL cycloheximide were treated on the cultures for 15 minutes, then lysed on ice in lysis buffer (10mM Tris pH 7.5, 150mM NaCl, 5mM MgCl₂, 0.5mM DTT, 100 μ g/mL cycloheximide, EDTA-free protease inhibitor (Roche), 1% NP-40, 20U/mL SuperAse-In (ambion)).

The lysates were incubated in ice for 15 minutes, and centrifuged for 10 minutes at 20,000×g. Total RNA concentration of lysate was measured by Qubit RNA BR Assay (Life Technologies), and the same amount of RNA was used across samples. The supernatant was split into two tubes for ribosome footprinting and RNA-seq library generation.

Ribosome footprinting: The lysates were treated with 15µL of RNase I (Ambion) in 600µL total reaction volume for 45 min at room temperature, and the reaction was stopped by adding 30µL of SuperAse-In (Ambion). Sucrose cushion was performed with 1.7g sucrose in 3.9mL polysome buffer (10mM Tris pH 7.5, 150mM NaCl, 5mM MgCl₂, 0.5mM DTT, 100µg/mL cycloheximide, 20U/mL SuperAse-In), 4 hours at 70,000rpm. The pellet was resuspended with 700mL QIAzol (QIAGEN) reagent, incubated for 5 minutes at room temperature, 140µL chloroform was added, vortexed for 15 seconds, and incubated again for 2 minutes at room temperature. The sample was centrifuged for 15 minutes at 12,000×g, the 350µL supernatant was mixed with 525µL 100% EtOH. The mixture was loaded on an RNeasy Mini column (QIAGEN), and the RNA was extracted. 26~34nt ribosome footprints were size-selected by Urea-PAGE, gel extraction and RNA purification. Ribo-Zero Gold Kit (Illumina) was used for rRNA removal after the size selection. The rRNA depleted ribosome footprints were dephosphorylated by T4 polynucleotide kinase treatment, then Universal miRNA Cloning Linker (NEB) was added to the 3' ends. Reverse transcription reaction was performed with NI-NI-9 primers as previously described (N. T. Ingolia et al., 2012). The cDNA was circularized by CircLigase II (Epicentre) reaction, and subjected to the PCR for final library generation.

RNA-seq: Total RNA was purified by a combination of QIAzol and RNeasy Mini as described. Ribo-Zero Gold Kit was used for rRNA removal. RNA-seq library was generated from the total RNA by ScriptSeq v2 Library Preparation Kit (Epicentre).

Ribosome profiling data processing

Illumina HiSeq 2000 or 2500 were used for deep sequencing of the libraries. Sequencing results were processed by following a previously published pipeline (N. T. Ingolia et al., 2012). FASTX-Toolkit (http://hannonlab.cshl.edu/fastx_toolkit/) was used for the initial processing of the reads.

Ribosome footprinting libraries: Only adapter-containing reads were clipped. Reads shorter than 25nt were discarded. The first nucleotide of the reads was trimmed. rRNA-mapped reads were discarded before genomic alignment.

RNA-seq libraries: Only adapter-containing reads were clipped, rRNA-mapped reads were discarded.

The processed reads were mapped to the UCSC genome database (mouse: mm9, human: hg19) by Tophat (2.0.11) with Bowtie2 (2.2.2). Maximum 1 mismatch was allowed for the alignments.

Ribosome profiling data analysis

Aligned reads were counted by either a Python package HTSeq (htseq-count) or an R package GenomicAlignments (summarizeOverlaps) (Anders, Pyl, & Huber, 2015; Lawrence et al., 2013). Reads only in the CDS regions were counted. Transcripts with low read counts (<128 reads) were discarded. An R package DESeq (1.20) was used for calculating

normalized expression from either ribosome footprinting or RNA-seq data based on a negative binomial distribution and generalized linear model (Anders & Huber, 2010). For the mouse data, replicates were initially analyzed independently to confirm reproducibility, and then analyzed in combination for the final analysis. For the human neuron data, biological triplicates were handled by DESeq. Translation efficiency was calculated based on the DESeq expression output. 5'UTR estimated folding energy table was extracted from the UCSC genome database (mm9, hg19). For the 5'UTR estimated folding energy comparison, a control group with similar group size was randomly selected for each comparison to avoid potential bias from sample size differences. For the transcript coordinate calculation, the A site of each footprint was inferred by using a rounded value of the half point of the footprint length.

Mouse primary cortical neuron culture

Dissociated primary cortical neurons were prepared from E15 developing brain (CD1 strain). Developing cortices were dissected in the dissecting medium (Dulbecco's Modified Eagle Medium (DMEM) with 20% horse serum, 0.5mM GlutaMax, 6 μ M glucose, Gibco), digested with TrypLE (Gibco), and plated at a concentration of 3×10^6 cells for a plate. Culture plates were pre-coated with 15 μ g/mL poly-L-ornithine. Cultures were maintained under Neurobasal (Gibco) medium with a serum-free supplement B-27 (Gibco) and 0.5mM GlutaMax (Gibco).

5'UTR and IRES reporter assays

5'UTR stem-loop reporters: Additional 101 nucleotides were inserted into the 5'UTR region of the pGL4.53(luc2/PGK) vector (Promega). Estimated folding energy of the anticipated

5'UTR sequences were calculated by the Vienna RNA Package RNAfold (2.1.1) (Lorenz et al., 2011).

5'UTR CACNA1C/1D reporters: 5'UTR sequence of CACNA1C/1D genes were retrieved from UCSC genome database (hg19, CACNA1C: uc009zdu.1, CACNA1D: uc003dgu.5). and cloned into the 5'UTR region of the pGL4.53(luc2/PGK) (Promega) vector.

IRES reporters: pFR-HCV-xb, pFR-CrPV-xb vectors (from Phil Sharp Lab) were obtained from the Addgene depository (#11510, #11509, respectively). C-terminal myc-tagged

LRRK2 vectors and N-terminal V5-tagged S15 vectors were used as previously described

(Martin, Kim, Lee, et al., 2014). The vectors were transfected into mouse cortical neurons at DIV 5 by Lipofectamine 2000 (Invitrogen) reagent. Culture medium was replaced (half-change) every 24 hours to minimize any potential effects from the growth condition

including starvation. Luciferase activity was measured at DIV 7 by Luciferase Assay System (Promega) (for the 5'UTR reporters) or Dual-Glo Luciferase Assay System (Promega) (for the IRES reporters) with Glomax 20/20 Luminometer (Promega). The lysates were subjected to the total RNA purification with DNase treatment for the transcript level measurement. For the 5'UTR reporters, luciferase mRNAs were spiked-in for qPCR input normalization.

0kcal/mol:

```
AAGATCACAACCTATAACCTAAGCATCACCTCTACAACCTACGATCACCCTATAAA  
GATCACAACCTATAACCTAAGCATCACCTCTACAACCTACGATCACCCT
```

30kcal/mol:

```
AAGATCACAACCTATAACCTAAGCATCACCTCTACAACCTACGATCACCCTATAAG  
GTGGAATTTGTAACGTAGAGGCTTGTATTGAGTACTAGTACGATCTA
```


(100nM, Stemgent), SB431542 (10 μ M, R&D Systems), CHIR99021 (3 μ M, Stemgent), and pumorphine (2 μ M, Sigma) for the first five days. For the next six days, cells were maintained in Neurobasal medium (Gibco) containing B-27 supplement minus vitamin A (Gibco), N-2 supplement (Gibco) along with LDN193189 and CHIR99021. In the final stage, colonies were made into single cell suspension and seeded at density of 4 \times 10⁶ cells/cm² on poly-ornithine and laminin coated plate in neurobasal media containing B27 minus vitamin A, BDNF (20ng/mL, Peprotech), GDNF (20ng/mL, Peprotech), TGF β (1ng/mL, R&D Systems), ascorbic acid (0.2mM, Sigma), Dibutyryl-cAMP (0.5mM, Sigma) and DAPT (10 μ M, Stemgent) until maturation. DA neurons were cultured for > 60 differentiation days before measurements.

Ingenuity pathway analysis and gene ontology

Ingenuity Pathway Analysis (QIAGEN) was used for the pathway analysis in GS LRRK2 human dopamine neurons. TE fold change (1.2 in log₂ cutoff) was used, 255 genes were analyzed with a brain tissues expression profile preset. For gene ontology, a Cytoscape (3.2.1) plug-in ClueGo (2.1.7) was used (Bindea et al., 2009). Total 388 genes with increased TE in GS LRRK2 (1 in log₂ cutoff) were selected. ‘Biological Process’ and ‘Molecular Function’ pathways were selected for the analysis.

Immunoblotting

Brain tissues were lysed with an automated homogenizer in RIPA buffer with 1% SDS (20mM Tris-HCl (pH 7.5), 150mM NaCl, 1mM EDTA, 1% NP-40, 1% sodium deoxycholate, 1% SDS, protease inhibitors). Lysates were incubated on a rotator for 1 hour at

4°C, and spun down for 10 min × 12,000g at 4°C. Supernatant was collected, protein concentration was measured and the lysate was mixed with 2x Laemmli sample buffer. The following antibodies were used for western blots: α -LRRK2 (1:1000, Cell Signaling #13046), α -Ca_v1.2 (1:1000, clone 4D10, Sigma SAB1402709), α -Ca_v1.3 (1:1000, rabbit polyclonal antibody generated in Amy Lee's laboratory) (Nunez-Santana et al., 2014), α - β -actin (Cell Signaling, 13E5 clone, HRP conjugated). Generation and characterization of α -S15 and α -phospho-S15 (T136) antibodies were previously described (Martin, Kim, Lee, et al., 2014).

Immunocytochemistry of human iPSCs and DA neurons

Cells were fixed with 4% paraformaldehyde for 15 minutes at room temperature, then permeabilized with 0.03% Triton X-100 for 15 min. The cells were washed, and blocked for 1 hour with 10% goat serum in PBS. The blocked cells were subsequently incubated with primary antibody for overnight at 4°C. On the following day, the cells were incubated with secondary antibody for 1 hour at room temperature in a light controlled condition. After 3× wash with PBS buffer, the cells were mounted on cover slides with mounting media containing DAPI. All images were taken for analysis with Zeiss AxioObserver Z1 or LSM710 (Carl Zeiss) confocal laser scanning microscope under 20× or 40× oil objectives. For pluripotent stem cell markers, 2-3 random fields were captured for analysis. For DAPI, TH and TUJ1 counting, 6 random fields were captured and total 600-800 cells were counted in each condition for analysis. The following primary antibodies were used for immunocytochemistry: α -TUJ1 (1:2000, Covance MMS-435P), α -TH (1:1000, EMD Millipore AB152), α -OCT4, α -NANOG, α -SOX2, α -SSEA4 (1:200 for all, Cell Signaling, StemLight™ Pluripotency Antibody Kit #9656).

T136A S15 overexpression and isradipine treatment in human DA neurons

Human cDNA expressing T136A S15 allele was cloned into pAM/CBA-pI-WPRE-bGH vector, and AAV virus (AAV2 serotype) was generated (Vector Biolabs). 2 μ l of 2 \times 10⁶ GC/mL virus was used for one well of human DA neurons (approx. 4 \times 10⁶ cells, differentiation day > 60), and incubated for 5 days with minimum culture medium change (half-change, once every 3 days) before measurements. Cells were exposed to isradipine (1 μ M) for 2 hours in prior to measurements.

Intracellular Ca²⁺ imaging of human DA neurons

Membrane permeable acetoxymethylester (AM) form of Fluo-4 (Thermo Fisher Scientific) or Fura-2 (K_d 0.14M; Invitrogen) was used to monitor intracellular Ca²⁺ levels. Human DA neurons (at differentiation day 60-80) were loaded with Fluo-4-AM or Fura-2-AM for 30min at 2 μ M final concentration. Neurons were washed three times with HEPES-buffered ACSF (NaCl 125mM, KCl 5mM, HEPES 10mM, MgCl₂ 1mM, CaCl₂ 2mM, glucose 25mM, pH 7.4, osmolality 310 mosM), and incubated at RT in the dark for additional 20–25minutes to allow for complete dye de-esterification. Cells were placed in a 30-32°C heated adaptor and images was taken by inverted epifluorescence microscope (Nikon TE300) with a 40 \times /1.35NA oil-immersion objective. The imaging chamber was superfused with HEPES-buffered ACSF at a flow rate of 1mL/min. For Fluo-4-AM, live imaging was conducted with excitation wavelength of 485 nm and emission wavelength of 525nm. For Fura-2-AM, cells were illuminated at two excitation wavelengths (340 and 380nm) by Polychrome V (TILL Photonics) and emission was captured with a cooled CCD camera (Hamamatsu ImagEM)

connected to a computer running Slidebook imaging software (Intelligent Imaging Innovations). Ratiometric images (F340/F380) were taken every 120ms with exposure time of 20ms. Regions of interests (ROIs) in the soma were selected for further analysis. ROI F340/F380 ratios were converted to Ca^{2+} concentrations, using a standard curve generated under the exact acquisition conditions (Calcium Calibration Buffer Kits, Invitrogen).

Whole-cell patch clamp Ca^{2+} current recordings of human DA neurons

Spontaneous and evoked action potentials (APs): HEKA EPC10 amplifier (HEKA Elektronik) was used. Human DA neurons were visualized under a 40 \times water immersion objective by fluorescence and DIC optics (Carl Zeiss), and the chamber was constantly perfused at a rate of 1-2mL/min at 32 $^{\circ}$ C with bath solution (NaCl 137mM, KCl 5mM, CaCl_2 2mM, MgCl_2 1mM, HEPES 10mM, glucose 10mM). pH of bath solution was adjusted to 7.4 with NaOH, and osmolarity was at 300–310mosM. Patch pipettes (2–5 $\text{M}\Omega$) were pulled from borosilicate glass (BF-150, Sutter Instruments) using a Flaming-Brown micropipette puller (P-1000, Sutter Instruments) and filled with pipette solution (K-gluconate 126mM, KCl 8mM, HEPES 20mM, EGTA 0.2mM, NaCl 2mM, MgATP 3mM, Na_3GTP 0.5mM, adjusted to pH 7.3 with KOH, adjusted to 290-300mosM with sucrose). Resting membrane potential was recorded in current clamp mode at 0pA immediately after establishing a whole-cell configuration. Series resistance (R_{series}) and input resistance (R_{in}) were calculated from a 5mV pulse and monitored throughout the experiment. Unstable recordings (>10% fluctuation of R_{series} value) during the course of experiments were rejected from further analysis. Series of hyperpolarizing and depolarizing step currents were injected to measure

intrinsic properties and to elicit APs. Presence of a sag in the membrane potential and the AP firing pattern were checked in current-clamp immediately after rupturing the membrane.

Voltage clamp: External solution (TEA-MeSO₃ 140mM, HEPES 10mM, BaCl₂ or CaCl₂ 10mM, pH was adjusted to 7.4 with CsOH, osmolarity was adjusted to 300-310mosM with glucose) and internal solution (pipet solution) (CsMeSO₃ 135mM, CsCl 5mM, MgCl₂ 1mM, MgATP 4mM, HEPES 5mM, EGTA 5mM, pH was adjusted to 7.3 with CsOH, and osmolarity was adjusted to 290-300mosM with glucose) were used. Currents were recorded by holding the cell at -90mV, before stepping to various potentials from -60mV to +50mV for 250ms in 10mV increments. Tetrodotoxin (1μM) was used to ensure blockade of voltage-gated sodium currents. Data were acquired by PatchMaster software (HEKA Elektronik), sampled at 10kHz, and filtered at 2.9kHz. Ca²⁺ currents were analyzed using Clampfit 10.5 software (Molecular devices).

Ramp voltage clamp: Cultures were transferred to a recording chamber on a fixed-stage inverted microscope (Diaphot 200; Nikon). The recording chamber was perfused (2 ml/min, 25°C) with HEPES-based solution: 130mM NaCl, 1mM MgCl₂, 10mM BaCl₂, 10mM HEPES, 10mM dextrose, 10mM sucrose and 15mM CsCl at pH 7.4 and osmolarity of ~320mosM. Internal pipette solutions contained the following: 180mM *N*-methyl-D-glucamine, 40mM HEPES, 4mM MgCl₂, 12mM phosphocreatine, 0.1mM leupeptin, 2mM Na₂ATP, 0.5mM Na₃GTP, 5mM BAPTA, pH 7.2–7.3 and osmolarity of ~290 mosM.

Somatic whole-cell patch-clamp recordings were obtained with a Multi-Clamp 700A amplifier (Molecular Devices) connected to an Intel-based PC running pClamp10 (Molecular Devices). The signals were filtered at 1kHz and digitized at 10kHz with Digidata 1440A (Molecular Devices). Recording voltage was either fixed to +10mV, or current–voltage

relationships were calculated with current responses to voltage ramps (0.7mV/ms) from -60 to 80 mV. Cell capacitance (measured using PClamp 10 automatic compensation) was used to calculate peak Ca^{2+} current densities (pA/pF). At the end of each experiment, Ca^{2+} current–voltage relationships were corrected for leaks currents measured in the presence of Cd^{2+} (200 μM), a non-selective Ca^{2+} channels antagonist. L-VGCC currents were estimated by subtracting Ca^{2+} currents in the presence of isradipine (1 μM) from total Ca^{2+} currents. Peak Ca^{2+} current densities were measured from current–voltage relationships using Clampfit 10 (Axon Instruments) and IgorPro 6 software.

Acknowledgements

This work was supported by grants from the NIH P50 NS38377 and the JPB Foundation. I.M. is supported by NIH/NIA grant K01-01AG050718. Y.X. is supported by NIH/NIA grant K01-AG046366 and The William N. & Bernice E. Bumpus Foundation Innovation Awards. T.M.D. is the Leonard and Madlyn Abramson Professor in Neurodegenerative Diseases. The authors acknowledge the joint participation by the Adrienne Helis Malvin Medical Research Foundation through its direct engagement in the continuous active conduct of medical research in conjunction with The Johns Hopkins Hospital and the Johns Hopkins University School of Medicine and the Foundation's Parkinson's Disease Program M-2014. The $\text{Ca}_v1.2$ antibody is a generous gift from J.W. Hell, and the IRES reporters are gifts from P.A. Sharp's laboratory (Addgene #11509, #11510). We thank R. Green and M.K. Meffert for discussion; H. Kim and the Stem Cell Core for iPSC generation; J.H. Shin and the Lieber Institute for Brain Development for supporting deep sequencing of human DA neuron

samples. I-H. Wu created Fig. 3-1A and 3-12A.

This chapter was modified from:

- 1) A manuscript originally submitted to *Science*: Kim JW, Yin X, Martin I, Xie Z, Perez-Rosello T, Jhaldiyal A, Xiong Y, Abalde-Atristain L, Kumar M, Eacker SM, Karuppagounder S, Lee A, Surmeier DJ, Ingolia NT, Dawson TM, Dawson VL. Pathogenic LRRK2 mutation alters neuronal translome resulting in dysregulated calcium homeostasis.
- 2) Kim JW, Abalde-Atristain L, Jia H, Dawson VL, Dawson TM. Protein translation in Parkinson's disease. In: Verstreken P, Ed., *Parkinson's Disease: Molecular Mechanisms Underlying Pathology*. San Diego: Academic Press, 2017:281-309.

Figure 3-1. Broad alteration in mRNA translation through structured 5'UTR in GS LRRK2 mouse brain.

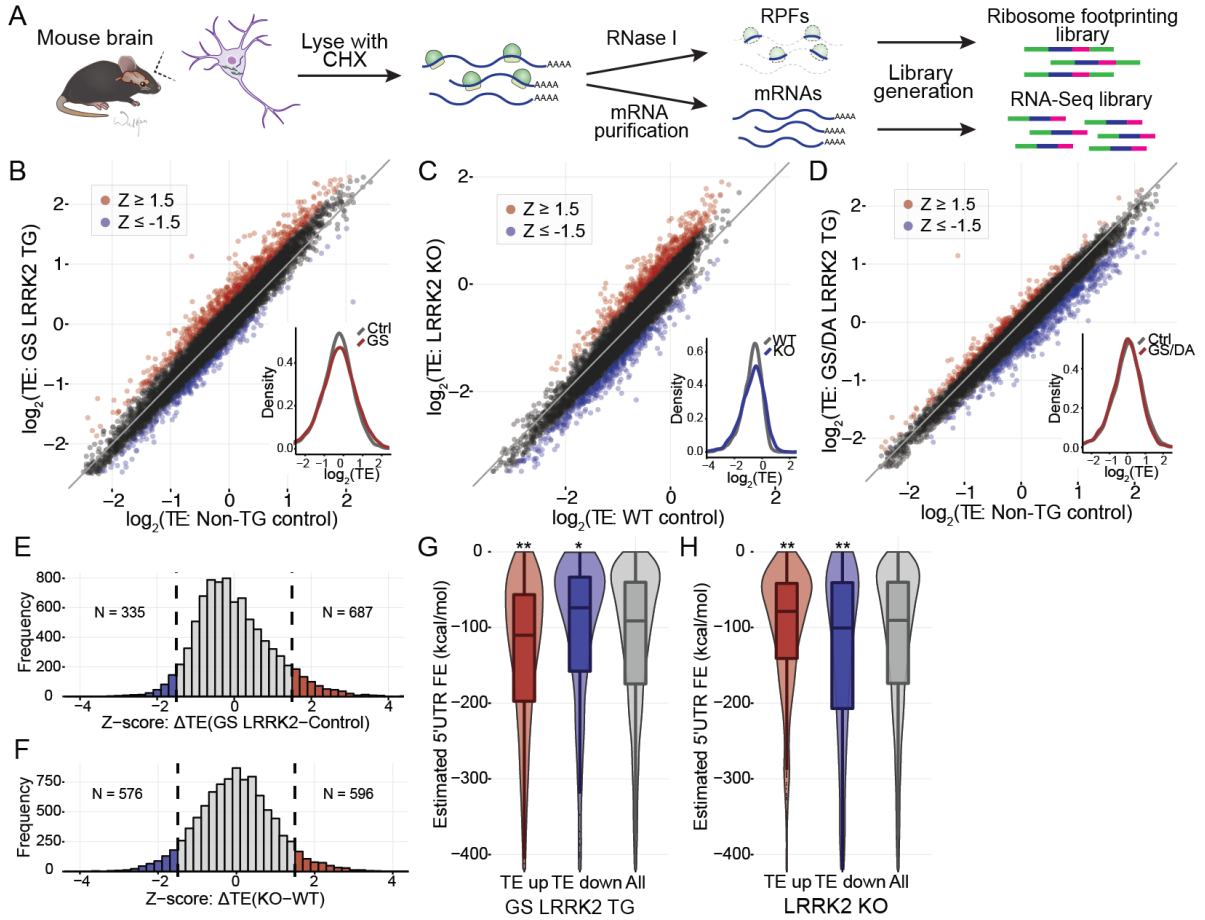


Figure 3-1. Broad alteration in mRNA translation through structured 5'UTR in GS LRRK2 mouse brain.

Ribosome profiling was performed with GS, GS/DA LRRK2 TG and LRRK2 knockout (KO) mouse brains. (A) A schematic of ribosome profiling workflow with mouse brain tissue. Caudate putamen tissues of ~3 months old mice were dissected, 3 mice were pooled and processed. (B to D), TE was calculated to estimate translational activity of genes. TE was derived by normalizing RPF read abundance by RNA-seq read abundance. Global TE distribution between (B) GS LRRK2 TG and non-TG control, (C) LRRK2 KO and WT, or (D) GS/DA LRRK2 TG and non-TG control was compared by scatterplots and density plots. All values are in \log_2 , and each data point represents a single transcript. In scatterplots, centerline is a guideline with slope of 1, meaning that the dots on the line do not have TE value differences between the genotypes. GS LRRK2 TG and KO show distortion in global translation efficiency distribution compared to the control, while GS/DA LRRK2 TG shows much similar TE distribution to the control mice (standard deviation of TE differences: 0.226 (GS LRRK2 vs control), 0.273 (LRRK2 KO vs WT), 0.179 (GS/DA LRRK2 vs control). Standard z-score was calculated, and ± 1.5 cut-off was used to select TE up and TE down genes. TE up genes: red, TE down genes: blue. (E and F) Histogram of TE differences (delta TE, Δ TE) between (E) GS LRRK2 TG and non-TG control, or (F) LRRK2 KO and WT. Z-score ± 1.5 cut-off was used for selecting TE up and TE down genes from each comparison, and TE values are in \log_2 . (G and H), Correlation between estimated 5'UTR folding energy and translation efficiency changes in (G) GS LRRK2 TG, or (H) LRRK2 KO. In GS LRRK2 TG brain, TE up genes tend to have complex 5'UTR secondary structure, while TE down genes tend to have simple 5'UTR secondary structure than the average. LRRK2 KO brain

samples show an opposite trend. The results suggest that increased LRRK2 kinase activity shifts translational preference, favoring mRNAs with complex 5'UTR secondary structure. 5'UTR folding energy for transcripts was retrieved from UCSC genome database (mm9). When there are multiple transcript isoforms with different 5'UTR sequences, transcript with the lowest 5'UTR folding energy was selected. The same z-score ± 1.5 cut-off was used. Group sizes: GS TG (TE up: 687, TE down: 335), KO (TE up: 596, TE down: 576). Each ribosome profiling experiment was firstly analyzed independently to ensure reproducibility. Two independent results were analyzed by DESeq. (n=2). Box plot overlaid with violin plot visualizes the median, the first and the third quartile along with the data distribution pattern. Statistical significance was determined by one-way ANOVA with Bonferroni correction. * p<0.05, ** p<0.01.

Figure 3-2. LRRK2 protein expression levels in LRRK2 mouse models.

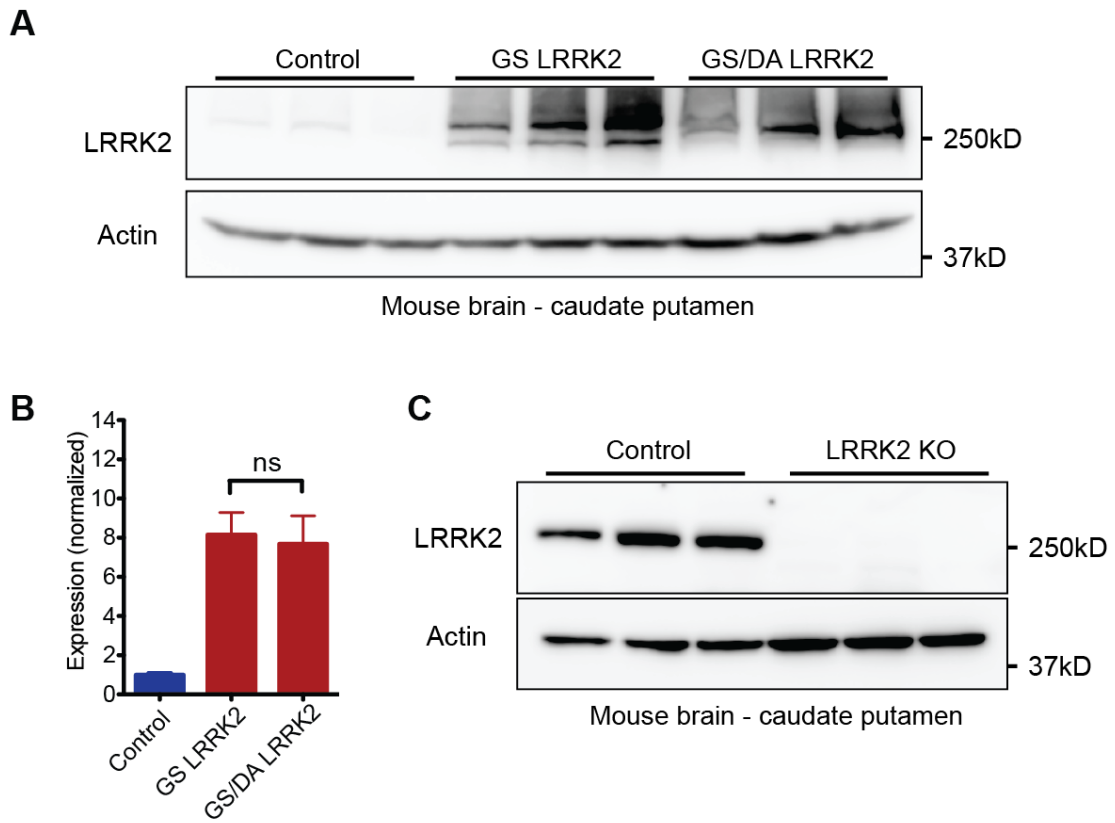


Figure 3-2. LRRK2 protein expression levels in LRRK2 mouse models.

(A) LRRK2 protein levels in the caudate putamen of LRRK2 mouse models at the timepoint used for ribosome profiling experiments were measured. LRRK2 protein levels in GS, GS/DA transgenic mice and non-transgenic control mice. Average LRRK2 expression levels (normalized): 8.15 (GS), 7.68 (GS/DA). (B) Quantification of LRRK2 expression levels. (C) LRRK2 knockout mice with wild-type control mice. Mice were sacrificed at 3 months old, and biological triplicates were used. Statistical significance was determined by Kruskal-Wallis nonparametric test with Dunn's post-test, ns=no significance.

Figure 3-3. Translation regulatory mechanisms unchanged in LRRK2 mouse models.

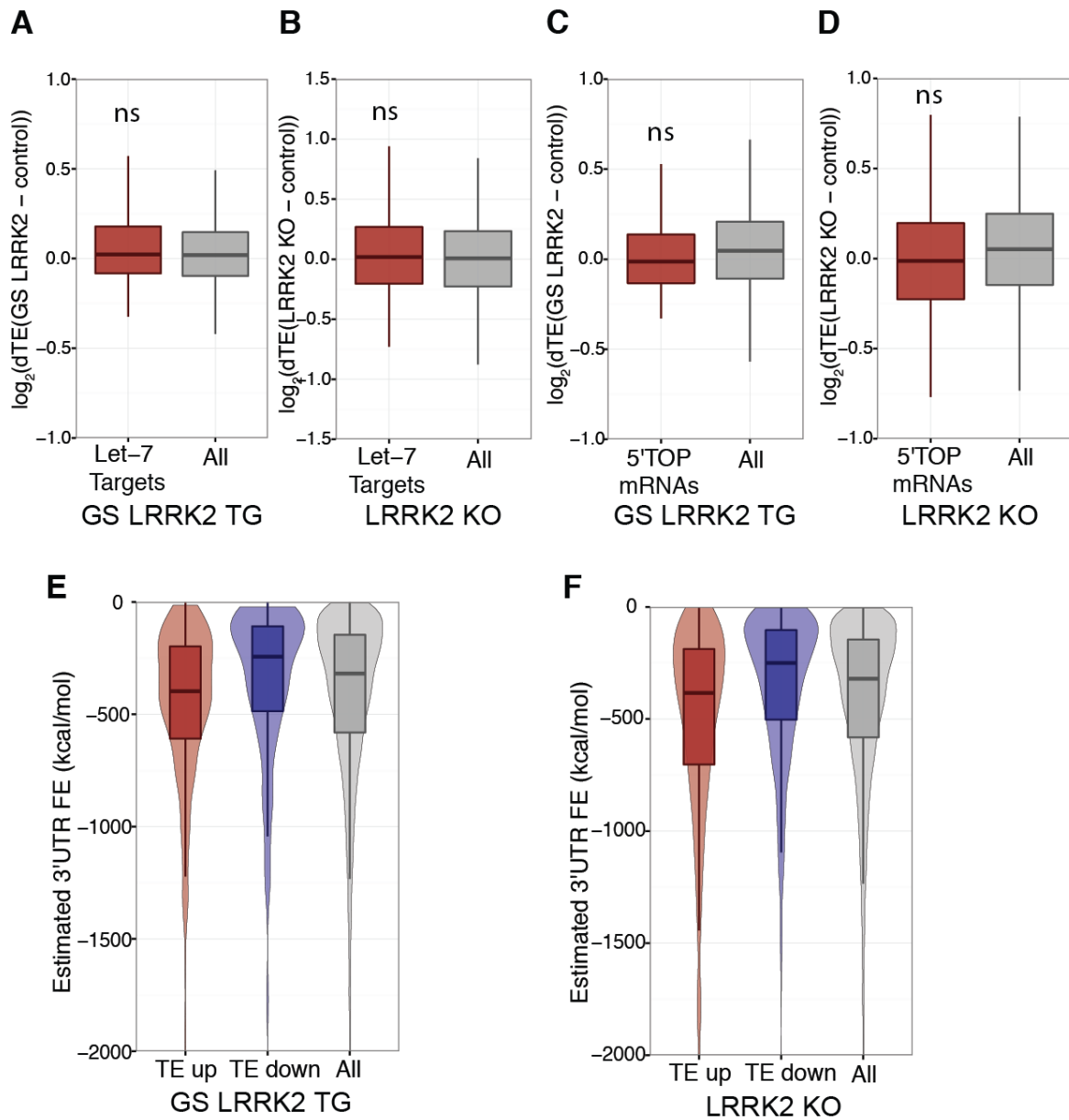


Figure 3-3. Translation regulatory mechanisms unchanged in LRRK2 mouse models.

(A and B) TE differences of let-7 family miRNA targets in LRRK2 mouse models. Let-7 family miRNA targets were previously reported as LRRK2 translation targets in *Drosophila* models (S. Gehrke et al., 2010). Mouse let-7 targets were downloaded from the miRWalk 2.0 database (date: 6/7/2016), and compared between different LRRK2 models. The result indicates that the let-7 target mRNAs are not differentially regulated in any LRRK2 mouse models (Wilcoxon signed-rank test). (C and D) TE differences of 5'TOP mRNAs in LRRK2 mouse models. 5'TOP mRNAs are translationally regulated by mTOR signaling pathway through phosphorylation of 4E-BP (Thoreen et al., 2012). Genetic interaction between LRRK2 and mTOR was previously reported, and 4E-BP was suggested as a LRRK2 phosphorylation substrate (Imai et al., 2008). Our data do not show any differential regulation of 5'TOP mRNAs in LRRK2 mouse models (Wilcoxon signed-rank test). (E and F) 3'UTR secondary structure folding energy differences between TE up and TE down genes (z-score ± 1.5 was used). Unlike the 5'UTR folding energy comparison, 3'UTR folding energy does not show opposite distribution in LRRK2 TG and LRRK2 KO mice.

Figure 3-4. Phosphorylation of S15 mediates structured 5'UTR bias in GS LRRK2 neurons.

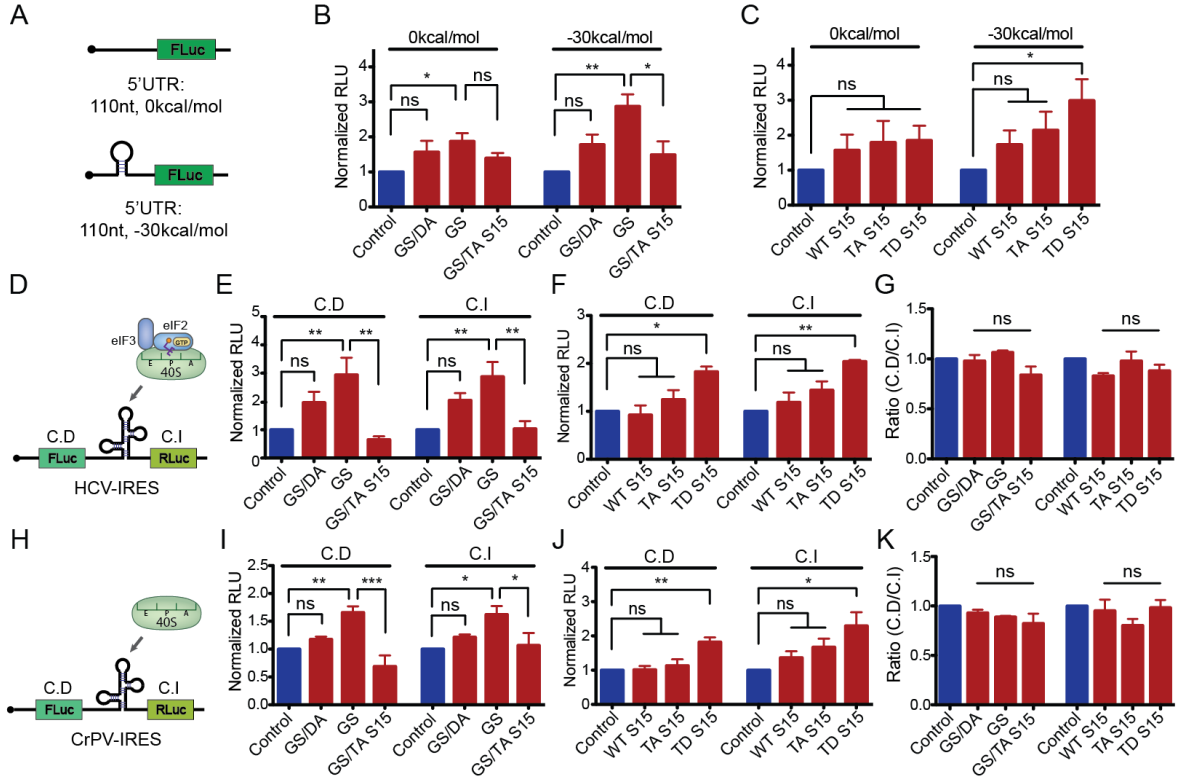


Figure 3-4. Phosphorylation of S15 mediates structured 5'UTR bias in GS LRRK2 neurons.

(A) A schematic of 5'UTR stem-loop reporter. 5'UTR sequences with no predicted secondary structure (0kcal/mol) or a hairpin structure (-30kcal/mol) were inserted into a firefly luciferase expression vector. Both reporters have the same length of inserted sequences (110nt). RNAfold from ViennaRNA was used for folding energy calculation (Lorenz et al., 2011). (B and C) 5'UTR luciferase reporter assays. -30kcal/mol reporter shows about two-fold higher increase than 0kcal/mol reporter in GS LRRK2. Co-expression of TA S15 is able to suppress the effects of GS LRRK2, and the effects of GS/DA LRRK2 are not statistically significant in both reporters. Similar to GS LRRK2, TD S15 shows significantly increased expression only in -30kcal/mol reporter. Reporter transcript levels do not show significant changes in all conditions. n=5, n=4, respectively. (D) A schematic of HCV (hepatitis C virus) IRES (internal ribosome entry site) reporter. HCV IRES does not require additional initiation factors other than eIF3 and ternary complex to initiate translation. (E to G) HCV IRES reporter assays. GS LRRK2 and TD S15 show S15 phosphorylation-dependent translation increase in both cap-dependent (C.D) and cap-independent (C.I) reporter expression, leaving the C.D/C.I ratios unchanged. It demonstrates that RNA helicase activity is not required for the 5'UTR-mediated shift in translation. n=4 (LRRK2) and n=3 (S15), respectively. (H) A schematic of CrPV (cricket paralysis virus) IRES reporter. CrPV IRES is known to directly recruit 40S subunit to the IRES and also mimic Met-tRNAⁱ, thereby initiating translation without any initiation factors. (I to K) CrPV IRES reporter assays. Similar to the HCV IRES results, S15 phosphorylation-dependent translational increase is observed in GS LRRK2 neurons in both cap-dependent and cap-

independent reporter expression. n=4 and n=3, respectively. All reporter assays were performed in primary mouse cortical neurons with transient transfection, and each experiment is an average of triplicates. WT: wild-type. Fluc: firefly luciferase, RLuc: *Renilla* luciferase. RLU: relative light units. Statistical significance was determined by one-way ANOVA with Bonferroni correction. Error bars indicate s.e.m. * p<0.05, ** p<0.01, *** p<0.001, ns=no significance.

Figure 3-5. Reporter transcript levels measurement for stem-loop and IRES reporter assays.

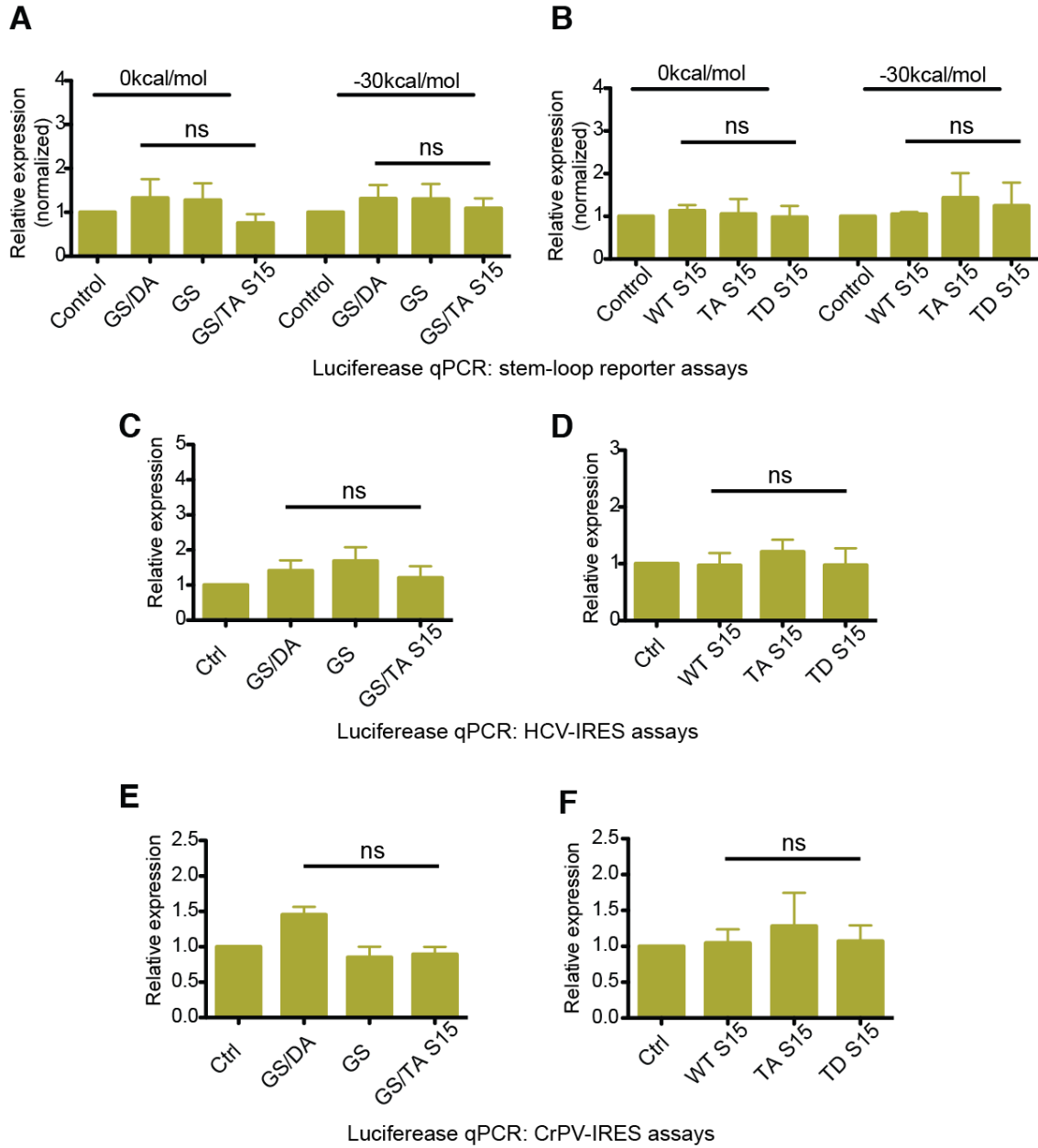


Figure 3-5. Reporter transcript levels measurement for stem-loop and IRES reporter assays.

(A and B) Luciferase transcript levels were measured by qPCR for the stem-loop reporter luciferase assays. Control mRNA was spiked-in to the lysate and used to normalize the input. Transcript levels of the reporter are not affected by LRRK2 or S15 expression. One-way ANOVA was used to determine statistical significance. (C to F) qPCR measurement of luciferase transcript levels in the IRES reporter assays. One-way ANOVA with Bonferroni correction was used, and there were no significant changes in the reporter transcript levels detected. ns=no significance.

Figure 3-6. DA differentiation and ribosome profiling of LRRK2 hiPSC lines.

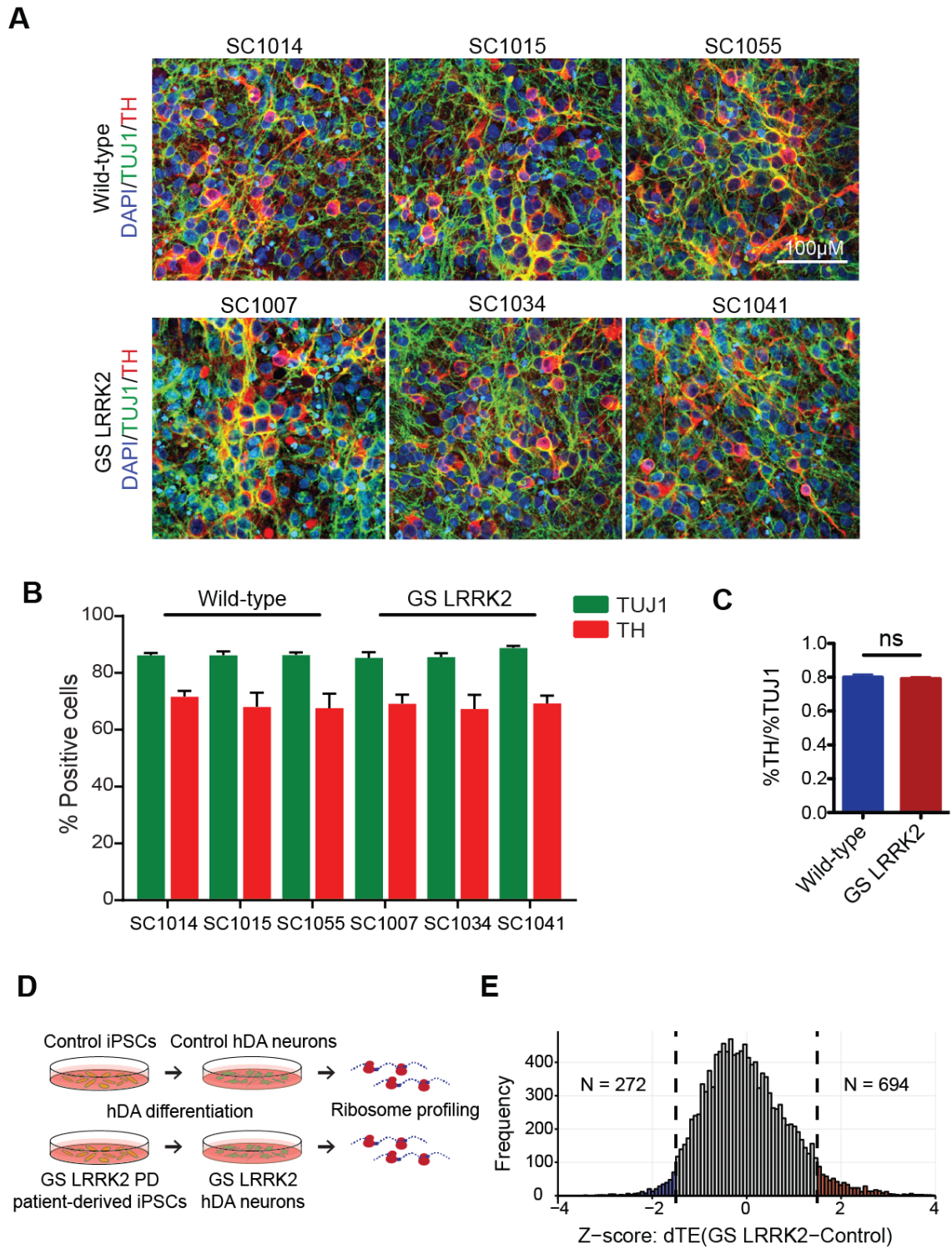


Figure 3-6. DA differentiation and ribosome profiling of LRRK2 hiPSC lines.

(A) TH/TUJ1 immunocytochemistry was performed to assess the efficiency of DA neuronal differentiation from the hiPSC lines. (B) Quantification of TH and TUJ1 positive cells over all DAPI-stained cells on the human DA neuron cultures. (C) A ratio of TH positive neurons over TUJ1 positive neurons. TH differentiation efficiency was calculated by the proportion of TH positive neurons over all TUJ1 positive neurons. No significant difference was found in the TH differentiation efficiency between the cell lines. Unpaired t-test was used to examine statistical significance. ns=no significance. (D) A schematic of ribosome profiling experiments with human DA neurons differentiated from hiPSCs. DA neurons were differentiated for 60 days for the ribosome profiling experiments. (E) Δ TE (GS LRRK2 – WT) distribution histogram demonstrates the genes selected for TE up (red) and down (blue) analysis. Z-score ± 1.5 cut-off was used.

Figure 3-7. GS LRRK2 human DA neurons have increased cytosolic Ca^{2+} concentration.

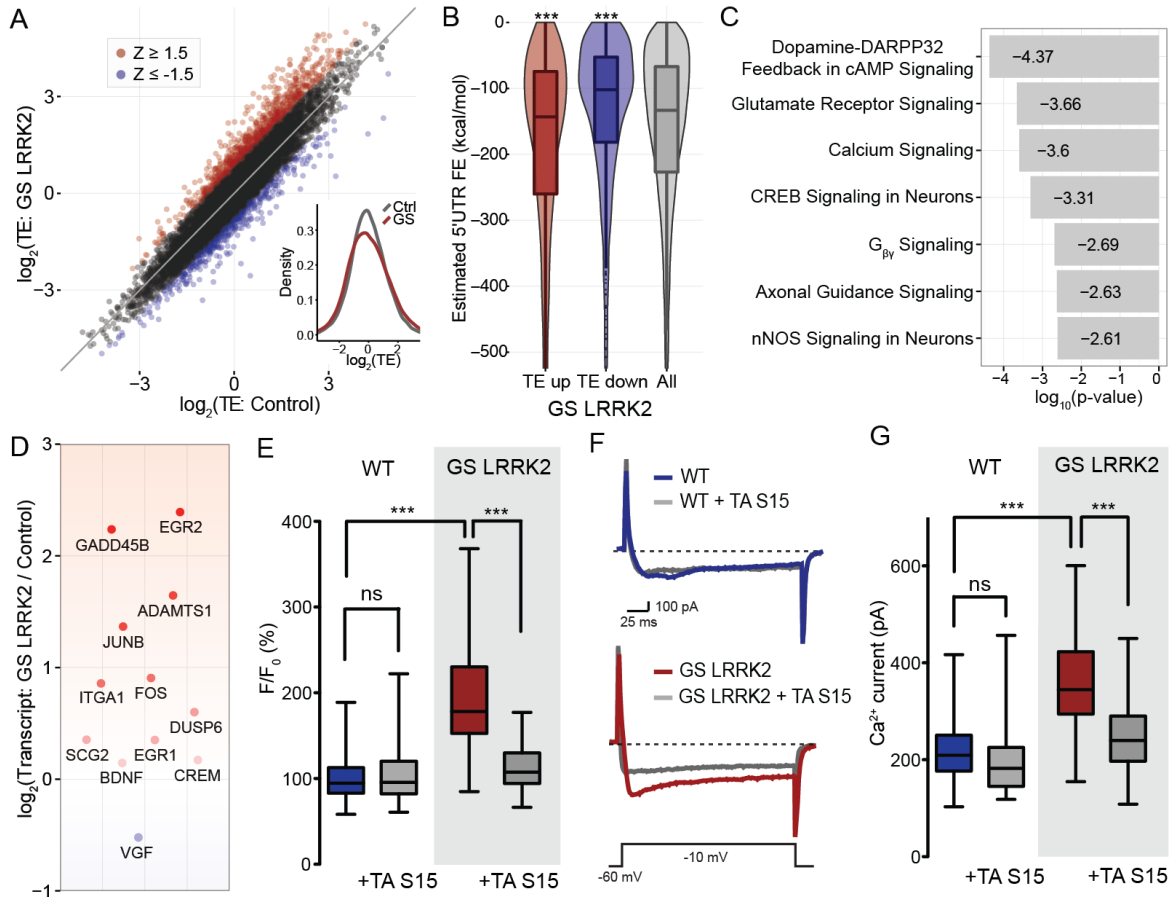
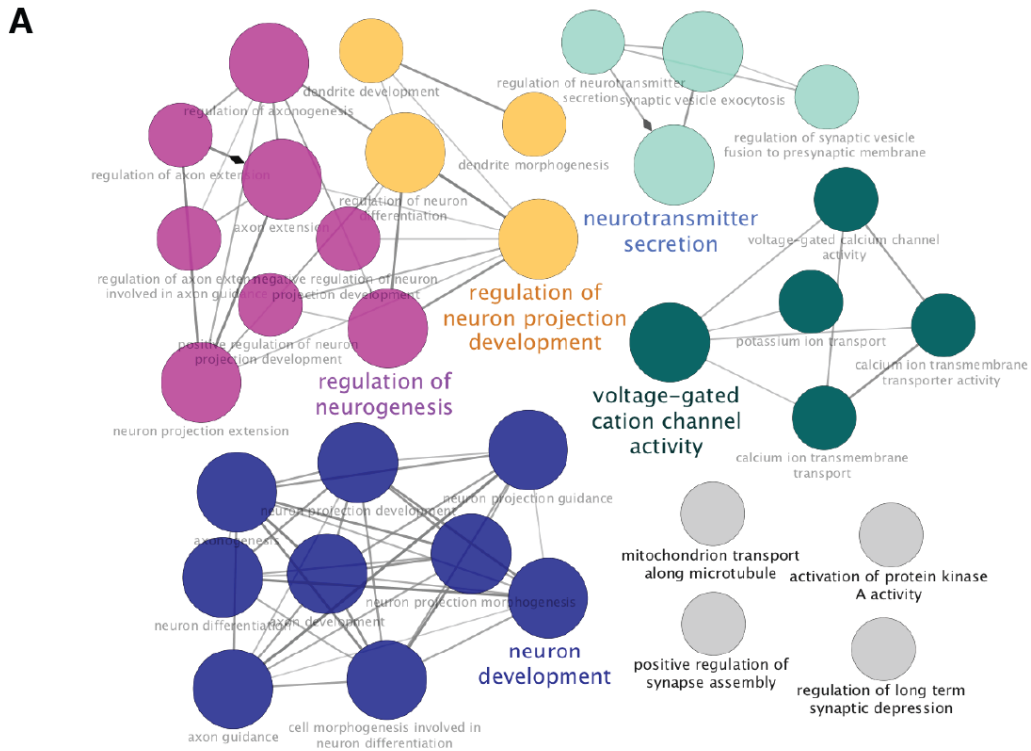


Figure 3-7. GS LRRK2 human DA neurons have increased cytosolic Ca²⁺ concentration.

Ribosome profiling was performed with human DA neurons differentiated from hiPSCs. Control hiPSC lines were derived from three healthy individuals, and GS LRRK2 hiPSC lines were derived from three PD patients bearing the GS LRRK2 mutation. The six lines were differentiated into DA neurons and cultured 60 days for maturation. **(A)** TE distribution comparison of GS LRRK2 and wild-type human DA neurons. The result shows broadly altered TE distribution in GS LRRK2 neurons, which is consistent with the mouse ribosome profiling data. Ribosome profiling data from the three independent cell lines per genotype were jointly analyzed by DESeq (Anders & Huber, 2010). Z-score ± 1.5 cut-off was used to select TE up (red) and down (blue) genes. **(B)** Estimated 5'UTR folding energy of TE up and down genes. Similar to the TG mouse brain result, the TE up genes in GS LRRK2 human DA neurons tend to have complex 5'UTR secondary structure, while TE down genes tend to have simpler 5'UTR secondary structure. UCSC genome (hg19) dataset was used for 5'UTR folding energy estimation. Group sizes: 934 genes for TE up, 541 genes for TE down. Statistical significance was determined by one-way ANOVA with Bonferroni correction. **(C)** Ingenuity Pathway Analysis was performed with the TE values of human DA neurons. The top pathways are associated with neuronal Ca²⁺ influx, suggesting that Ca²⁺ influx may be increased in GS LRRK2 human DA neurons. Cutoff: 1.2 fold change (log₂), 257 genes. **(D)** Induction of activity-regulated gene in GS LRRK2 human DA neurons. As neuronal Ca²⁺ influx serves as an upstream regulator of activity-regulated gene expression, elevated activity-regulated gene expression also suggests increased Ca²⁺ influx in GS LRRK2 neurons. Activity-regulated gene list was extracted from a previous study (Xiang et al., 2007). **(E)**

Intracellular Ca^{2+} level was measured by Fluo-4 Ca^{2+} indicator. TA S15 transgene under a CAG promoter was delivered by adeno-associated virus serotype 2 (AAV2) to human DA neurons. Control (without TA S15) neurons were transduced with the same dose of AAV2 virus expressing GFP or mCherry transgene. Ca^{2+} concentration was measured at 5 days post infection. Three different lines were independently analyzed and pooled for statistical analysis. Statistical significance was tested by one-way ANOVA with Bonferroni correction. n=165 (WT), n=175 (WT+TA S15), n=154 (GS LRRK2), n=138 (GS LRRK2+TA S15). **(F)** Whole-cell patch clamp recording was performed to measure Ca^{2+} currents in human DA neurons. Similar to the intracellular Ca^{2+} concentration results, the recordings show that Ca^{2+} current is significantly increased in GS LRRK2 human DA neurons, and it is reduced by TA S15 overexpression. The same AAV2 virus was used to express TA S15, and the neurons were voltage clamped for Ca^{2+} current measurement after 5 days of transduction. **(G)** Quantification of Ca^{2+} peak currents. Three different lines per genotype were pooled for analysis. Average Ca^{2+} peak current values are 218.11pA (WT), 199.77pA (WT+TA S15), 358.68pA (GS LRRK2), 242.75pA (GS LRRK2+TA S15). Statistical significance was derived by one-way ANOVA with Bonferroni correction. n=30 for all conditions. * p<0.05, ** p<0.01, *** p<0.001, ns=no significance.

Figure 3-8. Pathway analyses of human DA neuron ribosome profiling.



B

GO Term	Corrected Term P Value
voltage-gated cation channel activity	1.79684E-05
voltage-gated calcium channel activity	4.97914E-03
calcium ion transmembrane transporter activity	2.73658E-03

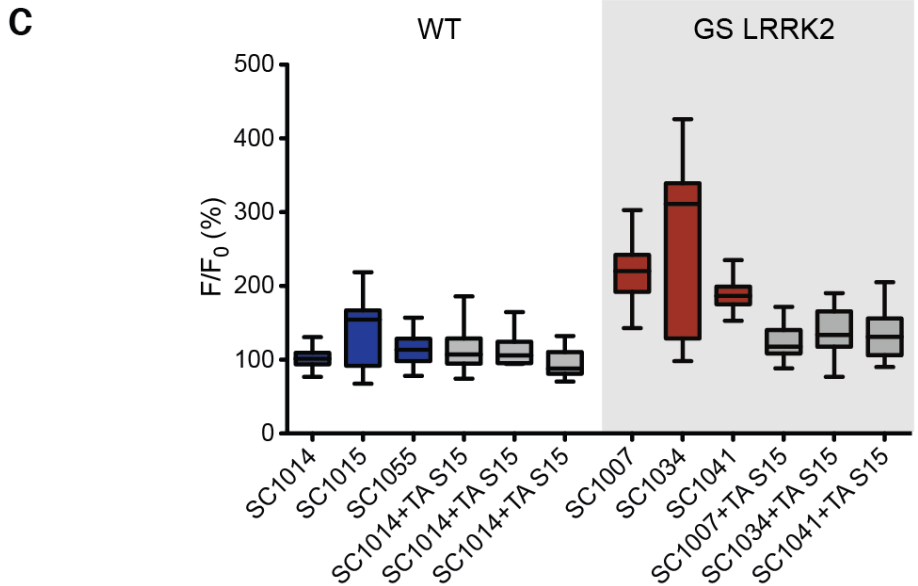


Figure 3-8. Pathway analyses of human DA neuron ribosome profiling.

(A) Gene ontology analysis by ClueGO software from the TE up genes in GS LRRK2 human DA neurons (fold change > 1 in log₂) (Bindea et al., 2009). Five major groups (neurotransmitter transmission, regulation of neuron projection development, regulation of neurogenesis, neuron development, voltage-gated cation channel activity) were suggested to be the most affected pathways by the analysis. All the groups are relevant to neuronal physiology. (B) A table of suggested gene ontology terms relevant to Ca²⁺ influx. Consistent with the ingenuity pathway analysis result, voltage-gated Ca²⁺ channel activity was shown to be affected by GS LRRK2 by gene ontology analysis as well. (C) Fluo-4 intracellular Ca²⁺ imaging results with TA S15 overexpression are plotted by each individual line. The results show that the increased Ca²⁺ levels are consistent with their genotypes. Group sizes: n=51 (SC1014), n=44 (SC1015), n=51 (SC1055), n=51 (SC1014+TA S15), n=51 (SC1015+TA S15), n=40 (SC1055+TA S15), n=51 (SC1007), n=51 (SC1034), n=52 (SC1041), n=50 (SC1007+TA S15), n=45 (SC1034+TA S15), n=43 (SC1041+TA S15).

Figure 3-9. $Ca_v1.2$ expression is increased in GS LRRK2 human DA neurons.

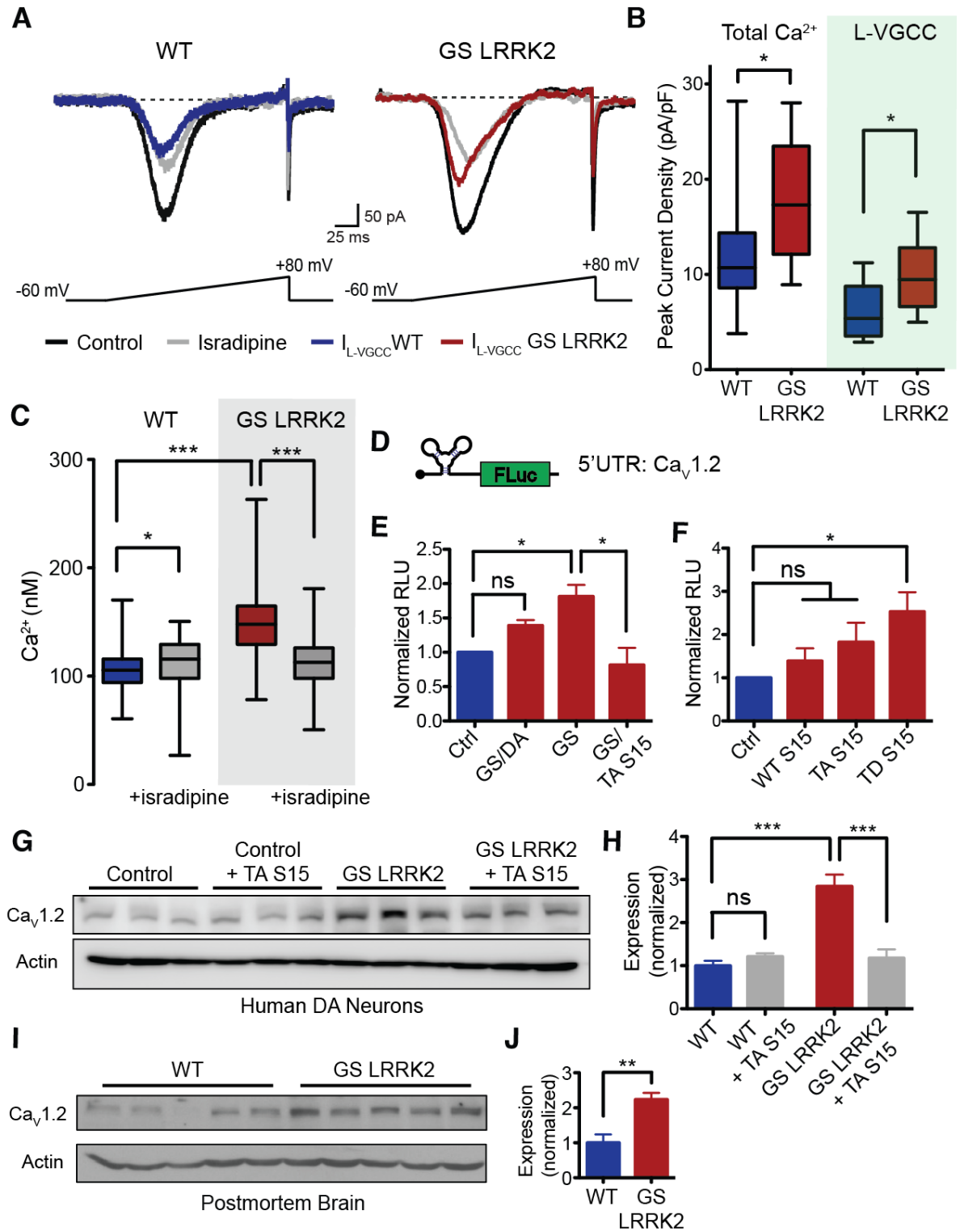
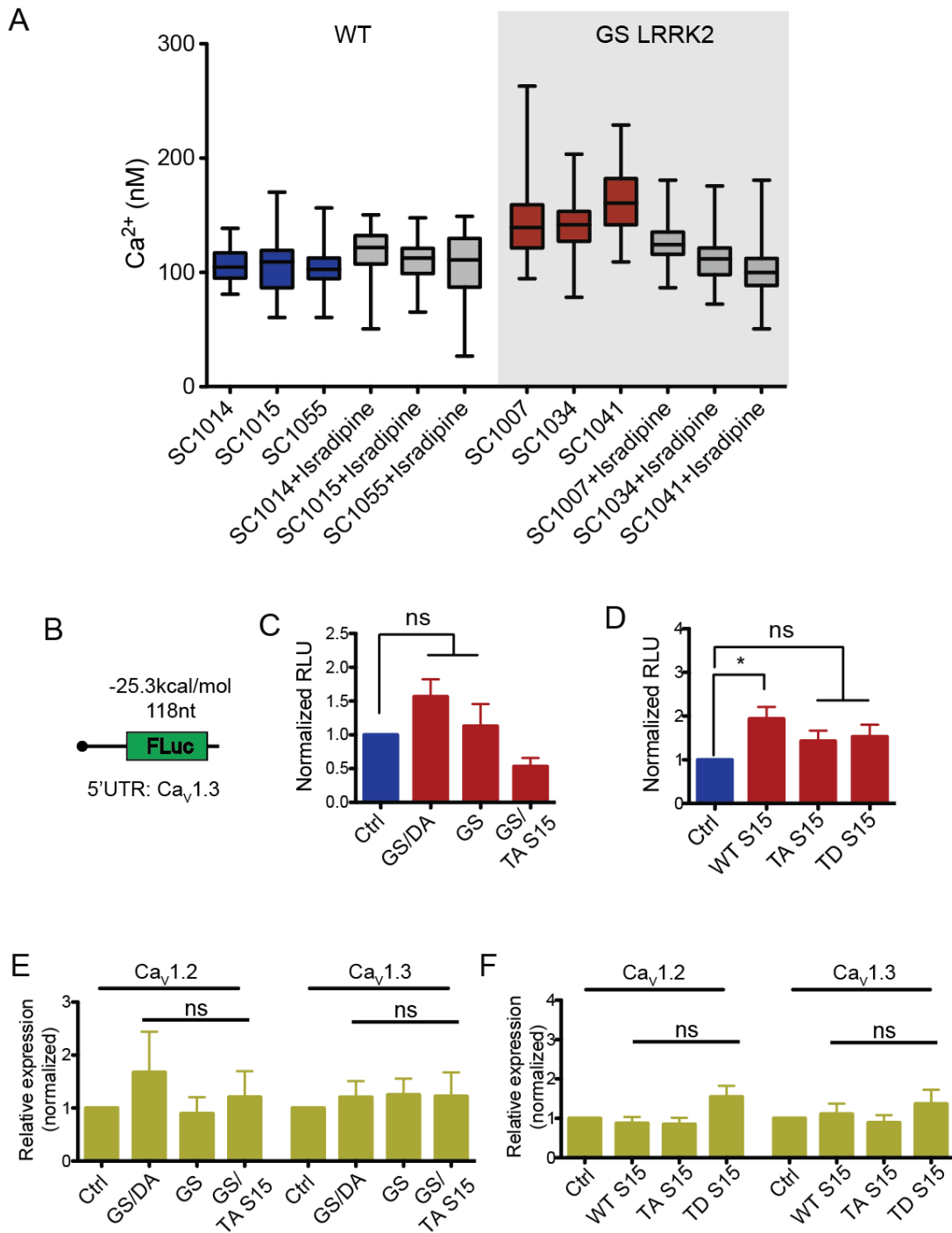


Figure 3-9. Ca_v1.2 expression is increased in GS LRRK2 human DA neurons.

(A) Ca²⁺ peak current density measurement with selective L-VGCC antagonist isradipine. L-VGCC currents were obtained by subtracting Ca²⁺ current after isradipine treatment from total Ca²⁺ current. (B) Quantification of Ca²⁺ peak current density. Total Ca²⁺ peak current was normalized to cell capacitance (pA/pF). Three lines of each genotype were pooled for analysis, and statistical significance was tested by Mann-Whitney nonparametric test. n=22 (WT), n=12 (WT+isradipine), n=23 (GS LRRK2), n=10 (GS LRRK2+isradipine). (C) Intracellular Ca²⁺ concentration with isradipine treatment was measured using ratiometric Ca²⁺ indicator Fura-2. 1μM isradipine was treated for 2 hours before measurement, and fluorescence intensity was converted to absolute Ca²⁺ concentration. The results show that intracellular Ca²⁺ concentration is increased by ~40% in GS LRRK2 human DA neurons, and isradipine treatment reduces the elevated intracellular Ca²⁺ concentration. Average Ca²⁺ concentrations for the neurons are 104.21nM (WT), 112.33nM (WT+isradipine), 150.45nM (GS LRRK2), 112.25nM (GS LRRK2+isradipine). Three different lines were pooled and statistical significance was tested by one-way ANOVA with Bonferroni correction (Extended Data Fig. 10a). n=166 (WT), n=161 (WT+isradipine), n=180 (GS LRRK2), n=204 (GS LRRK2+isradipine). (D) A schematic of 5'UTR luciferase reporter of CACNA1C, which encodes the Ca_v1.2 L-VGCC. 5'UTR sequences of CACNA1C (313nt, uc009zdu.1, UCSC hg19) were inserted into the 5'UTR region of a firefly luciferase expression vector. (E and F) 5'UTR luciferase reporter assays were performed in mouse primary cortical neurons with transient transfection. The results demonstrate that 5'UTR sequences of CACNA1C induces reporter expression in GS LRRK2 in an S15 phosphorylation-dependent manner. Each experiment is an average of triplicates, n=3 and n=4, respectively. (G) Ca_v1.2 protein level is

significantly increased in GS LRRK2 human DA neurons, and it is reduced by TA S15 overexpression. TA S15 transgene or control transgene expressing GFP or mCherry was delivered by AAV2, and protein levels were measured at 5 days post infection. WT lanes: SC1014, SC1015, SC1055, GS LRRK2 lanes: SC1007, SC1034, SC1041, respectively. **(H)** Quantification of $Ca_v1.2$ expression in human DA neurons. Statistical significance was tested by one-way ANOVA with Bonferroni correction. **(I)** Steady-state $Ca_v1.2$ expression is increased in GS LRRK2 PD brain samples. Postmortem striatal brain samples were collected from wild-type control individuals or GS LRRK2 PD patients. **(J)** Quantification of $Ca_v1.2$ expression in postmortem samples. Statistical significance was determined by Mann-Whitney nonparametric test, n=5, different individuals. Error bars indicate s.e.m. * p<0.05, ** p<0.01, *** p<0.001, ns=no significance.

Figure 3-10. Increased L-VGCC current in GS LRRK2 human DA neurons.



Luciferase qPCR: 5'UTR reporter assays

Figure 3-10. Increased L-VGCC current in GS LRRK2 human DA neurons.

(A) Fura-2 intracellular Ca^{2+} imaging results plotted by each individual line show that the increased Ca^{2+} levels are consistent with their genotypes, and isradipine treatment reduces intracellular Ca^{2+} levels in all three GS LRRK2 lines. Group sizes: n=60 (SC1014), n=51 (SC1015), n=55 (SC1055), n=60 (SC1014+isradipine), n=36 (SC1015+isradipine), n=65 (SC1055+isradipine), n=62 (SC1007), n=49 (SC1034), n=69 (SC1041), n=65 (SC1007+isradipine), n=58 (SC1034+isradipine), n=81 (SC1041+isradipine). (B) A schematic of 5'UTR luciferase reporter of human CACNA1D (uc003dgu.5). (C and D) $\text{Ca}_v1.3$ (CACNA1D) 5'UTR reporter assays were performed in mouse primary cortical neurons. Unlike $\text{Ca}_v1.2$ (CACNA1C) 5'UTR reporter, no significant expression change was detected with GS LRRK2 or TD S15 overexpression. Overexpression of wild-type S15 showed a mild yet significant expression increase. Statistical significance was tested by one-way ANOVA with Bonferroni correction. Group sizes: n=3 (LRRK2), n=4 (S15), each experiment is an average of triplicates. (E and F) Luciferase transcript qPCR to measure transcript levels of the 5'UTR reporters (CACNA1C, CACNA1D). One-way ANOVA with Bonferroni correction was used, and there was no significant transcript level change detected in all reporter assays. * $p < 0.05$, ns=no significance.

Figure 3-11. Ca_v1.2 expression is increased in GS LRRK2 human DA neurons.

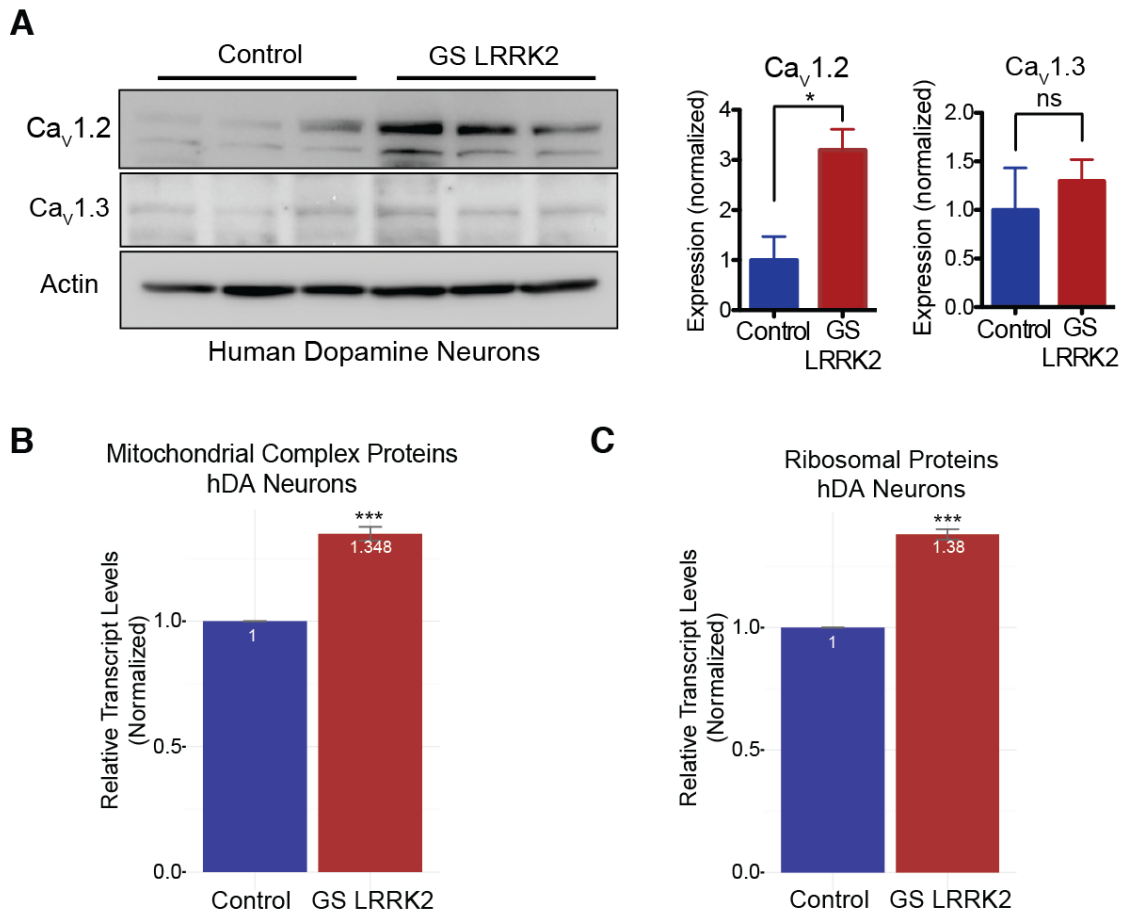


Figure 3-11. Ca_v1.2 expression is increased in GS LRRK2 human DA neurons.

(A) Ca_v1.2, not Ca_v1.3, protein level is increased in GS LRRK2 human DA neurons. Ca_v1.2 steady-state protein levels measured by western blot are increased by approx. 3-fold in GS LRRK2 human DA neurons. WT lanes: SC1014, SC1015, SC1055, GS LRRK2 lanes: SC1007, SC1034, SC1041, respectively. (B and C) Transcript levels of metabolism-related genes (ribosomal proteins, nuclear encoded mitochondrial complex proteins). GS LRRK2 human DA neurons have significantly increased transcript levels of the two groups, suggesting that GS LRRK2 DA neurons may have increased metabolic demands. Group sizes: 81 (mitochondrial genes), 85 (ribosomal proteins). Statistical significance was tested by unpaired t-test. * p<0.05, *** p<0.001, ns=no significance.

Figure 3-12. Translation-mediated stress model in GS LRRK2 DA neurons.

A

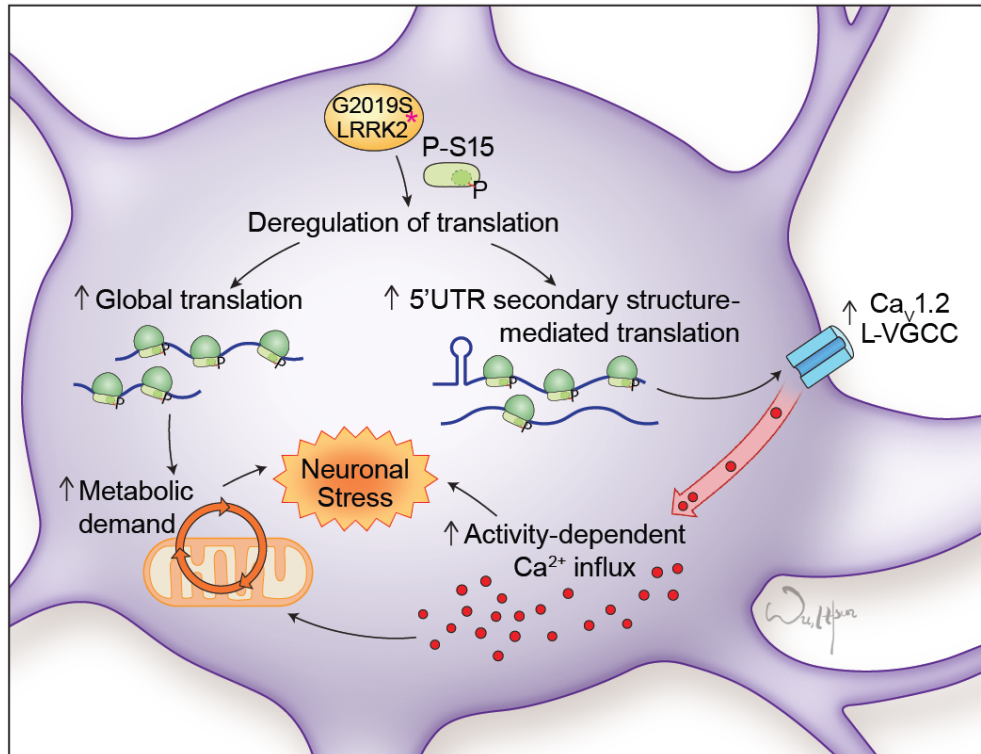


Figure 3-12. Translation-mediated stress model in GS LRRK2 DA neurons.

(A) A schematic of DA neuron stress model in GS LRRK2 Parkinson's disease brain.

Illustration: I-Hsun Wu.

Chapter 4. Discussion and Conclusions

While disruption in diverse cellular pathways is associated with Parkinson's disease (PD), recent studies have suggested a role of deregulated mRNA translation in PD pathogenesis. In addition to the effects of G2019S LRRK2 on translation, mutations in eIF4G1 and PINK1 have also been linked to aberrant translation. Ribosome profiling provides ample and thorough information on translational regulation, and has become the gold standard to study defective translational regulation. Our study provides a comprehensive interpretation on the translational profiles from mammalian PD models for the first time. We believe that our approach can be expanded to study translational defects in other PD-linked mutations, and ultimately to other neurodegenerative diseases as well.

Target identification for translational abnormality in PD models

In the previous studies, we showed that 5'UTR-mediated translational shift causes a broad alteration in G2019S LRRK2 translome. It is possible that there are additional susceptible genes caused by other PD-linked mutations that can contribute to cell-type specific stress in PD. To test this hypothesis, it would be particularly interesting to survey genome-wide translation profiling from the PD-linked mutations. If the target genes identified are important to dopamine (DA) neuronal survival, it may provide a clue to explain the susceptibility of DA neurons. Recently, more advanced tools for 'omics' study have been developed, including ribosome profiling – a genome-wide profiling method for translational regulation – and stable isotope labeling by amino acids in cell culture (SILAC) – a quantitative proteomic tool by incorporation of non-radioactive isotopes (Kitchen,

Rozowsky, Gerstein, & Nairn, 2014). These techniques will allow us to test those hypotheses through genome-wide and proteome-wide expression profiles with PD-linked mutants. For example, a recent study suggested a translational change in mitochondrial gene expression in PINK1 mutants (Stephan Gehrke et al., 2015). Therefore, translational profiling on PINK1 mutants with a focus on mitochondrial gene expression changes may be informative. Moreover, it is still unclear how PD-linked eIF4G1 mutations affect translational initiation. Thus, biochemical approaches as well as gene expression analysis can help investigate the molecular mechanisms of eIF4G1 mutations on translation. It is also of particular interest to survey the effects of α -synuclein mutations, from its suggested genetic relationship with eIF4G1 and translation. Furthermore, it might be important to test the potential effects of aforementioned mutants on the expression of α -synuclein. Excessive α -synuclein expression has a clear link to PD pathology (Moore et al., 2005). Thus, any translational defects increasing α -synuclein expression can be potentially harmful as they may exacerbate α -synuclein aggregation.

DA neuron-specific expression profiling

Although it is critical to understand dopamine neuron specificity in PD, substantia nigra pars compacta (SNc) dopamine neurons are small in number. This is the reason why obtaining dopamine neuron specific expression data has been challenging. Recent advances on genetic tools to study cell type-specific expression may be particularly informative to understand PD. For example, translating ribosome affinity purification (TRAP) has been shown to provide clean and reproducible data from a specific neuronal population. Briefly, TRAP models are expressing enhanced green fluorescent protein (EGFP)-tagged ribosomal protein L10a

(Rpl10a) under cell-type specific promoters (Heiman et al., 2008). For dopamine neurons, dopamine transporter (DAT) promoter-driven TRAP (DAT-TRAP) mice have been generated, and the expression profile was successfully generated (Brichta et al., 2015). Combined with PD mouse models, DAT-TRAP mice can provide specific gene expression changes from dopamine neurons in mouse brain, thereby expanding our knowledge on the effects of PD genes on gene expression including translational defects.

Ca²⁺ homeostasis and SNc dopamine neuronal specificity

A central question in PD has been to understand the relatively selective degeneration of SNc dopamine neurons. As previously mentioned, L-type voltage-gated Ca²⁺ channels (L-VGCCs) is thought to play a role in this selective vulnerability. L-VGCCs in SNc dopamine neurons open throughout their autonomous pacemaking, while the channels in ventral tegmental area (VTA) dopamine neurons do not. It has been shown that L-VGCC activities elevate intracellular Ca²⁺ level in SNc dopamine neurons, and thereby causing a higher basal oxidative stress level. The idea is supported by the observation that L-VGCC blocker treatment rescues elevated basal oxidative levels in SNc dopamine neurons. In this regard, our studies showing that 5'UTR-mediated translational alteration in G2019S LRRK2 dopamine neurons causes elevated Ca²⁺ influx including L-type voltage-gated Ca²⁺ channel (L-VGCC) current suggest a potential explanation on the mechanisms that how G2019S LRRK2 mutation contributes to the selective degeneration in familial PD. It may be informative to investigate potential relationships between intracellular Ca²⁺ homeostasis and other PD-linked mutations as well.

Ca²⁺ homeostasis, cellular metabolism and neurotoxicity

As previously discussed, higher basal metabolism and reduced mitochondrial reserve capacity have been identified as distinctive characteristics of SNc dopamine neurons. As mitochondrial defect is regarded as a common cellular phenotype in all PD models including genetic and pharmacological models, mitochondrial stress has been thought to be a major cause of neurotoxicity in different PD cases. In a case of G2019S LRRK2 mutation, high-cost translational defects and increased levels of L-VGCCs may have more detrimental effects in SNc dopamine neurons. However, more direct and causal links between translational abnormalities and metabolic demands, and also mitochondrial stress and neurotoxicity models need to be established. For example, in the case of increased bulk translation with G2019S LRRK2 mutation, measuring basal metabolism rate as well as mitochondrial oxidative stress with LRRK2 kinase inhibitors and/or protein synthesis inhibitors may be informative. Also, monitoring the effects of S15 phosphorylation on metabolism and mitochondrial stress will support the suggested role of S15 phosphorylation in PD pathology. Furthermore, investigating the relationship between Ca²⁺ homeostasis and mitochondrial stress in different subtypes of midbrain dopamine neurons will provide more detailed information on the molecular mechanisms of selective neurotoxicity.

Translation and Ca²⁺ as a druggable target in PD

There are many translational inhibitors found in nature and also synthesized in the laboratory, targeting different stages in protein synthesis. Therefore, it may be promising to test translational inhibitors as a PD treatment, especially in the cases of increased translation and metabolic demands. Furthermore, in regard to the well-characterized roles of mechanistic

target of rapamycin (mTOR) in translation and metabolism, since rapamycin attenuates neurodegenerative phenotypes in diverse PD models and it is a compound already approved by the FDA for the treatment of other conditions, modulating the mTOR pathway with rapamycin seems a promising therapeutic approach for PD. At the same time, new mTOR inhibitors discovered recently also have a potential as a PD treatment, with the advantage that, unlike to rapamycin, some of them can completely block all pathways downstream to mTOR (Y. C. Kim & Guan, 2015). In addition, L-VGCC inhibitors are now under clinical trials based on the hypothesis that L-VGCC activity in SNc dopamine neurons primes the neurons for chronic neuronal stress. Although these trials bring a high hope to reduce basal cellular stress caused by L-VGCC activity in SNc dopamine neurons, the current study focuses on the Ca_v1.3 activity. Although Ca_v1.3 activity might be important for the basal Ca²⁺ influx in SNc dopamine neurons, our gene expression profiling results suggest that dysregulation of Ca²⁺ homeostasis in PD-linked mutants seem to be multifactorial - multiple channels and various genes are involved. Therefore, our new findings encourage us to devise new and creative hypotheses comprehensively addressing the regulation of Ca²⁺ homeostasis in dopamine neurons. Identification and validation of new small molecules that can remedy Ca²⁺ dysregulation in dopamine neurons will make a promising next step, especially for the G2019S LRRK2 PD cases. Collectively, these efforts will ultimately result in more specific and safer design and assignment of disease-modifying agents for patients suffering from the devastating PD.

This chapter was modified from: Kim JW, Abalde-Atristain L, Jia H, Dawson VL, Dawson TM. Protein translation in Parkinson's disease. In: Verstreken P, Ed., Parkinson's Disease:

Molecular Mechanisms Underlying Pathology. San Diego: Academic Press, 2017:281-309.

References

- Alegre-Abarrategui, J., Christian, H., Lufino, M. M., Mutihac, R., Venda, L. L., Ansorge, O., & Wade-Martins, R. (2009). LRRK2 regulates autophagic activity and localizes to specific membrane microdomains in a novel human genomic reporter cellular model. *Hum Mol Genet*, *18*(21), 4022-4034. doi:10.1093/hmg/ddp346
- Anders, S., & Huber, W. (2010). Differential expression analysis for sequence count data. *Genome Biol*, *11*(10), R106. doi:10.1186/gb-2010-11-10-r106
- Anders, S., Pyl, P. T., & Huber, W. (2015). HTSeq--a Python framework to work with high-throughput sequencing data. *Bioinformatics*, *31*(2), 166-169. doi:10.1093/bioinformatics/btu638
- Anger, A. M., Armache, J. P., Berninghausen, O., Habeck, M., Subklewe, M., Wilson, D. N., & Beckmann, R. (2013). Structures of the human and Drosophila 80S ribosome. *Nature*, *497*(7447), 80-85. doi:10.1038/nature12104
- Bhattacharya, A., Kaphzan, H., Alvarez-Dieppa, A. C., Murphy, J. P., Pierre, P., & Klann, E. (2012). Genetic removal of p70 S6 kinase 1 corrects molecular, synaptic, and behavioral phenotypes in fragile X syndrome mice. *Neuron*, *76*(2), 325-337. doi:10.1016/j.neuron.2012.07.022
- Bindea, G., Mlecnik, B., Hackl, H., Charoentong, P., Tosolini, M., Kirilovsky, A., . . . Galon, J. (2009). ClueGO: a Cytoscape plug-in to decipher functionally grouped gene ontology and pathway annotation networks. *Bioinformatics*, *25*(8), 1091-1093. doi:10.1093/bioinformatics/btp101

- Brar, G. A., & Weissman, J. S. (2015). Ribosome profiling reveals the what, when, where and how of protein synthesis. *Nat Rev Mol Cell Biol*, *16*(11), 651-664.
doi:10.1038/nrm4069
- Brichta, L., Shin, W., Jackson-Lewis, V., Blesa, J., Yap, E. L., Walker, Z., . . . Greengard, P. (2015). Identification of neurodegenerative factors using translome-regulatory network analysis. *Nat Neurosci*, *18*(9), 1325-1333. doi:10.1038/nn.4070
- Chan, C. S., Guzman, J. N., Ilijic, E., Mercer, J. N., Rick, C., Tkatch, T., . . . Surmeier, D. J. (2007). 'Rejuvenation' protects neurons in mouse models of Parkinson's disease. *Nature*, *447*(7148), 1081-1086. doi:10.1038/nature05865
- Chartier-Harlin, M. C., Dachsel, J. C., Vilarino-Guell, C., Lincoln, S. J., LePrete, F., Hulihan, M. M., . . . Farrer, M. J. (2011). Translation initiator EIF4G1 mutations in familial Parkinson disease. *Am J Hum Genet*, *89*(3), 398-406.
doi:10.1016/j.ajhg.2011.08.009
- Cleary, J. D., & Ranum, L. P. W. (2013). Repeat-associated non-ATG (RAN) translation in neurological disease. *Human Molecular Genetics*, *22*(R1), R45-51.
- Cookson, M. R. (2012). Cellular effects of LRRK2 mutations. *Biochem. Soc. Trans.*, *40*(5), 1070-1073.
- Cookson, M. R. (2015). LRRK2 Pathways Leading to Neurodegeneration. *Curr Neurol Neurosci Rep*, *15*(7), 42. doi:10.1007/s11910-015-0564-y
- Crombie, T., Swaffield, J. C., & Brown, A. J. (1992). Protein folding within the cell is influenced by controlled rates of polypeptide elongation. *J Mol Biol*, *228*(1), 7-12.
- Darnell, J. C., & Klann, E. (2013). The translation of translational control by FMRP: therapeutic targets for FXS. *Nat Neurosci*, *16*(11), 1530-1536. doi:10.1038/nn.3379

- Dawson, T. M., & Dawson, V. L. (2017). Mitochondrial Mechanisms of Neuronal Cell Death: Potential Therapeutics. *Annu Rev Pharmacol Toxicol*, *57*, 437-454.
doi:10.1146/annurev-pharmtox-010716-105001
- Dever, T. E., & Green, R. (2012). The elongation, termination, and recycling phases of translation in eukaryotes. *Cold Spring Harb Perspect Biol*, *4*(7), a013706.
doi:10.1101/cshperspect.a013706
- Dhungel, N., Eleuteri, S., Li, L.-b., Kramer, N. J., Chartron, J. W., Spencer, B., . . . Gitler, A. D. (2015). Parkinson's disease genes VPS35 and EIF4G1 interact genetically and converge on α -synuclein. *Neuron*, *85*(1), 76-87.
- Dodson, M. W., Zhang, T., Jiang, C., Chen, S., & Guo, M. (2012). Roles of the Drosophila LRRK2 homolog in Rab7-dependent lysosomal positioning. *Hum Mol Genet*, *21*(6), 1350-1363. doi:10.1093/hmg/ddr573
- Funayama, M., Hasegawa, K., Kowa, H., Saito, M., Tsuji, S., & Obata, F. (2002). A new locus for Parkinson's disease (PARK8) maps to chromosome 12p11.2-q13.1. *Ann Neurol*, *51*(3), 296-301.
- Gehrke, S., Imai, Y., Sokol, N., & Lu, B. (2010). Pathogenic LRRK2 negatively regulates microRNA-mediated translational repression. *Nature*, *466*(7306), 637-641.
doi:10.1038/nature09191
- Gehrke, S., Wu, Z., Klinkenberg, M., Sun, Y., Auburger, G., Guo, S., & Lu, B. (2015). PINK1 and Parkin Control Localized Translation of Respiratory Chain Component mRNAs on Mitochondria Outer Membrane. *Cell Metabolism*, *21*(1), 95-108.

- Gillardon, F. (2009). Interaction of elongation factor 1-alpha with leucine-rich repeat kinase 2 impairs kinase activity and microtubule bundling in vitro. *Neuroscience*, *163*(2), 533-539.
- Gkogkas, C. G., Khoutorsky, A., Ran, I., Rampakakis, E., Nevarko, T., Weatherill, D. B., . . . Sonenberg, N. (2013). Autism-related deficits via dysregulated eIF4E-dependent translational control. *Nature*, *493*(7432), 371-377.
- Greggio, E., Jain, S., Kingsbury, A., Bandopadhyay, R., Lewis, P., Kaganovich, A., . . . Cookson, M. R. (2006). Kinase activity is required for the toxic effects of mutant LRRK2/dardarin. *Neurobiol Dis*, *23*(2), 329-341. doi:10.1016/j.nbd.2006.04.001
- Guzman, J. N., Sanchez-Padilla, J., Wokosin, D., Kondapalli, J., Ilijic, E., Schumacker, P. T., & Surmeier, D. J. (2010). Oxidant stress evoked by pacemaking in dopaminergic neurons is attenuated by DJ-1. *Nature*, *468*(7324), 696-700.
- Halliday, M., Radford, H., Sekine, Y., Moreno, J., Verity, N., le Quesne, J., . . . Mallucci, G. R. (2015). Partial restoration of protein synthesis rates by the small molecule ISRIB prevents neurodegeneration without pancreatic toxicity. *Cell Death Dis*, *6*, e1672. doi:10.1038/cddis.2015.49
- Harding, H. P., Novoa, I., Zhang, Y., Zeng, H., Wek, R., Schapira, M., & Ron, D. (2000). Regulated translation initiation controls stress-induced gene expression in mammalian cells. *Mol Cell*, *6*(5), 1099-1108.
- Heiman, M., Schaefer, A., Gong, S., Peterson, J. D., Day, M., Ramsey, K. E., . . . Heintz, N. (2008). A translational profiling approach for the molecular characterization of CNS cell types. *Cell*, *135*(4), 738-748. doi:10.1016/j.cell.2008.10.028

- Herzig, M. C., Kolly, C., Persohn, E., Theil, D., Schweizer, T., Hafner, T., . . . Shimshek, D. R. (2011). LRRK2 protein levels are determined by kinase function and are crucial for kidney and lung homeostasis in mice. *Hum Mol Genet*, *20*(21), 4209-4223. doi:10.1093/hmg/ddr348
- Hinnebusch, A. G., Ivanov, I. P., & Sonenberg, N. (2016). Translational control by 5'-untranslated regions of eukaryotic mRNAs. *Science*, *352*(6292), 1413-1416. doi:10.1126/science.aad9868
- Huang, X., Chen, Y., Zhang, H., Ma, Q., Zhang, Y. W., & Xu, H. (2012). Salubrinal attenuates beta-amyloid-induced neuronal death and microglial activation by inhibition of the NF-kappaB pathway. *Neurobiol Aging*, *33*(5), 1007 e1009-1017. doi:10.1016/j.neurobiolaging.2011.10.007
- Imai, Y., Gehrke, S., Wang, H.-Q., Takahashi, R., Hasegawa, K., Oota, E., & Lu, B. (2008). Phosphorylation of 4E-BP by LRRK2 affects the maintenance of dopaminergic neurons in *Drosophila*. *EMBO J*, *27*(18), 2432-2443.
- Ingolia, N. T. (2016). Ribosome Footprint Profiling of Translation throughout the Genome. *Cell*, *165*(1), 22-33. doi:10.1016/j.cell.2016.02.066
- Ingolia, N. T., Brar, G. A., Rouskin, S., McGeachy, A. M., & Weissman, J. S. (2012). The ribosome profiling strategy for monitoring translation in vivo by deep sequencing of ribosome-protected mRNA fragments. *Nat Protoc*, *7*(8), 1534-1550. doi:10.1038/nprot.2012.086
- Ingolia, N. T., Ghaemmaghami, S., Newman, J. R. S., & Weissman, J. S. (2009). Genome-wide analysis in vivo of translation with nucleotide resolution using ribosome profiling. *Science*, *324*(5924), 218-223.

- Jackson, R. J., Hellen, C. U. T., & Pestova, T. V. (2010). The mechanism of eukaryotic translation initiation and principles of its regulation. *Nature Reviews Molecular Cell Biology*, *11*(2), 113-127.
- Jaleel, M., Nichols, R. J., Deak, M., Campbell, D. G., Gillardon, F., Knebel, A., & Alessi, D. R. (2007). LRRK2 phosphorylates moesin at threonine-558: characterization of how Parkinson's disease mutants affect kinase activity. *Biochem J*, *405*(2), 307-317.
doi:10.1042/BJ20070209
- Kett, L. R., Boassa, D., Ho, C. C., Rideout, H. J., Hu, J., Terada, M., . . . Dauer, W. T. (2012). LRRK2 Parkinson disease mutations enhance its microtubule association. *Hum Mol Genet*, *21*(4), 890-899. doi:10.1093/hmg/ddr526
- Khaliq, Z. M., & Bean, B. P. (2010). Pacemaking in dopaminergic ventral tegmental area neurons: depolarizing drive from background and voltage-dependent sodium conductances. *J Neurosci*, *30*(21), 7401-7413. doi:10.1523/JNEUROSCI.0143-10.2010
- Kim, H.-J., Raphael, A. R., LaDow, E. S., McGurk, L., Weber, R. A., Trojanowski, J. Q., . . . Bonini, N. M. (2013). Therapeutic modulation of eIF2 α phosphorylation rescues TDP-43 toxicity in amyotrophic lateral sclerosis disease models. *Nat Genet*.
- Kim, Y. C., & Guan, K. L. (2015). mTOR: a pharmacologic target for autophagy regulation. *J Clin Invest*, *125*(1), 25-32. doi:10.1172/JCI73939
- Kitchen, R. R., Rozowsky, J. S., Gerstein, M. B., & Nairn, A. C. (2014). Decoding neuroproteomics: integrating the genome, translome and functional anatomy. *Nat Neurosci*, *17*(11), 1491-1499. doi:10.1038/nn.3829

- Kriks, S., Shim, J. W., Piao, J., Ganat, Y. M., Wakeman, D. R., Xie, Z., . . . Studer, L. (2011). Dopamine neurons derived from human ES cells efficiently engraft in animal models of Parkinson's disease. *Nature*, *480*(7378), 547-551. doi:10.1038/nature10648
- Kthiri, F., Gautier, V., Le, H. T., Prere, M. F., Fayet, O., Malki, A., . . . Richarme, G. (2010). Translational defects in a mutant deficient in YajL, the bacterial homolog of the parkinsonism-associated protein DJ-1. *J Bacteriol*, *192*(23), 6302-6306. doi:10.1128/JB.01077-10
- Lawrence, M., Huber, W., Pages, H., Aboyoun, P., Carlson, M., Gentleman, R., . . . Carey, V. J. (2013). Software for computing and annotating genomic ranges. *PLoS Comput Biol*, *9*(8), e1003118. doi:10.1371/journal.pcbi.1003118
- Lee, Y., Karuppagounder, S. S., Shin, J.-H., Lee, Y.-I., Ko, H. S., Swing, D., . . . Dawson, T. M. (2013). Parthanatos mediates AIMP2-activated age-dependent dopaminergic neuronal loss. *Nature Neuroscience*, *16*(10), 1392-1400.
- Lees, A. J., Hardy, J., & Revesz, T. (2009). Parkinson's disease. *Lancet*, *373*(9680), 2055-2066. doi:10.1016/S0140-6736(09)60492-X
- Lin, C. H., Tsai, P. I., Wu, R. M., & Chien, C. T. (2010). LRRK2 G2019S mutation induces dendrite degeneration through mislocalization and phosphorylation of tau by recruiting autoactivated GSK3 α . *J Neurosci*, *30*(39), 13138-13149. doi:10.1523/JNEUROSCI.1737-10.2010
- Lin, W., Wadlington, N. L., Chen, L., Zhuang, X., Brorson, J. R., & Kang, U. J. (2014). Loss of PINK1 attenuates HIF-1 α induction by preventing 4E-BP1-dependent switch in protein translation under hypoxia. *J. Neurosci.*, *34*(8), 3079-3089.

- Lorenz, R., Bernhart, S. H., Honer Zu Siederdisen, C., Tafer, H., Flamm, C., Stadler, P. F., & Hofacker, I. L. (2011). ViennaRNA Package 2.0. *Algorithms Mol Biol*, 6, 26.
doi:10.1186/1748-7188-6-26
- Ma, T., Trinh, M. A., Wexler, A. J., Bourbon, C., Gatti, E., Pierre, P., . . . Klann, E. (2013). Suppression of eIF2 α kinases alleviates Alzheimer's disease-related plasticity and memory deficits. *Nature Neuroscience*.
- MacLeod, D., Dowman, J., Hammond, R., Leete, T., Inoue, K., & Abeliovich, A. (2006). The familial Parkinsonism gene LRRK2 regulates neurite process morphology. *Neuron*, 52(4), 587-593. doi:10.1016/j.neuron.2006.10.008
- Macleod, D. A., Rhinn, H., Kuwahara, T., Zolin, A., Di Paolo, G., Maccabe, B. D., . . . Abeliovich, A. (2013). RAB7L1 Interacts with LRRK2 to Modify Intraneuronal Protein Sorting and Parkinson's Disease Risk. *Neuron*, 77(3), 425-439.
- Manzoni, C., Mamais, A., Dihanich, S., McGoldrick, P., Devine, M. J., Zerle, J., . . . Lewis, P. A. (2013). Pathogenic Parkinson's disease mutations across the functional domains of LRRK2 alter the autophagic/lysosomal response to starvation. *Biochem Biophys Res Commun*, 441(4), 862-866. doi:10.1016/j.bbrc.2013.10.159
- Martin, I., Abalde-Atristain, L., Kim, J. W., Dawson, T. M., & Dawson, V. L. (2014). Aberrant protein synthesis in G2019S LRRK2 Drosophila Parkinson disease-related phenotypes. *Fly (Austin)*, 8(3), 165-169. doi:10.4161/19336934.2014.983382
- Martin, I., Kim, J. W., Dawson, V. L., & Dawson, T. M. (2014). LRRK2 pathobiology in Parkinson's disease. *J Neurochem*, 131(5), 554-565. doi:10.1111/jnc.12949

- Martin, I., Kim, J. W., Lee, B. D., Kang, H. C., Xu, J. C., Jia, H., . . . Dawson, V. L. (2014). Ribosomal protein s15 phosphorylation mediates LRRK2 neurodegeneration in Parkinson's disease. *Cell*, *157*(2), 472-485. doi:10.1016/j.cell.2014.01.064
- Matta, S., Van Kolen, K., da Cunha, R., van den Bogaart, G., Mandemakers, W., Miskiewicz, K., . . . Verstreken, P. (2012). LRRK2 controls an EndoA phosphorylation cycle in synaptic endocytosis. *Neuron*, *75*(6), 1008-1021. doi:10.1016/j.neuron.2012.08.022
- Mayford, M., Bach, M. E., Huang, Y. Y., Wang, L., Hawkins, R. D., & Kandel, E. R. (1996). Control of memory formation through regulated expression of a CaMKII transgene. *Science*, *274*(5293), 1678-1683.
- Moore, D. J., West, A. B., Dawson, V. L., & Dawson, T. M. (2005). Molecular pathophysiology of Parkinson's disease. *Annu Rev Neurosci*, *28*, 57-87. doi:10.1146/annurev.neuro.28.061604.135718
- Moreno, J. A., Radford, H., Peretti, D., Steinert, J. R., Verity, N., Martin, M. G., . . . Mallucci, G. R. (2012). Sustained translational repression by eIF2 α -P mediates prion neurodegeneration. *Nature*, *485*(7399), 507-511.
- Nikonova, E. V., Xiong, Y., Tanis, K. Q., Dawson, V. L., Vogel, R. L., Finney, E. M., . . . Dawson, T. M. (2012). Transcriptional responses to loss or gain of function of the leucine-rich repeat kinase 2 (LRRK2) gene uncover biological processes modulated by LRRK2 activity. *Hum Mol Genet*, *21*(1), 163-174. doi:10.1093/hmg/ddr451
- Nunez-Santana, F. L., Oh, M. M., Antion, M. D., Lee, A., Hell, J. W., & Disterhoft, J. F. (2014). Surface L-type Ca²⁺ channel expression levels are increased in aged hippocampus. *Aging Cell*, *13*(1), 111-120. doi:10.1111/acel.12157

- Ottone, C., Galasso, A., Gemei, M., Pisa, V., Gigliotti, S., Piccioni, F., . . . Verrotti di Pianella, A. (2011). Diminution of eIF4E activity suppresses parkin mutant phenotypes. *Gene*, *470*(1-2), 12-19. doi:10.1016/j.gene.2010.09.003
- Pacelli, C., Giguere, N., Bourque, M. J., Levesque, M., Slack, R. S., & Trudeau, L. E. (2015). Elevated Mitochondrial Bioenergetics and Axonal Arborization Size Are Key Contributors to the Vulnerability of Dopamine Neurons. *Curr Biol*, *25*(18), 2349-2360. doi:10.1016/j.cub.2015.07.050
- Parisiadou, L., Xie, C., Cho, H. J., Lin, X., Gu, X. L., Long, C. X., . . . Cai, H. (2009). Phosphorylation of ezrin/radixin/moesin proteins by LRRK2 promotes the rearrangement of actin cytoskeleton in neuronal morphogenesis. *J Neurosci*, *29*(44), 13971-13980. doi:10.1523/JNEUROSCI.3799-09.2009
- Parisiadou, L., Yu, J., Sgobio, C., Xie, C., Liu, G., Sun, L., . . . Cai, H. (2014). LRRK2 regulates synaptogenesis and dopamine receptor activation through modulation of PKA activity. *Nat Neurosci*, *17*(3), 367-376. doi:10.1038/nn.3636
- Parsyan, A., Svitkin, Y., Shahbazian, D., Gkogkas, C., Lasko, P., Merrick, W. C., & Sonenberg, N. (2011). mRNA helicases: the tacticians of translational control. *Nat Rev Mol Cell Biol*, *12*(4), 235-245. doi:10.1038/nrm3083
- Philippart, F., Destreel, G., Merino-Sepulveda, P., Henny, P., Engel, D., & Seutin, V. (2016). Differential Somatic Ca²⁺ Channel Profile in Midbrain Dopaminergic Neurons. *J Neurosci*, *36*(27), 7234-7245. doi:10.1523/JNEUROSCI.0459-16.2016
- Plowey, E. D., Cherra, S. J., 3rd, Liu, Y. J., & Chu, C. T. (2008). Role of autophagy in G2019S-LRRK2-associated neurite shortening in differentiated SH-SY5Y cells. *J Neurochem*, *105*(3), 1048-1056. doi:10.1111/j.1471-4159.2008.05217.x

- Ramonet, D., Daher, J. P., Lin, B. M., Stafa, K., Kim, J., Banerjee, R., . . . Moore, D. J. (2011). Dopaminergic neuronal loss, reduced neurite complexity and autophagic abnormalities in transgenic mice expressing G2019S mutant LRRK2. *PLoS One*, 6(4), e18568. doi:10.1371/journal.pone.0018568
- Rhin, H., Qiang, L., Yamashita, T., Rhee, D., Zolin, A., Vanti, W., & Abeliovich, A. (2012). Alternative α -synuclein transcript usage as a convergent mechanism in Parkinson's disease pathology. *Nat Commun*, 3, 1084.
- Santini, E., Huynh, T. N., MacAskill, A. F., Carter, A. G., Pierre, P., Ruggero, D., . . . Klann, E. (2013). Exaggerated translation causes synaptic and behavioural aberrations associated with autism. *Nature*, 493(7432), 411-415.
- Scarffe, L. A., Stevens, D. A., Dawson, V. L., & Dawson, T. M. (2014). Parkin and PINK1: much more than mitophagy. *Trends Neurosci*, 37(6), 315-324. doi:10.1016/j.tins.2014.03.004
- Scheper, G. C., van der Knaap, M. S., & Proud, C. G. (2007). Translation matters: protein synthesis defects in inherited disease. *Nat Rev Genet*, 8(9), 711-723. doi:10.1038/nrg2142
- Sen, N. D., Zhou, F., Ingolia, N. T., & Hinnebusch, A. G. (2015). Genome-wide analysis of translational efficiency reveals distinct but overlapping functions of yeast DEAD-box RNA helicases Ded1 and eIF4A. *Genome Res*, 25(8), 1196-1205. doi:10.1101/gr.191601.115
- Sharma, A., Hoeffler, C. A., Takayasu, Y., Miyawaki, T., McBride, S. M., Klann, E., & Zukin, R. S. (2010). Dysregulation of mTOR signaling in fragile X syndrome. *J Neurosci*, 30(2), 694-702. doi:10.1523/JNEUROSCI.3696-09.2010

- Smith, W. W., Pei, Z., Jiang, H., Dawson, V. L., Dawson, T. M., & Ross, C. A. (2006). Kinase activity of mutant LRRK2 mediates neuronal toxicity. *Nature Neuroscience*, 9(10), 1231-1233.
- Sonenberg, N., & Hinnebusch, A. G. (2009). Regulation of Translation Initiation in Eukaryotes: Mechanisms and Biological Targets. *Cell*, 136(4), 731-745.
- Stafa, K., Tsika, E., Moser, R., Musso, A., Glauser, L., Jones, A., . . . Moore, D. J. (2014). Functional interaction of Parkinson's disease-associated LRRK2 with members of the dynamin GTPase superfamily. *Hum Mol Genet*, 23(8), 2055-2077.
doi:10.1093/hmg/ddt600
- Su, Y. C., & Qi, X. (2013). Inhibition of excessive mitochondrial fission reduced aberrant autophagy and neuronal damage caused by LRRK2 G2019S mutation. *Hum Mol Genet*, 22(22), 4545-4561. doi:10.1093/hmg/ddt301
- Surmeier, D. J., Guzman, J. N., Sanchez, J., & Schumacker, P. T. (2012). Physiological phenotype and vulnerability in Parkinson's disease. *Cold Spring Harb Perspect Med*, 2(7), a009290. doi:10.1101/cshperspect.a009290
- Taymans, J. M., Nkiliza, A., & Chartier-Harlin, M. C. (2015). Deregulation of protein translation control, a potential game-changing hypothesis for Parkinson's disease pathogenesis. *Trends Mol Med*, 21(8), 466-472. doi:10.1016/j.molmed.2015.05.004
- Thoreen, C. C., Chantranupong, L., Keys, H. R., Wang, T., Gray, N. S., & Sabatini, D. M. (2012). A unifying model for mTORC1-mediated regulation of mRNA translation. *Nature*, 486(7396), 109-113.

- Vattem, K. M., & Wek, R. C. (2004). Reinitiation involving upstream ORFs regulates ATF4 mRNA translation in mammalian cells. *Proc Natl Acad Sci U S A*, *101*(31), 11269-11274. doi:10.1073/pnas.0400541101
- Wang, X., Yan, M. H., Fujioka, H., Liu, J., Wilson-Delfosse, A., Chen, S. G., . . . Zhu, X. (2012). LRRK2 regulates mitochondrial dynamics and function through direct interaction with DLP1. *Hum Mol Genet*, *21*(9), 1931-1944. doi:10.1093/hmg/dds003
- West, A. B., Moore, D. J., Biskup, S., Bugayenko, A., Smith, W. W., Ross, C. A., . . . Dawson, T. M. (2005). Parkinson's disease-associated mutations in leucine-rich repeat kinase 2 augment kinase activity. *Proc. Natl. Acad. Sci. U.S.A.*, *102*(46), 16842-16847.
- West, A. B., Moore, D. J., Choi, C., Andrabi, S. A., Li, X., Dikeman, D., . . . Dawson, T. M. (2007). Parkinson's disease-associated mutations in LRRK2 link enhanced GTP-binding and kinase activities to neuronal toxicity. *Human Molecular Genetics*, *16*(2), 223-232.
- Wu, X., Tang, K. F., Li, Y., Xiong, Y. Y., Shen, L., Wei, Z. Y., . . . Qin, S. Y. (2012). Quantitative assessment of the effect of LRRK2 exonic variants on the risk of Parkinson's disease: a meta-analysis. *Parkinsonism Relat Disord*, *18*(6), 722-730. doi:10.1016/j.parkreldis.2012.04.013
- Xiang, G., Pan, L., Xing, W., Zhang, L., Huang, L., Yu, J., . . . Zhou, Y. (2007). Identification of activity-dependent gene expression profiles reveals specific subsets of genes induced by different routes of Ca(2+) entry in cultured rat cortical neurons. *J Cell Physiol*, *212*(1), 126-136. doi:10.1002/jcp.21008

Appendices

1/20/17, 10:27 AM

ELSEVIER ORDER DETAILS

Jan 20, 2017

This Agreement between ("You") and Elsevier ("Elsevier") consists of your order details and the terms and conditions provided by Elsevier and Copyright Clearance Center.

Order Number	501224399
Order date	Jan 15, 2017
Licensed Content Publisher	Elsevier
Licensed Content Publication	Elsevier Books
Licensed Content Title	Parkinson's Disease
Licensed Content Author	J.W. Kim,L. Abalde-Atristain,H. Jia,I. Martin,T.M. Dawson,V.L. Dawson
Licensed Content Date	2017
Licensed Content Volume Number	n/a
Licensed Content Issue Number	n/a
Licensed Content Pages	29
Start Page	281
End Page	309
Type of Use	reuse in a thesis/dissertation
Intended publisher of new work	other
Portion	full chapter
Format	electronic
Are you the author of this Elsevier chapter?	Yes
How many pages did you author in this Elsevier book?	29
Will you be translating?	No
Order reference number	
Title of your thesis/dissertation	MOLECULAR MECHANISMS OF TRANSLATIONAL ABNORMALITY IN PARKINSON'S DISEASE-LINKED G2019S LEUCINE-RICH REPEAT KINASE 2 (LRRK2) EXPRESSING NEURONS
Expected completion date	Mar 2017
Estimated size (number of pages)	100
Elsevier VAT number	GB 494 6272 12

Requestor Location Jungwoo W Kim
733 N Broadway, Suite 732

BALTIMORE, MD 21205
United States
Attn: Jungwoo W Kim

Billing Type Invoice

Billing Address Jungwoo W Kim
733 N Broadway, Suite 732

BALTIMORE, MD 21205
United States
Attn: Jungwoo W Kim

Total 0.00 USD

Terms and Conditions

INTRODUCTION

1. The publisher for this copyrighted material is Elsevier. By clicking "accept" in connection with completing this licensing transaction, you agree that the following terms and conditions apply to this transaction (along with the Billing and Payment terms and conditions established by Copyright Clearance Center, Inc. ("CCC"), at the time that you opened your Rightslink account and that are available at any time at <http://myaccount.copyright.com>).

GENERAL TERMS

2. Elsevier hereby grants you permission to reproduce the aforementioned material subject to the terms and conditions indicated.

3. Acknowledgement: If any part of the material to be used (for example, figures) has appeared in our publication with credit or acknowledgement to another source, permission must also be sought from that source. If such permission is not obtained then that material may not be included in your publication/copies. Suitable acknowledgement to the source must be made, either as a footnote or in a reference list at the end of your publication, as follows:

"Reprinted from Publication title, Vol /edition number, Author(s), Title of article / title of chapter, Pages No., Copyright (Year), with permission from Elsevier [OR APPLICABLE SOCIETY COPYRIGHT OWNER]." Also Lancet special credit - "Reprinted from The Lancet, Vol. number, Author(s), Title of article, Pages No., Copyright (Year), with permission from Elsevier."

4. Reproduction of this material is confined to the purpose and/or media for which permission is hereby given.

5. Altering/Modifying Material: Not Permitted. However figures and illustrations may be altered/adapted minimally to serve your work. Any other abbreviations, additions, deletions and/or any other alterations shall be made only with prior written authorization of Elsevier Ltd. (Please contact Elsevier at permissions@elsevier.com). No modifications can be made to any Lancet figures/tables and they must be reproduced in full.

6. If the permission fee for the requested use of our material is waived in this instance, please be advised that your future requests for Elsevier materials may attract a fee.

7. **Reservation of Rights:** Publisher reserves all rights not specifically granted in the combination of (i) the license details provided by you and accepted in the course of this licensing transaction, (ii) these terms and conditions and (iii) CCC's Billing and Payment terms and conditions.

8. **License Contingent Upon Payment:** While you may exercise the rights licensed immediately upon issuance of the license at the end of the licensing process for the transaction, provided that you have disclosed complete and accurate details of your proposed use, no license is finally effective unless and until full payment is received from you (either by publisher or by CCC) as provided in CCC's Billing and Payment terms and conditions. If full payment is not received on a timely basis, then any license preliminarily granted shall be deemed automatically revoked and shall be void as if never granted. Further, in the event that you breach any of these terms and conditions or any of CCC's Billing and Payment terms and conditions, the license is automatically revoked and shall be void as if never granted. Use of materials as described in a revoked license, as well as any use of the materials beyond the scope of an unrevoked license, may constitute copyright infringement and publisher reserves the right to take any and all action to protect its copyright in the materials.

9. **Warranties:** Publisher makes no representations or warranties with respect to the licensed material.

10. **Indemnity:** You hereby indemnify and agree to hold harmless publisher and CCC, and their respective officers, directors, employees and agents, from and against any and all claims arising out of your use of the licensed material other than as specifically authorized pursuant to this license.

11. **No Transfer of License:** This license is personal to you and may not be sublicensed, assigned, or transferred by you to any other person without publisher's written permission.

12. **No Amendment Except in Writing:** This license may not be amended except in a writing signed by both parties (or, in the case of publisher, by CCC on publisher's behalf).

13. **Objection to Contrary Terms:** Publisher hereby objects to any terms contained in any purchase order, acknowledgment, check endorsement or other writing prepared by you, which terms are inconsistent with these terms and conditions or CCC's Billing and Payment terms and conditions. These terms and conditions, together with CCC's Billing and Payment terms and conditions (which are incorporated herein), comprise the entire agreement between you and publisher (and CCC) concerning this licensing transaction. In the event of any conflict between your obligations established by these terms and conditions and those established by CCC's Billing and Payment terms and conditions, these terms and conditions shall control.

14. **Revocation:** Elsevier or Copyright Clearance Center may deny the permissions described in this License at their sole discretion, for any reason or no reason, with a full refund payable to you. Notice of such denial will be made using the contact information provided by you. Failure to receive such notice will not alter or invalidate the denial. In no event will Elsevier or Copyright Clearance Center be responsible or liable for any costs, expenses or damage incurred by you as a result of a denial of your permission request, other than a refund of the amount(s) paid by you to Elsevier and/or Copyright Clearance Center for denied permissions.

LIMITED LICENSE

The following terms and conditions apply only to specific license types:

15. **Translation:** This permission is granted for non-exclusive world English rights only

unless your license was granted for translation rights. If you licensed translation rights you may only translate this content into the languages you requested. A professional translator must perform all translations and reproduce the content word for word preserving the integrity of the article.

16. Posting licensed content on any Website: The following terms and conditions apply as follows: Licensing material from an Elsevier journal: All content posted to the web site must maintain the copyright information line on the bottom of each image; A hyper-text must be included to the Homepage of the journal from which you are licensing at

<http://www.sciencedirect.com/science/journal/xxxx> or the Elsevier homepage for books at <http://www.elsevier.com>; Central Storage: This license does not include permission for a scanned version of the material to be stored in a central repository such as that provided by Heron/XanEdu.

Licensing material from an Elsevier book: A hyper-text link must be included to the Elsevier homepage at <http://www.elsevier.com> . All content posted to the web site must maintain the copyright information line on the bottom of each image.

Posting licensed content on Electronic reserve: In addition to the above the following clauses are applicable: The web site must be password-protected and made available only to bona fide students registered on a relevant course. This permission is granted for 1 year only. You may obtain a new license for future website posting.

17. For journal authors: the following clauses are applicable in addition to the above:

Preprints:

A preprint is an author's own write-up of research results and analysis, it has not been peer-reviewed, nor has it had any other value added to it by a publisher (such as formatting, copyright, technical enhancement etc.).

Authors can share their preprints anywhere at any time. Preprints should not be added to or enhanced in any way in order to appear more like, or to substitute for, the final versions of articles however authors can update their preprints on arXiv or RePEc with their Accepted Author Manuscript (see below).

If accepted for publication, we encourage authors to link from the preprint to their formal publication via its DOI. Millions of researchers have access to the formal publications on ScienceDirect, and so links will help users to find, access, cite and use the best available version. Please note that Cell Press, The Lancet and some society-owned have different preprint policies. Information on these policies is available on the journal homepage.

Accepted Author Manuscripts: An accepted author manuscript is the manuscript of an article that has been accepted for publication and which typically includes author-incorporated changes suggested during submission, peer review and editor-author communications.

Authors can share their accepted author manuscript:

- immediately
 - o via their non-commercial person homepage or blog
 - o by updating a preprint in arXiv or RePEc with the accepted manuscript
 - o via their research institute or institutional repository for internal institutional uses or as part of an invitation-only research collaboration work-group
 - o directly by providing copies to their students or to research collaborators for their personal use

- for private scholarly sharing as part of an invitation-only work group on commercial sites with which Elsevier has an agreement
- after the embargo period
 - via non-commercial hosting platforms such as their institutional repository
 - via commercial sites with which Elsevier has an agreement

In all cases accepted manuscripts should:

- link to the formal publication via its DOI
- bear a CC-BY-NC-ND license - this is easy to do
- if aggregated with other manuscripts, for example in a repository or other site, be shared in alignment with our hosting policy not be added to or enhanced in any way to appear more like, or to substitute for, the published journal article.

Published journal article (JPA): A published journal article (PJA) is the definitive final record of published research that appears or will appear in the journal and embodies all value-adding publishing activities including peer review co-ordination, copy-editing, formatting, (if relevant) pagination and online enrichment.

Policies for sharing publishing journal articles differ for subscription and gold open access articles:

Subscription Articles: If you are an author, please share a link to your article rather than the full-text. Millions of researchers have access to the formal publications on ScienceDirect, and so links will help your users to find, access, cite, and use the best available version. Theses and dissertations which contain embedded PJAs as part of the formal submission can be posted publicly by the awarding institution with DOI links back to the formal publications on ScienceDirect.

If you are affiliated with a library that subscribes to ScienceDirect you have additional private sharing rights for others' research accessed under that agreement. This includes use for classroom teaching and internal training at the institution (including use in course packs and courseware programs), and inclusion of the article for grant funding purposes.

Gold Open Access Articles: May be shared according to the author-selected end-user license and should contain a [CrossMark logo](#), the end user license, and a DOI link to the formal publication on ScienceDirect.

Please refer to Elsevier's [posting policy](#) for further information.

18. **For book authors** the following clauses are applicable in addition to the above:

Authors are permitted to place a brief summary of their work online only. You are not allowed to download and post the published electronic version of your chapter, nor may you scan the printed edition to create an electronic version. **Posting to a repository:** Authors are permitted to post a summary of their chapter only in their institution's repository.

19. **Thesis/Dissertation:** If your license is for use in a thesis/dissertation your thesis may be submitted to your institution in either print or electronic form. Should your thesis be published commercially, please reapply for permission. These requirements include permission for the Library and Archives of Canada to supply single copies, on demand, of the complete thesis and include permission for Proquest/UMI to supply single copies, on demand, of the complete thesis. Should your thesis be published commercially, please reapply for permission. Theses and dissertations which contain embedded PJAs as part of the formal submission can be posted publicly by the awarding institution with DOI links

back to the formal publications on ScienceDirect.

Elsevier Open Access Terms and Conditions

You can publish open access with Elsevier in hundreds of open access journals or in nearly 2000 established subscription journals that support open access publishing. Permitted third party re-use of these open access articles is defined by the author's choice of Creative Commons user license. See our [open access license policy](#) for more information.

Terms & Conditions applicable to all Open Access articles published with Elsevier:

Any reuse of the article must not represent the author as endorsing the adaptation of the article nor should the article be modified in such a way as to damage the author's honour or reputation. If any changes have been made, such changes must be clearly indicated.

The author(s) must be appropriately credited and we ask that you include the end user license and a DOI link to the formal publication on ScienceDirect.

If any part of the material to be used (for example, figures) has appeared in our publication with credit or acknowledgement to another source it is the responsibility of the user to ensure their reuse complies with the terms and conditions determined by the rights holder.

Additional Terms & Conditions applicable to each Creative Commons user license:

CC BY: The CC-BY license allows users to copy, to create extracts, abstracts and new works from the Article, to alter and revise the Article and to make commercial use of the Article (including reuse and/or resale of the Article by commercial entities), provided the user gives appropriate credit (with a link to the formal publication through the relevant DOI), provides a link to the license, indicates if changes were made and the licensor is not represented as endorsing the use made of the work. The full details of the license are available at <http://creativecommons.org/licenses/by/4.0>.

CC BY NC SA: The CC BY-NC-SA license allows users to copy, to create extracts, abstracts and new works from the Article, to alter and revise the Article, provided this is not done for commercial purposes, and that the user gives appropriate credit (with a link to the formal publication through the relevant DOI), provides a link to the license, indicates if changes were made and the licensor is not represented as endorsing the use made of the work. Further, any new works must be made available on the same conditions. The full details of the license are available at <http://creativecommons.org/licenses/by-nc-sa/4.0>.

CC BY NC ND: The CC BY-NC-ND license allows users to copy and distribute the Article, provided this is not done for commercial purposes and further does not permit distribution of the Article if it is changed or edited in any way, and provided the user gives appropriate credit (with a link to the formal publication through the relevant DOI), provides a link to the license, and that the licensor is not represented as endorsing the use made of the work. The full details of the license are available at <http://creativecommons.org/licenses/by-nc-nd/4.0>.

Any commercial reuse of Open Access articles published with a CC BY NC SA or CC BY NC ND license requires permission from Elsevier and will be subject to a fee.

Commercial reuse includes:

- Associating advertising with the full text of the Article
- Charging fees for document delivery or access
- Article aggregation
- Systematic distribution via e-mail lists or share buttons

Posting or linking by commercial companies for use by customers of those companies.

20. **Other Conditions:** Permission is granted to submit your article in electronic format. This license permits you to post this Elsevier article online on your Institution's website if the content is embedded within your thesis.

v1.9

**JOHN WILEY AND SONS LICENSE
TERMS AND CONDITIONS**

Feb 21, 2017

This Agreement between Jungwoo W Kim ("You") and John Wiley and Sons ("John Wiley and Sons") consists of your license details and the terms and conditions provided by John Wiley and Sons and Copyright Clearance Center.

License Number	4053711210162
License date	Feb 21, 2017
Licensed Content Publisher	John Wiley and Sons
Licensed Content Publication	Journal of Neurochemistry
Licensed Content Title	LRRK2 pathobiology in Parkinson's disease
Licensed Content Author	Ian Martin,Jungwoo Wren Kim,Valina L. Dawson,Ted M. Dawson
Licensed Content Date	Oct 10, 2014
Licensed Content Pages	12
Type of use	Dissertation/Thesis
Requestor type	Author of this Wiley article
Format	Print and electronic
Portion	Full article
Will you be translating?	No
Title of your thesis / dissertation	MOLECULAR MECHANISMS OF TRANSLATIONAL ABNORMALITY IN PARKINSON'S DISEASE-LINKED G2019S LEUCINE-RICH REPEAT KINASE 2 (LRRK2) EXPRESSING NEURONS
Expected completion date	Mar 2017
Expected size (number of pages)	100
Requestor Location	Jungwoo W Kim 733 N Broadway, Suite 732 BALTIMORE, MD 21205 United States Attn: Jungwoo W Kim
Publisher Tax ID	EU826007151
Billing Type	Invoice
Billing Address	Jungwoo W Kim 733 N Broadway, Suite 732 BALTIMORE, MD 21205

United States
Attn: Jungwoo W Kim

Total 0.00 USD

[Terms and Conditions](#)

TERMS AND CONDITIONS

This copyrighted material is owned by or exclusively licensed to John Wiley & Sons, Inc. or one of its group companies (each a "Wiley Company") or handled on behalf of a society with which a Wiley Company has exclusive publishing rights in relation to a particular work (collectively "WILEY"). By clicking "accept" in connection with completing this licensing transaction, you agree that the following terms and conditions apply to this transaction (along with the billing and payment terms and conditions established by the Copyright Clearance Center Inc., ("CCC's Billing and Payment terms and conditions"), at the time that you opened your RightsLink account (these are available at any time at <http://myaccount.copyright.com>).

Terms and Conditions

- The materials you have requested permission to reproduce or reuse (the "Wiley Materials") are protected by copyright.
- You are hereby granted a personal, non-exclusive, non-sub licensable (on a stand-alone basis), non-transferable, worldwide, limited license to reproduce the Wiley Materials for the purpose specified in the licensing process. This license, **and any CONTENT (PDF or image file) purchased as part of your order**, is for a one-time use only and limited to any maximum distribution number specified in the license. The first instance of republication or reuse granted by this license must be completed within two years of the date of the grant of this license (although copies prepared before the end date may be distributed thereafter). The Wiley Materials shall not be used in any other manner or for any other purpose, beyond what is granted in the license. Permission is granted subject to an appropriate acknowledgement given to the author, title of the material/book/journal and the publisher. You shall also duplicate the copyright notice that appears in the Wiley publication in your use of the Wiley Material. Permission is also granted on the understanding that nowhere in the text is a previously published source acknowledged for all or part of this Wiley Material. Any third party content is expressly excluded from this permission.
- With respect to the Wiley Materials, all rights are reserved. Except as expressly granted by the terms of the license, no part of the Wiley Materials may be copied, modified, adapted (except for minor reformatting required by the new Publication), translated, reproduced, transferred or distributed, in any form or by any means, and no derivative works may be made based on the Wiley Materials without the prior permission of the respective copyright owner. **For STM Signatory Publishers clearing permission under the terms of the [STM Permissions Guidelines](#) only, the terms of the license are extended to include subsequent editions and for editions in other languages, provided such editions are for the work as a whole in situ and does not involve the separate exploitation of the permitted figures or extracts,**

You may not alter, remove or suppress in any manner any copyright, trademark or other notices displayed by the Wiley Materials. You may not license, rent, sell, loan, lease, pledge, offer as security, transfer or assign the Wiley Materials on a stand-alone basis, or any of the rights granted to you hereunder to any other person.

- The Wiley Materials and all of the intellectual property rights therein shall at all times remain the exclusive property of John Wiley & Sons Inc, the Wiley Companies, or their respective licensors, and your interest therein is only that of having possession of and the right to reproduce the Wiley Materials pursuant to Section 2 herein during the continuance of this Agreement. You agree that you own no right, title or interest in or to the Wiley Materials or any of the intellectual property rights therein. You shall have no rights hereunder other than the license as provided for above in Section 2. No right, license or interest to any trademark, trade name, service mark or other branding ("Marks") of WILEY or its licensors is granted hereunder, and you agree that you shall not assert any such right, license or interest with respect thereto
- NEITHER WILEY NOR ITS LICENSORS MAKES ANY WARRANTY OR REPRESENTATION OF ANY KIND TO YOU OR ANY THIRD PARTY, EXPRESS, IMPLIED OR STATUTORY, WITH RESPECT TO THE MATERIALS OR THE ACCURACY OF ANY INFORMATION CONTAINED IN THE MATERIALS, INCLUDING, WITHOUT LIMITATION, ANY IMPLIED WARRANTY OF MERCHANTABILITY, ACCURACY, SATISFACTORY QUALITY, FITNESS FOR A PARTICULAR PURPOSE, USABILITY, INTEGRATION OR NON-INFRINGEMENT AND ALL SUCH WARRANTIES ARE HEREBY EXCLUDED BY WILEY AND ITS LICENSORS AND WAIVED BY YOU.
- WILEY shall have the right to terminate this Agreement immediately upon breach of this Agreement by you.
- You shall indemnify, defend and hold harmless WILEY, its Licensors and their respective directors, officers, agents and employees, from and against any actual or threatened claims, demands, causes of action or proceedings arising from any breach of this Agreement by you.
- IN NO EVENT SHALL WILEY OR ITS LICENSORS BE LIABLE TO YOU OR ANY OTHER PARTY OR ANY OTHER PERSON OR ENTITY FOR ANY SPECIAL, CONSEQUENTIAL, INCIDENTAL, INDIRECT, EXEMPLARY OR PUNITIVE DAMAGES, HOWEVER CAUSED, ARISING OUT OF OR IN CONNECTION WITH THE DOWNLOADING, PROVISIONING, VIEWING OR USE OF THE MATERIALS REGARDLESS OF THE FORM OF ACTION, WHETHER FOR BREACH OF CONTRACT, BREACH OF WARRANTY, TORT, NEGLIGENCE, INFRINGEMENT OR OTHERWISE (INCLUDING, WITHOUT LIMITATION, DAMAGES BASED ON LOSS OF PROFITS, DATA, FILES, USE, BUSINESS OPPORTUNITY OR CLAIMS OF THIRD PARTIES), AND WHETHER OR NOT THE PARTY HAS BEEN ADVISED OF THE POSSIBILITY OF SUCH DAMAGES. THIS LIMITATION SHALL APPLY NOTWITHSTANDING ANY

FAILURE OF ESSENTIAL PURPOSE OF ANY LIMITED REMEDY PROVIDED HEREIN.

- Should any provision of this Agreement be held by a court of competent jurisdiction to be illegal, invalid, or unenforceable, that provision shall be deemed amended to achieve as nearly as possible the same economic effect as the original provision, and the legality, validity and enforceability of the remaining provisions of this Agreement shall not be affected or impaired thereby.
- The failure of either party to enforce any term or condition of this Agreement shall not constitute a waiver of either party's right to enforce each and every term and condition of this Agreement. No breach under this agreement shall be deemed waived or excused by either party unless such waiver or consent is in writing signed by the party granting such waiver or consent. The waiver by or consent of a party to a breach of any provision of this Agreement shall not operate or be construed as a waiver of or consent to any other or subsequent breach by such other party.
- This Agreement may not be assigned (including by operation of law or otherwise) by you without WILEY's prior written consent.
- Any fee required for this permission shall be non-refundable after thirty (30) days from receipt by the CCC.
- These terms and conditions together with CCC's Billing and Payment terms and conditions (which are incorporated herein) form the entire agreement between you and WILEY concerning this licensing transaction and (in the absence of fraud) supersedes all prior agreements and representations of the parties, oral or written. This Agreement may not be amended except in writing signed by both parties. This Agreement shall be binding upon and inure to the benefit of the parties' successors, legal representatives, and authorized assigns.
- In the event of any conflict between your obligations established by these terms and conditions and those established by CCC's Billing and Payment terms and conditions, these terms and conditions shall prevail.
- WILEY expressly reserves all rights not specifically granted in the combination of (i) the license details provided by you and accepted in the course of this licensing transaction, (ii) these terms and conditions and (iii) CCC's Billing and Payment terms and conditions.
- This Agreement will be void if the Type of Use, Format, Circulation, or Requestor Type was misrepresented during the licensing process.
- This Agreement shall be governed by and construed in accordance with the laws of the State of New York, USA, without regards to such state's conflict of law rules. Any legal action, suit or proceeding arising out of or relating to these Terms and Conditions or the breach thereof shall be instituted in a court of competent jurisdiction in New

York County in the State of New York in the United States of America and each party hereby consents and submits to the personal jurisdiction of such court, waives any objection to venue in such court and consents to service of process by registered or certified mail, return receipt requested, at the last known address of such party.

WILEY OPEN ACCESS TERMS AND CONDITIONS

Wiley Publishes Open Access Articles in fully Open Access Journals and in Subscription journals offering Online Open. Although most of the fully Open Access journals publish open access articles under the terms of the Creative Commons Attribution (CC BY) License only, the subscription journals and a few of the Open Access Journals offer a choice of Creative Commons Licenses. The license type is clearly identified on the article.

The Creative Commons Attribution License

The [Creative Commons Attribution License \(CC-BY\)](#) allows users to copy, distribute and transmit an article, adapt the article and make commercial use of the article. The CC-BY license permits commercial and non-

Creative Commons Attribution Non-Commercial License

The [Creative Commons Attribution Non-Commercial \(CC-BY-NC\) License](#) permits use, distribution and reproduction in any medium, provided the original work is properly cited and is not used for commercial purposes.(see below)

Creative Commons Attribution-Non-Commercial-NoDerivs License

The [Creative Commons Attribution Non-Commercial-NoDerivs License](#) (CC-BY-NC-ND) permits use, distribution and reproduction in any medium, provided the original work is properly cited, is not used for commercial purposes and no modifications or adaptations are made. (see below)

Use by commercial "for-profit" organizations

Use of Wiley Open Access articles for commercial, promotional, or marketing purposes requires further explicit permission from Wiley and will be subject to a fee.

Further details can be found on Wiley Online Library
<http://olabout.wiley.com/WileyCDA/Section/id-410895.html>

Other Terms and Conditions:

v1.10 Last updated September 2015

Questions? customercare@copyright.com or +1-855-239-3415 (toll free in the US) or +1-978-646-2777.

ELSEVIER LICENSE TERMS AND CONDITIONS

Jan 15, 2017

This Agreement between Jungwoo W Kim ("You") and Elsevier ("Elsevier") consists of your license details and the terms and conditions provided by Elsevier and Copyright Clearance Center.

License Number	4030401277243
License date	Jan 15, 2017
Licensed Content Publisher	Elsevier
Licensed Content Publication	Cell
Licensed Content Title	Ribosomal Protein s15 Phosphorylation Mediates LRRK2 Neurodegeneration in Parkinson's Disease
Licensed Content Author	Ian Martin, Jungwoo Wren Kim, Byoung Dae Lee, Ho Chul Kang, Jin-Chong Xu, Hao Jia, Jeannette Stankowski, Min-Sik Kim, Jun Zhong, Manoj Kumar, Shaida A. Andrabi, Yulan Xiong, Dennis W. Dickson, Zbigniew K. Wszolek, Akhilesh Pandey, Ted M. Dawson, Valina L. Dawson
Licensed Content Date	10 April 2014
Licensed Content Volume Number	157
Licensed Content Issue Number	2
Licensed Content Pages	14
Start Page	472
End Page	485
Type of Use	reuse in a thesis/dissertation
Portion	full article
Format	electronic
Are you the author of this Elsevier article?	Yes
Will you be translating?	No
Order reference number	
Title of your thesis/dissertation	MOLECULAR MECHANISMS OF TRANSLATIONAL ABNORMALITY IN PARKINSON'S DISEASE-LINKED G2019S LEUCINE-RICH REPEAT KINASE 2 (LRRK2) EXPRESSING NEURONS
Expected completion date	Mar 2017
Estimated size (number of pages)	100

Elsevier VAT number GB 494 6272 12
Requestor Location Jungwoo W Kim
733 N Broadway, Suite 732

BALTIMORE, MD 21205
United States
Attn: Jungwoo W Kim

Total 0.00 USD
Terms and Conditions

INTRODUCTION

1. The publisher for this copyrighted material is Elsevier. By clicking "accept" in connection with completing this licensing transaction, you agree that the following terms and conditions apply to this transaction (along with the Billing and Payment terms and conditions established by Copyright Clearance Center, Inc. ("CCC"), at the time that you opened your Rightslink account and that are available at any time at <http://myaccount.copyright.com>).

GENERAL TERMS

2. Elsevier hereby grants you permission to reproduce the aforementioned material subject to the terms and conditions indicated.
3. Acknowledgement: If any part of the material to be used (for example, figures) has appeared in our publication with credit or acknowledgement to another source, permission must also be sought from that source. If such permission is not obtained then that material may not be included in your publication/copies. Suitable acknowledgement to the source must be made, either as a footnote or in a reference list at the end of your publication, as follows:
"Reprinted from Publication title, Vol /edition number, Author(s), Title of article / title of chapter, Pages No., Copyright (Year), with permission from Elsevier [OR APPLICABLE SOCIETY COPYRIGHT OWNER]." Also Lancet special credit - "Reprinted from The Lancet, Vol. number, Author(s), Title of article, Pages No., Copyright (Year), with permission from Elsevier."
4. Reproduction of this material is confined to the purpose and/or media for which permission is hereby given.
5. Altering/Modifying Material: Not Permitted. However figures and illustrations may be altered/adapted minimally to serve your work. Any other abbreviations, additions, deletions and/or any other alterations shall be made only with prior written authorization of Elsevier Ltd. (Please contact Elsevier at permissions@elsevier.com). No modifications can be made to any Lancet figures/tables and they must be reproduced in full.
6. If the permission fee for the requested use of our material is waived in this instance, please be advised that your future requests for Elsevier materials may attract a fee.
7. Reservation of Rights: Publisher reserves all rights not specifically granted in the combination of (i) the license details provided by you and accepted in the course of this licensing transaction, (ii) these terms and conditions and (iii) CCC's Billing and Payment terms and conditions.
8. License Contingent Upon Payment: While you may exercise the rights licensed immediately upon issuance of the license at the end of the licensing process for the transaction, provided that you have disclosed complete and accurate details of your proposed

use, no license is finally effective unless and until full payment is received from you (either by publisher or by CCC) as provided in CCC's Billing and Payment terms and conditions. If full payment is not received on a timely basis, then any license preliminarily granted shall be deemed automatically revoked and shall be void as if never granted. Further, in the event that you breach any of these terms and conditions or any of CCC's Billing and Payment terms and conditions, the license is automatically revoked and shall be void as if never granted. Use of materials as described in a revoked license, as well as any use of the materials beyond the scope of an unrevoked license, may constitute copyright infringement and publisher reserves the right to take any and all action to protect its copyright in the materials.

9. **Warranties:** Publisher makes no representations or warranties with respect to the licensed material.

10. **Indemnity:** You hereby indemnify and agree to hold harmless publisher and CCC, and their respective officers, directors, employees and agents, from and against any and all claims arising out of your use of the licensed material other than as specifically authorized pursuant to this license.

11. **No Transfer of License:** This license is personal to you and may not be sublicensed, assigned, or transferred by you to any other person without publisher's written permission.

12. **No Amendment Except in Writing:** This license may not be amended except in a writing signed by both parties (or, in the case of publisher, by CCC on publisher's behalf).

13. **Objection to Contrary Terms:** Publisher hereby objects to any terms contained in any purchase order, acknowledgment, check endorsement or other writing prepared by you, which terms are inconsistent with these terms and conditions or CCC's Billing and Payment terms and conditions. These terms and conditions, together with CCC's Billing and Payment terms and conditions (which are incorporated herein), comprise the entire agreement between you and publisher (and CCC) concerning this licensing transaction. In the event of any conflict between your obligations established by these terms and conditions and those established by CCC's Billing and Payment terms and conditions, these terms and conditions shall control.

14. **Revocation:** Elsevier or Copyright Clearance Center may deny the permissions described in this License at their sole discretion, for any reason or no reason, with a full refund payable to you. Notice of such denial will be made using the contact information provided by you. Failure to receive such notice will not alter or invalidate the denial. In no event will Elsevier or Copyright Clearance Center be responsible or liable for any costs, expenses or damage incurred by you as a result of a denial of your permission request, other than a refund of the amount(s) paid by you to Elsevier and/or Copyright Clearance Center for denied permissions.

LIMITED LICENSE

The following terms and conditions apply only to specific license types:

15. **Translation:** This permission is granted for non-exclusive world **English** rights only unless your license was granted for translation rights. If you licensed translation rights you may only translate this content into the languages you requested. A professional translator must perform all translations and reproduce the content word for word preserving the integrity of the article.

16. **Posting licensed content on any Website:** The following terms and conditions apply as follows: Licensing material from an Elsevier journal: All content posted to the web site must maintain the copyright information line on the bottom of each image; A hyper-text must be

included to the Homepage of the journal from which you are licensing at <http://www.sciencedirect.com/science/journal/xxxx> or the Elsevier homepage for books at <http://www.elsevier.com>; Central Storage: This license does not include permission for a scanned version of the material to be stored in a central repository such as that provided by Heron/XanEdu.

Licensing material from an Elsevier book: A hyper-text link must be included to the Elsevier homepage at <http://www.elsevier.com> . All content posted to the web site must maintain the copyright information line on the bottom of each image.

Posting licensed content on Electronic reserve: In addition to the above the following clauses are applicable: The web site must be password-protected and made available only to bona fide students registered on a relevant course. This permission is granted for 1 year only. You may obtain a new license for future website posting.

17. For journal authors: the following clauses are applicable in addition to the above:

Preprints:

A preprint is an author's own write-up of research results and analysis, it has not been peer-reviewed, nor has it had any other value added to it by a publisher (such as formatting, copyright, technical enhancement etc.).

Authors can share their preprints anywhere at any time. Preprints should not be added to or enhanced in any way in order to appear more like, or to substitute for, the final versions of articles however authors can update their preprints on arXiv or RePEc with their Accepted Author Manuscript (see below).

If accepted for publication, we encourage authors to link from the preprint to their formal publication via its DOI. Millions of researchers have access to the formal publications on ScienceDirect, and so links will help users to find, access, cite and use the best available version. Please note that Cell Press, The Lancet and some society-owned have different preprint policies. Information on these policies is available on the journal homepage.

Accepted Author Manuscripts: An accepted author manuscript is the manuscript of an article that has been accepted for publication and which typically includes author-incorporated changes suggested during submission, peer review and editor-author communications.

Authors can share their accepted author manuscript:

- immediately
 - o via their non-commercial person homepage or blog
 - o by updating a preprint in arXiv or RePEc with the accepted manuscript
 - o via their research institute or institutional repository for internal institutional uses or as part of an invitation-only research collaboration work-group
 - o directly by providing copies to their students or to research collaborators for their personal use
 - o for private scholarly sharing as part of an invitation-only work group on commercial sites with which Elsevier has an agreement
- after the embargo period
 - o via non-commercial hosting platforms such as their institutional repository
 - o via commercial sites with which Elsevier has an agreement

In all cases accepted manuscripts should:

- link to the formal publication via its DOI
- bear a CC-BY-NC-ND license - this is easy to do
- if aggregated with other manuscripts, for example in a repository or other site, be shared in alignment with our hosting policy not be added to or enhanced in any way to appear more like, or to substitute for, the published journal article.

Published journal article (JPA): A published journal article (PJA) is the definitive final record of published research that appears or will appear in the journal and embodies all value-adding publishing activities including peer review co-ordination, copy-editing, formatting, (if relevant) pagination and online enrichment.

Policies for sharing publishing journal articles differ for subscription and gold open access articles:

Subscription Articles: If you are an author, please share a link to your article rather than the full-text. Millions of researchers have access to the formal publications on ScienceDirect, and so links will help your users to find, access, cite, and use the best available version. Theses and dissertations which contain embedded PJAs as part of the formal submission can be posted publicly by the awarding institution with DOI links back to the formal publications on ScienceDirect.

If you are affiliated with a library that subscribes to ScienceDirect you have additional private sharing rights for others' research accessed under that agreement. This includes use for classroom teaching and internal training at the institution (including use in course packs and courseware programs), and inclusion of the article for grant funding purposes.

Gold Open Access Articles: May be shared according to the author-selected end-user license and should contain a [CrossMark logo](#), the end user license, and a DOI link to the formal publication on ScienceDirect.

Please refer to Elsevier's [posting policy](#) for further information.

18. **For book authors** the following clauses are applicable in addition to the above:

Authors are permitted to place a brief summary of their work online only. You are not allowed to download and post the published electronic version of your chapter, nor may you scan the printed edition to create an electronic version. **Posting to a repository:** Authors are permitted to post a summary of their chapter only in their institution's repository.

19. **Thesis/Dissertation:** If your license is for use in a thesis/dissertation your thesis may be submitted to your institution in either print or electronic form. Should your thesis be published commercially, please reapply for permission. These requirements include permission for the Library and Archives of Canada to supply single copies, on demand, of the complete thesis and include permission for Proquest/UMI to supply single copies, on demand, of the complete thesis. Should your thesis be published commercially, please reapply for permission. Theses and dissertations which contain embedded PJAs as part of the formal submission can be posted publicly by the awarding institution with DOI links back to the formal publications on ScienceDirect.

Elsevier Open Access Terms and Conditions

You can publish open access with Elsevier in hundreds of open access journals or in nearly 2000 established subscription journals that support open access publishing. Permitted third party re-use of these open access articles is defined by the author's choice of Creative Commons user license. See our [open access license policy](#) for more information.

Terms & Conditions applicable to all Open Access articles published with Elsevier:

Any reuse of the article must not represent the author as endorsing the adaptation of the article nor should the article be modified in such a way as to damage the author's honour or reputation. If any changes have been made, such changes must be clearly indicated.

The author(s) must be appropriately credited and we ask that you include the end user license and a DOI link to the formal publication on ScienceDirect.

If any part of the material to be used (for example, figures) has appeared in our publication with credit or acknowledgement to another source it is the responsibility of the user to ensure their reuse complies with the terms and conditions determined by the rights holder.

Additional Terms & Conditions applicable to each Creative Commons user license:

CC BY: The CC-BY license allows users to copy, to create extracts, abstracts and new works from the Article, to alter and revise the Article and to make commercial use of the Article (including reuse and/or resale of the Article by commercial entities), provided the user gives appropriate credit (with a link to the formal publication through the relevant DOI), provides a link to the license, indicates if changes were made and the licensor is not represented as endorsing the use made of the work. The full details of the license are available at <http://creativecommons.org/licenses/by/4.0>.

CC BY NC SA: The CC BY-NC-SA license allows users to copy, to create extracts, abstracts and new works from the Article, to alter and revise the Article, provided this is not done for commercial purposes, and that the user gives appropriate credit (with a link to the formal publication through the relevant DOI), provides a link to the license, indicates if changes were made and the licensor is not represented as endorsing the use made of the work. Further, any new works must be made available on the same conditions. The full details of the license are available at <http://creativecommons.org/licenses/by-nc-sa/4.0>.

CC BY NC ND: The CC BY-NC-ND license allows users to copy and distribute the Article, provided this is not done for commercial purposes and further does not permit distribution of the Article if it is changed or edited in any way, and provided the user gives appropriate credit (with a link to the formal publication through the relevant DOI), provides a link to the license, and that the licensor is not represented as endorsing the use made of the work. The full details of the license are available at <http://creativecommons.org/licenses/by-nc-nd/4.0>.

Any commercial reuse of Open Access articles published with a CC BY NC SA or CC BY NC ND license requires permission from Elsevier and will be subject to a fee.

Commercial reuse includes:

- Associating advertising with the full text of the Article
- Charging fees for document delivery or access
- Article aggregation
- Systematic distribution via e-mail lists or share buttons

Posting or linking by commercial companies for use by customers of those companies.

20. Other Conditions:

v1.9

Questions? customercare@copyright.com or +1-855-239-3415 (toll free in the US) or +1-978-646-2777.

Copyright Clearance:

I-Hsun Wu hereby grants Jungwoo Wren Kim permission to use the figures listed below in his Ph.D. dissertation.

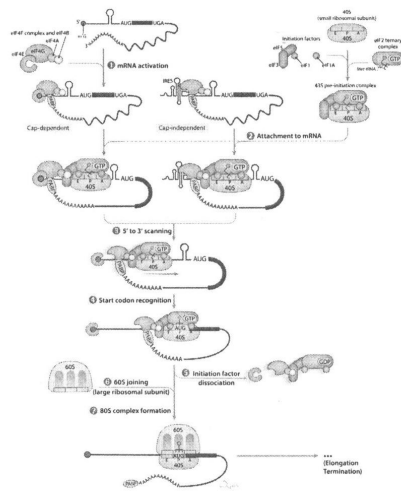


Figure 1-1

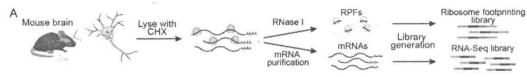


Figure 3-1A

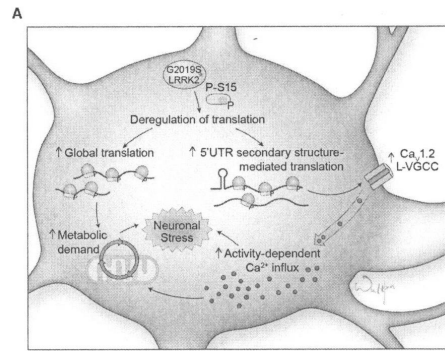


Figure 3-12A

19 February 2017

I-Hsun Wu, MA.
Research Associate (Scientific and Medical Illustrator)
Johns Hopkins University School of Medicine
Institute for Cell Engineering

Curriculum Vitae

CURRICULUM VITAE FOR Ph.D. CANDIDATES

The Johns Hopkins University School of Medicine

Jungwoo Wren Kim
Name

20 March 2017
Date of this version

Educational History:

Ph.D. expected	2017	Program in Cellular and Molecular Physiology Mentors: Valina L. Dawson, Ph.D. and Ted M. Dawson, M.D., Ph.D.	Johns Hopkins University School of Medicine
B.S.	2010	Biological Sciences	Seoul National University

Other Professional Experiences:

Undergraduate Research Assistant	2008-2010	Laboratory of Hyunsook Lee, Institute of Molecular Biology and Genetics, Seoul National University
----------------------------------	-----------	--

Scholarships:

Doctoral Scholarship	2010-2015	Korea Foundation of Advanced Studies, Stipend Support (\$10,000/year)
Undergraduate Scholarship	2004-2010	National S&T Undergraduate Scholarship, Stipend Support (full stipend)

Honors:

2017	David Israel Macht Research Award	The 40th Young Investigators' Day, Johns Hopkins University School of Medicine
2010	<i>summa cum laude</i>	Seoul National University
2009	Academic Excellence Award	College of Natural Sciences, Seoul National University

Peer-reviewed Publications:

- Kim JW**, Yin X, Martin I, Xie Z, Perez-Rosello T, Jhaldiyal A, Xiong Y, Abalde-Atristain L, Kumar M, Eacker SM, Karuppagounder S, Lee A, Surmeier DJ, Ingolia NT, Dawson TM, Dawson VL. Pathogenic LRRK2 mutation alters neuronal translome resulting in dysregulated calcium homeostasis. *under review (Science)*.
- Lee J, Stevens DA, Kang S-U, Jiang H, Lee Y-I, Ko HS, Scarffe LA, Umanah GE, Kang H, Ham S, Kam T-I, Allen K, Brahmachari S, **Kim JW**, Neifert S, Yun SP, Fiesel FC, Springer W, Dawson VL, Shin JH, Dawson TM. PINK1 primes parkin-mediated ubiquitination of PARIS in dopamine neuronal survival. *Cell Rep*. 2017 Jan;18(4):918-932.
- Martin I, **Kim JW**, Dawson VL, Dawson TM. LRRK2 pathobiology in Parkinson's disease. *J*.

Neurochem. 2014 Dec;131(5):554–65. Review.

Martin I, Abalde-Atristain L, **Kim JW**, Dawson TM, Dawson VL. Aberrant protein synthesis in G2019S LRRK2 Drosophila Parkinson disease-related phenotypes. *Fly* (Austin). 2014 Jul 3;8(3):165–9.

Martin I, **Kim JW**, Lee BD, Kang HC, Xu J-C, Jia H, Stankowski J, Kim M-S, Zhong J, Kumar M, Andrabi SA, Xiong Y, Dickson DW, Wszolek ZK, Pandey A, Dawson TM, Dawson VL. Ribosomal protein s15 phosphorylation mediates LRRK2 neurodegeneration in Parkinson's disease. *Cell*. 2014 Apr 10;157(2):472–85.

Highlighted in *Cell*, 157(2):291-293.

Highlighted in *ACS Chemical Biology*, 9(5):1067-1069.

Highlighted in *Movement Disorders*, 29(8):990.

Chapters:

Kim JW, Abalde-Atristain L, Jia H, Dawson VL, Dawson TM. Protein translation in Parkinson's disease. In: Verstreken P, Ed., *Parkinson's Disease: Molecular Mechanisms Underlying Pathology*. San Diego: Academic Press, 2017:281-309.

Presentations and Abstracts:

Kim JW, Yin X, Martin I, Xie Z, Perez-Rosello T, Jhaldiyal A, Xiong Y, Abalde-Atristain L, Kumar M, Eacker SM, Karuppagounder S, Lee A, Surmeier DJ, Ingolia NT, Dawson TM, Dawson VL. Broad Shift in 5'UTR-mediated mRNA Translation Leads to Calcium Dysregulation in G2019S LRRK2 Expressing Neurons. *Gordon Research Conference – Fragile X and Autism-Related Disorders* (2016). Poster Presentation.

Kim JW, Xie Z, Jhaldiyal A, Kumar M, Surmeier DJ, Dawson TM, Dawson VL. Aberrant Protein Synthesis Drives Ca²⁺-mediated Neuronal Stress in G2019S LRRK2 Parkinson's Disease. *Annual Meeting, The JPB Foundation* (2016). Poster Presentation.

Kim JW, Xie Z, Jhaldiyal A, Kumar M, Surmeier DJ, Dawson TM, Dawson VL. Aberrant Protein Synthesis Drives Ca²⁺-mediated Neuronal Stress in G2019S LRRK2 Parkinson's Disease. *The 9th Annual Symposium, Maryland Stem Cell Research Fund* (2016). Poster Presentation.

Kim JW, Martin I, Xiong Y, Eacker SM, Ingolia NT, Dawson TM, Dawson VL. Parkinson's disease-linked G2019S LRRK2 mutation alters mRNA translation in human dopamine neurons and LRRK2 transgenic mice. *Neuroscience 2015 Annual Meeting, Society for Neuroscience* (2015). Oral Presentation (Nanosymposium).